Available online at www.CivileJournal.org

# Civil Engineering Journal

(E-ISSN: 2476-3055; ISSN: 2676-6957)

Vol. 11, No. 06, June, 2025


# Optimizing Waste Foundry Sand in Concrete Considering Strength Properties for Sustainable Green Structures

Néstor Ulloa [1, 2*], Kerly Mishell Vaca Vallejo [3], Ana María Bucheli Campaña [4], Mery Mendoza Castillo [4], Byron Gabriel Vaca Vallejo [5]

[1] *Facultad de Mecánica, Escuela Superior Politécnica de Chimborazo (ESPOCH), Riobamba 060155, Ecuador.*

[2] *Grupo de Investigación y Desarrollo de Nanotecnología, Materiales y Manufactura (GIDENM), Escuela Superior Politécnica de Chimborazo, ESPOCH, Riobamba, Ecuador.*

[3] *Dipartimento Di Ingegneria Informatica, Modellistica, Elettronica E Sistemistica-DIMES, University of Calabria, Rende, 87036, Italy.*

[4] *Escuela Superior Politécnica de Chimborazo (ESPOCH), Sede Orellana, El Coca 220150, Ecuador.*

[5] *Facultad de Informática y Electrónica, Escuela Superior Politécnica de Chimborazo (ESPOCH), Riobamba, 060155, Ecuador.*

Received 02 March 2025; Revised 19 May 2025; Accepted 24 May 2025; Published 01 June 2025

**Abstract**

Incorporating waste foundry sand (WFS) into concrete is a sustainable approach to enhance green construction practices. Waste foundry sand is a byproduct of the metal casting industry and is often discarded in landfills, posing environmental concerns. Using it as a partial replacement for natural sand in concrete addresses both waste management and resource conservation. In this research paper, advanced machine learning models have been reported on the soft computing of the optimal waste foundry sand in concrete based on strength properties for sustainable green structures. The machine learning techniques such as “Group Methods Data Handling Neural Network (GMDH-NN)”, “Support Vector Machine (SVM)”, “K-Nearest Neighbors (KNN)”, “Tree Decision (Tree)” and “Random Forest (RF)” were applied on a database for the compressive strength containing 397 records, for elastic modulus containing 146 records, and for split tensile strength containing 242 records. Each record contains C-Cement content (kg/m³), WFS-Waste foundry sand content (kg/m³), W-Water content (kg/m³), SP-Super-plasticizer content (kg/m³), CA-Coarse aggregates content (kg/m³), FA-Fine aggregates content (kg/m³), TA-Total aggregates content (kg/m³), and Age-The concrete age at testing (days), considered as the input parameters and CS_WFS-Compressive strength of waste foundry sand concrete (MPa), E_WFS-Elastic modules of waste foundry sand concrete (GPa), and STS_WFS-Split tensile strength of waste foundry sand concrete (MPa), which are the output parameters. A 75/25 partitioning pattern for train/test of the database was used in line with established rules. At the end of the model operation, it can be observed that kNN, SVM, and RF were paramount in terms of performance and therefore outclassed the other models in the three-state strength condition of the WFS cement concrete. Hence, these were selected as the decisive models for the prediction of the compressive strength, elastic modulus, and splitting tensile strength of the WFS cement's concrete. The sensitivity analyses showed that Age, WFS/C and CA/C are more impactful on the compressive strength, Age, FA/TA, and W/C are more impactful on the elastic modulus; and 1000SP/C, WFS/C, and W/C are more impactful on the splitting tensile strength of the WFS cement concrete. Generally, these models provide a foundation for optimizing material use, ensuring quality, and meeting environmental goals. Industries leveraging these tools can produce eco-friendly, high-performance concrete while addressing waste management challenges and reducing their carbon footprint.

*Keywords:* Sustainable Green Structures; Waste Foundry Sand; Concrete Strength; Machine Learning.

* Corresponding author: nestor.ulloa@espoch.edu.ec

http://dx.doi.org/10.28991/CEJ-2025-011-06-023

# 1. Introduction

The construction industry is approaching a tipping point where embracing sustainability is no longer an option but a must. Extensive study has been conducted to identify the compelling reasons why this sector should continue to prioritize sustainability [1]. Notably, the building business has a considerable impact on energy consumption, waste output, resource depletion, and greenhouse gas emissions [2]. Addressing these environmental concerns is critical, and the construction industry has a tremendous opportunity to reduce its ecological impact through sustainable practices. Resource efficiency is a primary priority in this industry, which relies largely on natural resources such as water, raw materials, and electricity [3, 4]. The industry may greatly minimize resource consumption and waste output by using sustainable practices such as material recycling and optimized energy usage [5]. To address sustainability problems in the construction sector, environmentally friendly materials are created by combining various forms of waste or recycled materials into cementitious composites, either completely or partially replacing the major components of concrete [6]. For example, silica fume, fly ash, rice husk ash, and blast furnace slag are pozzolanic materials with high silica content. Other sustainable concretes include those made using recycled aggregate glass sands, waste foundry sand (WFS), tire rubber, and ceramic [7]. Waste foundry sand concrete (WFSC) is being used as an alternative to fine aggregate in ecologically friendly concrete production. However, the high cost of landfilling WFS creates substantial economic and environmental problems [8]. Experimental tests reveal that when WFS is substituted with fine aggregate at a rate of 15-20%, the mechanical parameters of the control concrete remain equivalent. However, beyond a 10% substitution level, strength qualities decrease [9]. WFS composition, mix proportions, percentage, and the physical properties of concrete materials all have an impact on this behavior. Mineral admixtures, fungal-treated WFS, and a low water-cement ratio can all help improve strength. When the water-cement ratio is less than 0.5030, adding WFS into concrete provides only limited benefits. Machine learning-based prediction models can assist in addressing these difficulties and ease the long-term reuse of WFS in industry [10].

Because of the development of AI, numerous soft-computing technologies have been used to forecast the properties of various types of concrete. For example, machine learning algorithms have been used to forecast the properties of recycled aggregate concrete, fiber-reinforced concrete, carbon fiber-reinforced concrete, geopolymer concrete, and concrete incorporating SCMs, including slag, fly ash, and silica fume. Among ML approaches, artificial neural networks (ANN), support vector regression (SVR), genetic engineering programming (GEPs), and decision trees (DT) are widely used [11]. According to the literature study, many studies used machine learning algorithms to estimate WFSC features. Shah et al. (2021) [12] employed sugarcane bagasse ash (SCBA) as a byproduct in green concrete production. Multi-expression programming (MEP) was utilized to create predictive models of the mechanical parameters of SCBA substitute concrete. The models were trained on literature data and validated with laboratory results. The results demonstrated strong approximation capability and effectively resolved modeling overfitting. The MEP-based modeling approach, followed by validation, cross-validation, and parametric analysis, may be helpful for accurate concrete property modeling. Behnood & Mohammadi (2021) [13] forecasted the mechanical properties of concrete, including waste foundry sand (WFS), using an artificial neural network (ANN) and the multi-objective multi-verse optimizer (MOMVO) method. A thorough database was compiled and modeled in MATLAB. Several optimal ANN models were developed for compressive strength, splitting tensile strength, modulus of elasticity, and flexural strength. The results demonstrated satisfactory accuracy in estimating properties. Parametric research found that water to cement, fine aggregate to total aggregate, and coarse aggregate to cement had the greatest impact.

Iqbal et al. (2021) [14] employed Multi-Expression Programming (MEP) to simulate the mechanical characteristics of concrete incorporating waste foundry sand (WFS), a significant environmental concern. The model accurately forecasts mechanical qualities when mix factors vary, eliminating mistakes and promoting the use of WFS in green concrete. This method can reduce landfill trash and contribute to sustainable construction. Also, Ghanizadeh et al. (2023) [15] used a hybrid ensemble learning (EL) approach that combines AdaBoost and forensic-based investigation optimization (FBIO) to estimate the strength and workability of concrete containing waste foundry sand (CCWFS). Data from 30 published articles were collected, and AdaBoost-FBIO was found to outperform other classical single ML approaches as well as the well-known random forest EL method. The models had $R^2$ values more than 0.90, and uncertainty analyses revealed that they were within the acceptable performance range. Ali et al. (2022) [16] studied decreasing the amount of fine aggregate used in concrete mixtures by partially substituting waste foundry sand (WFS). The WFS ratio and cure days were optimized in the study using the Central Composite Design tool in the Response Surface Methodology of the Design-Expert software [17]. The maximum mechanical qualities were attained after 56 days of cure and 20% replacement. Twenty percent was the ideal replacement level, while thirty percent was the typical replacement amount. For conventional concrete strength, WFS can replace 20% of the natural fine aggregate; for non-structural concrete, it can replace 30%.

ALYousef et al. (2023) [18] predicted the mechanical properties of waste foundry sand concrete (WFSC) using machine learning techniques [19, 20]. Predictive models were constructed using five machine learning (ML) techniques: gene expression programming (GEP), deep neural network (DNN), and optimizable Gaussian process regressor (OGPR). A database containing 397 and 169 compressive and flexural strength values was gathered. With higher accuracy and lower error levels, the DNN2 model performed better. In order to effectively estimate WFSC traits, the study recommends that future research employ ensemble and hybrid algorithms as well as post-hoc explanatory methodologies. All the above-discussed literature materials have presented the application of different AI techniques in predicting either the compressive strength or the tensile strength or the flexural strength and even at different curing regimes [21, 22]. However, none mentioned the prediction of the behavior of the waste foundry sand concrete in terms of compressive strength, splitting tensile strength, and the elastic modulus together in one research paper, giving authors the opportunity to comprehensively understand this type of concrete and be able to design for its production and practical use. It is understandable to observe from literature that 20% WFS by weight of the fine aggregates (FA) can replace FA for structural concrete requirements, while 30% replacement has been achieved as the optimal for non-structural uses. However, the application of more reliable and sustainable machine learning models has become necessary for the purpose of more sustainable concrete designs, production, and utilization in the field.

The reviewed literature provides a strong foundation for the present research work. Prior studies have extensively explored the environmental motivations for incorporating waste materials like waste foundry sand (WFS) into concrete, demonstrating its potential to reduce resource depletion and landfill impacts while promoting sustainable construction. Several researchers have applied machine learning (ML) and soft computing techniques to predict individual concrete properties, such as compressive strength, tensile strength, flexural strength, and modulus of elasticity, using data-driven models. Approaches such as artificial neural networks, gene expression programming, ensemble methods, and hybrid algorithms have been employed, showing promising predictive performance and offering useful insights into the impact of WFS and other supplementary materials on concrete behavior. However, the existing literature primarily focuses on isolated strength parameters or specific curing regimes, and no single study has comprehensively modeled multiple key mechanical properties, namely compressive strength, splitting tensile strength, and elastic modulus of WFS concrete in a unified framework [23]. This gap limits the full understanding required for robust concrete design and practical field application. The current research addresses this gap by integrating these three critical strength parameters into a single predictive modeling framework using soft computing techniques. By doing so, it enhances the reliability and sustainability of concrete mix designs incorporating WFS and contributes to the broader goal of developing greener and more resource-efficient construction practices.

In this research work, the strengths, such as the compressive strength, the splitting tensile strength, and the elastic modulus of the concrete mixed with waste foundry sand (WFS), have been reportedly predicted. This has been done by the application of different advanced machine learning techniques such as “Group Methods Data Handling Neural Network (GMDH-NN)”, “Support Vector Machine (SVM), “K-Nearest Neighbors (KNN)”, “Tree Decision (Tree)” and “Random Forest (RF)”.

## 2. Research Gap and Statement of Novelty

While numerous studies have investigated the use of waste foundry sand (WFS) as a partial replacement for fine aggregate in concrete, most have been limited to predicting individual mechanical properties such as compressive strength, flexural strength, or tensile strength, often under specific curing conditions or using a narrow selection of machine learning techniques. Additionally, these studies typically focus on a single property per model, which restricts the ability to comprehensively evaluate the structural performance of WFS concrete. There remains a lack of integrated, data-driven frameworks that simultaneously predict multiple key strength parameters namely compressive strength, splitting tensile strength, and elastic modulus—within a unified model, which is crucial for holistic design and sustainable application in real-world structures. Furthermore, despite the availability of advanced soft computing techniques, their collective application to optimize WFS content in concrete and support green construction practices remains underexplored.

This study presents a novel contribution by developing a robust soft computing framework that simultaneously predicts compressive strength, splitting tensile strength, and elastic modulus of concrete incorporating waste foundry sand. By employing five diverse machine-learning algorithms within the Weka data-mining environment, the research not only models the mechanical behavior of WFS concrete more comprehensively than previous works but also identifies the optimal WFS replacement levels for sustainable and structurally reliable concrete. This integrated approach advances the current understanding of WFS utilization and provides a practical tool for engineers and researchers aiming to design environmentally friendly and high-performance concrete mixes.

## 3. Research Methodology

### 3.1. Collection of Data and Preliminary Analysis

Three databases were compiled from the literature [11] for various mixing ratios of waste foundry sand concrete at different ages. The database for compressive strength contains 397 records, for elastic modulus 146 records, and for split tensile strength 242 records. Each record includes the following input parameters: C — Cement content (kg/m³), WFS — Waste foundry sand content (kg/m³), W — Water content (kg/m³), SP — Super-plasticizer content (kg/m³), CA — Coarse aggregates content (kg/m³), FA — Fine aggregates content (kg/m³), TA — Total aggregates content (kg/m³), and Age — The concrete age at testing (days). The output parameters are CS_WFS — Compressive strength of waste foundry sand concrete (MPa), E_WFS — Elastic modulus of waste foundry sand concrete (GPa), and STS_WFS — Split tensile strength of waste foundry sand concrete (MPa). In accordance with established data partitioning criteria for machine learning models [24], the collected records were divided into a training set (75%) and a validation set (25%) for each of the main concrete properties. The complete dataset is provided in the Appendix I, while Table 1 summarizes its statistical characteristics. Finally, Figure 1 presents the Pearson correlation matrix, histograms, and the relationships between variables. It can be observed that there is no strong internal consistency between the output parameters and the input variables, as shown in Figures 1-a, 1-b, and 1-c.

**Table 1. Statistical analysis of collected databases**

| | | | | | | | | |
|---|---|---|---|---|---|---|---|---|
| **Compressive Strength** | | | | | | | | |
| | **WFS/C** | **W/C** | **CA/C** | **FA/TA** | **WFS/FA** | **1000SP/C** | **Age** | **CS_WFS** |
| | **-** | **-** | **-** | **-** | **-** | **-** | **day** | **MPa** |
| **Training Set** | | | | | | | | |
| Max. | 1.2 | 0.6 | 4.2 | 0.7 | 2.3 | 17.8 | 365.0 | 53.8 |
| Min | 0.0 | 0.4 | 0.9 | 0.1 | 0.0 | 0.0 | 1.0 | 11.4 |
| Avg | 0.3 | 0.5 | 3.0 | 0.3 | 0.3 | 2.7 | 59.1 | 33.0 |
| SD | 0.3 | 0.0 | 0.5 | 0.1 | 0.4 | 5.0 | 89.8 | 8.7 |
| Var | 0.9 | 0.1 | 0.2 | 0.3 | 1.3 | 1.8 | 1.5 | 0.3 |
| **Validation Set** | | | | | | | | |
| Max. | 1.2 | 0.6 | 4.2 | 0.7 | 1.5 | 17.8 | 365.0 | 49.4 |
| Min | 0.0 | 0.4 | 0.9 | 0.1 | 0.0 | 0.0 | 7.0 | 15.6 |
| Avg | 0.3 | 0.5 | 3.0 | 0.3 | 0.3 | 2.3 | 52.9 | 32.0 |
| SD | 0.3 | 0.0 | 0.5 | 0.1 | 0.4 | 4.9 | 87.4 | 7.3 |
| Var | 0.9 | 0.1 | 0.2 | 0.3 | 1.2 | 2.1 | 1.7 | 0.2 |
| **Elastic Modulus** | | | | | | | | |
| | **WFS/C** | **W/C** | **CA/C** | **FA/TA** | **WFS/FA** | **1000SP/C** | **Age** | **E_WFS** |
| | **-** | **-** | **-** | **-** | **-** | **-** | **day** | **GPa** |
| **Training Set** | | | | | | | | |
| Max. | 1.3 | 0.6 | 3.3 | 0.5 | 2.3 | 15.9 | 365.0 | 45.7 |
| Min | 0.0 | 0.4 | 1.5 | 0.1 | 0.0 | 0.0 | 3.0 | 18.4 |
| Avg | 0.3 | 0.5 | 2.7 | 0.3 | 0.2 | 3.0 | 58.5 | 30.3 |
| SD | 0.3 | 0.0 | 0.5 | 0.1 | 0.3 | 5.2 | 95.6 | 6.8 |
| Var | 1.0 | 0.1 | 0.2 | 0.3 | 1.2 | 1.7 | 1.6 | 0.2 |
| **Validation Set** | | | | | | | | |
| Max. | 1.1 | 0.6 | 3.3 | 0.5 | 2.3 | 15.9 | 365.0 | 46.7 |
| Min | 0.0 | 0.4 | 1.5 | 0.1 | 0.0 | 0.0 | 7.0 | 21.2 |
| Avg | 0.3 | 0.5 | 2.6 | 0.3 | 0.2 | 2.8 | 82.4 | 30.9 |
| SD | 0.3 | 0.1 | 0.5 | 0.1 | 0.4 | 4.3 | 117.5 | 6.4 |
| Var | 1.0 | 0.1 | 0.2 | 0.3 | 1.6 | 1.5 | 1.4 | 0.2 |
| **Split Tensile Strength** | | | | | | | | |
| | **WFS/C** | **W/C** | **CA/C** | **FA/TA** | **WFS/FA** | **1000SP/C** | **Age** | **STS_WFS** |
| | **-** | **-** | **-** | **-** | **-** | **-** | **day** | **MPa** |
| **Training Set** | | | | | | | | |
| Max. | 1.3 | 0.6 | 4.2 | 0.7 | 1.5 | 17.8 | 365.0 | 4.9 |
| Min | 0.0 | 0.4 | 0.9 | 0.1 | 0.0 | 0.0 | 3.0 | 1.7 |
| Avg | 0.4 | 0.5 | 2.9 | 0.3 | 0.3 | 3.0 | 47.3 | 3.1 |
| SD | 0.3 | 0.0 | 0.6 | 0.1 | 0.4 | 5.7 | 73.3 | 0.7 |
| Var | 0.8 | 0.1 | 0.2 | 0.3 | 1.1 | 1.9 | 1.6 | 0.2 |
| **Validation Set** | | | | | | | | |
| Max. | 1.1 | 0.6 | 3.2 | 0.4 | 2.3 | 3.7 | 365.0 | 4.9 |
| Min | 0.0 | 0.4 | 2.4 | 0.1 | 0.0 | 0.0 | 7.0 | 2.2 |
| Avg | 0.3 | 0.5 | 2.8 | 0.3 | 0.3 | 1.3 | 72.5 | 3.7 |
| SD | 0.3 | 0.0 | 0.3 | 0.1 | 0.5 | 1.6 | 116.6 | 0.8 |
| Var | 0.9 | 0.1 | 0.1 | 0.2 | 1.5 | 1.2 | 1.6 | 0.2 |

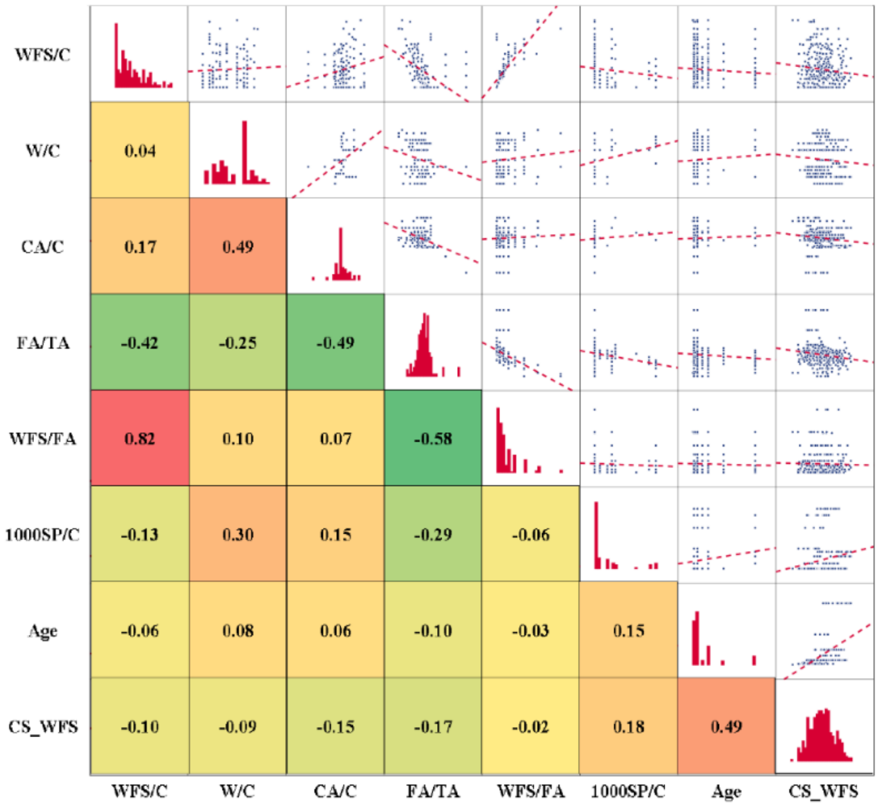


a) Compressive strength

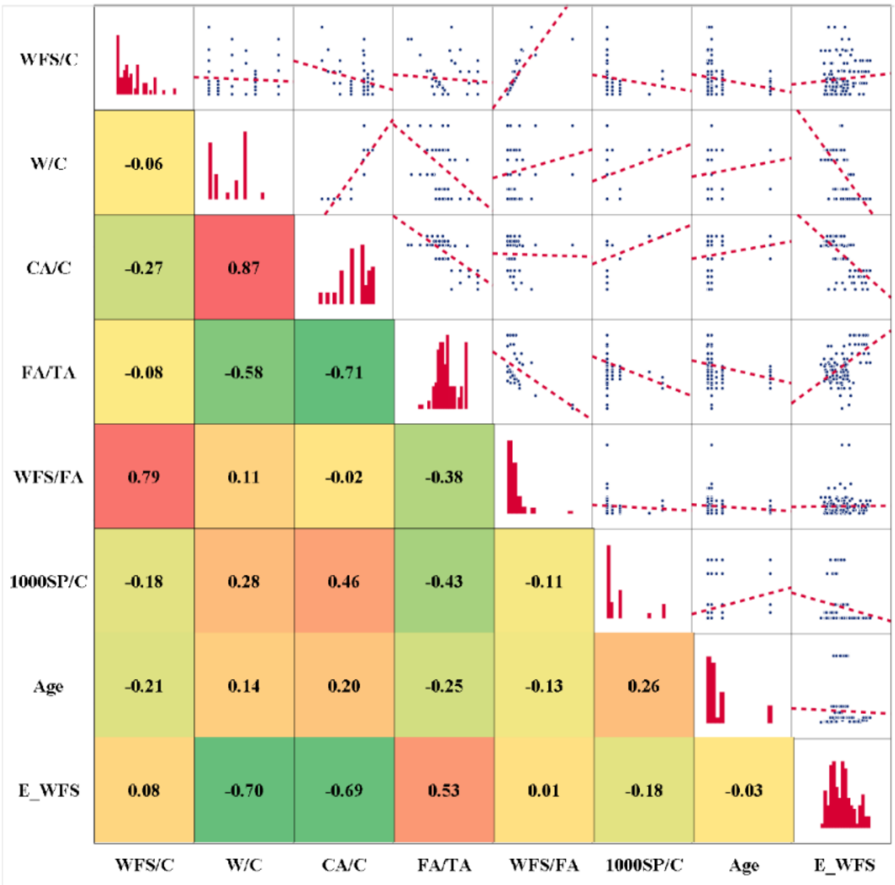


b) Elastic modulus

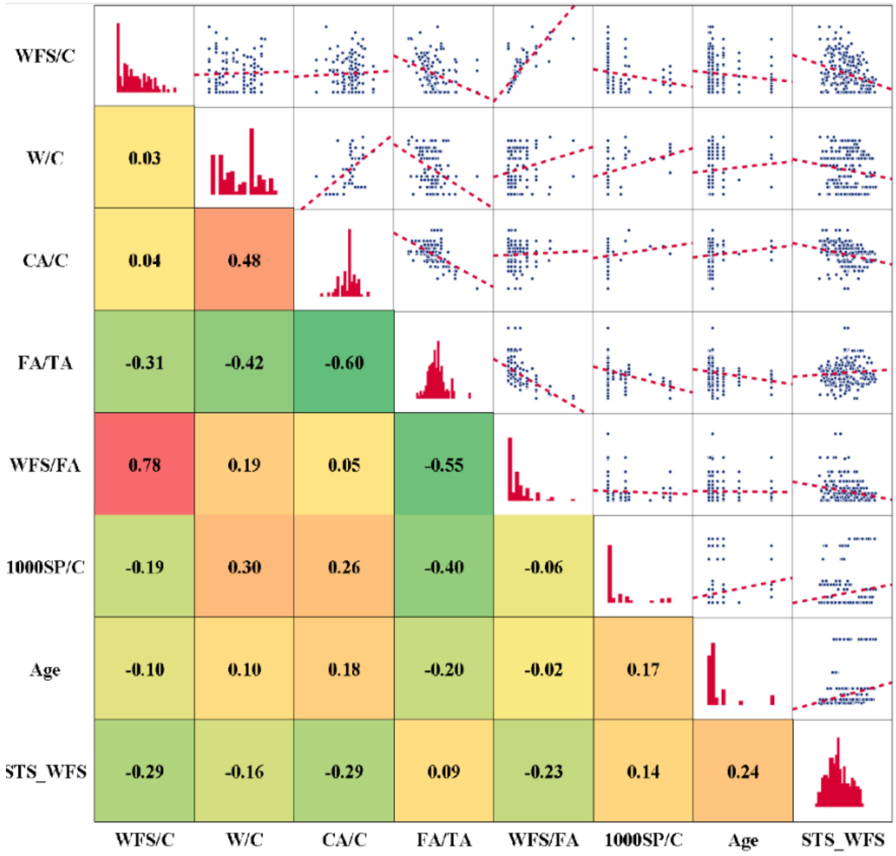


c) Split tensile strength

**Figure 1. Correlation, Distribution and Interpreting chart**

## 3.2. Sensitivity Analysis

A sensitivity analysis study on the compressive strength, tensile strength, and elastic modulus of waste foundry sand (WFS) cement concrete involves investigating how changes in the proportions of WFS and other concrete components (e.g., cement, aggregate, and water) affect these key mechanical properties. It is important to evaluate how varying the content of WFS influences the compressive strength (concrete's ability to resist axial load), tensile strength (concrete's capacity to resist tension), and flexural strength (concrete's ability to withstand bending stresses).A preliminary sensitivity analysis was carried out on the collected database to estimate the impact of each input on the (Y) values. “Single variable per time” technique is used to determine the “Sensitivity Index” (SI) for each input using Hoffman & Gardener (1983) [25] formula as follows:

$$SI\ (X_n) = \frac{Y(X_{max}) - Y(X_{min})}{Y(X_{max})} \tag{1}$$

A sensitivity index of 1.0 indicates complete sensitivity, whereas a sensitivity index below 0.01 suggests that the model is insensitive to changes in the parameter [25]. Figure 2 presents the results of sensitivity analyses for CS_WFS, E_WFS, and STS_WFS.

For compressive strength (CS_WFS), the sensitivity analysis shows that the constituents contributed as follows: curing age had a 41% influence, the WFS/C ratio 21%, the W/C ratio 2%, the CA/C ratio 21%, the FA/TA ratio 10%, the WFS/FA ratio 1%, and the 1000SP/C ratio 4% (see Figure 2-a). Analyzing these results highlights the following insights:

- **Curing Age (41%)**: This has the highest impact, indicating that curing significantly enhances compressive strength by ensuring proper cement hydration and improved matrix development.
- **WFS/C (21%) and CA/C (21%)**: These have equal influence, showing that the proportions of waste foundry sand and coarse aggregate relative to cement are critical. Adjusting these ratios likely affects the microstructure and load-bearing capacity of the concrete.
- **FA/TA (10%)**: The fine-to-total aggregate ratio moderately influences strength, emphasizing the importance of balanced aggregate proportions for optimized particle packing and reduced voids.

- **W/C (2%)**: The low influence suggests that the water-to-cement ratio was within an optimal range in most mixes, reducing variability in strength.
- **WFS/FA (1%)**: This minimal influence implies that WFS acts primarily as an inert filler without significantly altering compressive strength.
- **1000SP/C (4%)**: Superplasticizers have a slight effect, likely due to already optimized workability or mix designs.

Curing age remains the most critical factor, indicating that prolonged curing maximizes the strength potential of WFS concrete. The WFS/C and CA/C ratios are pivotal mix design parameters that directly affect mechanical performance, emphasizing the need for precise control during batching. FA/TA impacts particle distribution and void content, while W/C ratio demonstrates diminishing returns, suggesting hydration effects dominate once W/C ratios are optimized. Superplasticizers and WFS/FA play minor roles, with WFS largely functioning as a filler.

In practice, extended curing durations should be prioritized to fully leverage hydration and strength development. Optimizing the WFS/C ratio is essential to balance strength and sustainability, avoiding excessive replacement levels that could compromise strength. Aggregate proportions (CA/C and FA/TA) should be carefully managed to minimize voids and maximize particle interlock. Maintaining a controlled W/C ratio helps prevent excessive variability in strength. Regular testing and optimization of WFS/C and CA/C ratios are recommended, alongside leveraging advanced statistical methods to refine sensitivity analyses and improve prediction models.

For elastic modulus (E_WFS), the sensitivity analysis revealed the following contributions: curing age (30%), WFS/C (4%), W/C (15%), CA/C (11%), FA/TA (19%), WFS/FA (8%), and 1000SP/C (13%) (see Figure 2-b). Key interpretations include:

- **Curing Age (30%)**: The dominant factor indicates the critical role of hydration in determining concrete stiffness, as extended curing densifies the matrix and strengthens the bond between the cement paste and aggregates.
- **FA/TA (19%)**: This significantly impacts particle packing and matrix density, influencing stiffness. A higher fine aggregate proportion may improve the elastic modulus by reducing voids.
- **W/C (15%)**: A substantial effect is observed, as lower W/C ratios reduce porosity and enhance matrix density, leading to higher stiffness.
- **1000SP/C (13%)**: Moderately high impact suggests that superplasticizers improve workability, indirectly enhancing stiffness by promoting better compaction and fewer defects.
- **CA/C (11%)**: Coarse aggregate content significantly affects the elastic modulus due to the inherent stiffness and gradation of the aggregates.
- **WFS/FA (8%)**: This moderate influence indicates that replacing fine aggregate with WFS can alter the modulus, depending on the gradation, shape, and particle size of WFS.
- **WFS/C (4%)**: The minimal impact suggests WFS primarily acts as a filler rather than contributing directly to stiffness.

Curing age is vital for achieving the full stiffness potential, while FA/TA and W/C ratios contribute significantly by reducing voids and enhancing density. Superplasticizers improve compaction and matrix homogeneity, and coarse aggregates primarily govern mechanical stiffness. However, WFS/FA and WFS/C ratios show moderate to minimal effects.

Practically, extended curing should be prioritized to maximize the elastic modulus. Efficient curing techniques, such as water curing or curing compounds, should be employed. Aggregate proportions, particularly FA/TA and CA/C, should be optimized for balanced workability and stiffness. Controlling the W/C ratio is essential for achieving a denser, less porous matrix. Superplasticizers should be used judiciously to improve compaction without increasing water content. WFS content requires careful monitoring to avoid adverse effects on stiffness. Continued research is recommended to evaluate long-term stiffness and durability, and to explore how WFS gradation might positively influence stiffness under specific conditions.

For splitting tensile strength (STS_WFS), the analysis showed curing age (1%), WFS/C (25%), W/C (26%), CA/C (1%), FA/TA (8%), WFS/FA (1%), and 1000SP/C (38%) as the contributing factors (see Figure 2-c). Analysis yields these insights:

- **1000SP/C (38%)**: Superplasticizer content relative to cement has the greatest influence, highlighting the critical role of workability and compaction in reducing internal voids and ensuring proper bonding between the matrix and aggregates.
- **W/C (26%)**: A significant influence, indicating that lower W/C ratios reduce porosity and improve bond strength between aggregates and cement paste, which is crucial for tensile performance.

- **WFS/C (25%)**: Almost as influential as W/C, suggesting that WFS alters the microstructure and tensile strength depending on its quality, particle shape, and replacement level.
- **FA/TA (8%)**: Moderately affects tensile strength, as a higher FA/TA ratio improves particle packing, potentially enhancing resistance to cracking under tension.
- **Curing Age (1%)**: The low influence suggests that early hydration reactions primarily control tensile strength, with extended curing having less effect than on compressive strength.
- **CA/C (1%)**: Minimal impact indicates that coarse aggregate content does not significantly affect tensile behavior.
- **WFS/FA (1%)**: Negligible influence suggests WFS plays a secondary role when used as part of the fine aggregate system.

Superplasticizers play a prominent role in improving workability and eliminating defects during compaction, which directly affects tensile strength. Maintaining a low W/C ratio is crucial for minimizing porosity and ensuring matrix integrity under tensile stress. While WFS/C influences tensile strength through changes in the microstructure, excessive replacement levels may weaken the matrix if WFS is not pozzolanic or introduces defects. Fine aggregates enhance tensile behavior by improving particle interlock and reducing weak zones.

Curing age, CA/C, and WFS/FA have minimal influence on tensile strength compared to their effects on compressive strength and stiffness. The low role of curing suggests that tensile strength is mainly driven by early hydration reactions.

Practically, it is advisable to optimize superplasticizer dosage to achieve high workability and uniform compaction while avoiding excessive amounts that could lead to segregation. Controlling the W/C ratio remains essential for minimizing porosity and enhancing tensile strength. Careful balancing of WFS/C is necessary to avoid excessive replacement that could weaken the matrix. Maintaining an appropriate FA/TA ratio improves matrix packing and reduces weak planes in the concrete. Even though curing age has a limited impact on tensile strength, sufficient early curing is still important for proper hydration and strength development.

Recommendations include focusing on mix designs that emphasize superplasticizers, W/C ratio, and WFS content for tensile strength optimization. Further studies should investigate the optimal WFS replacement level and examine the influence of particle size and shape. Additionally, advanced modeling techniques, such as regression analysis or machine learning, should be employed to improve predictions of splitting tensile strength based on these parameters.

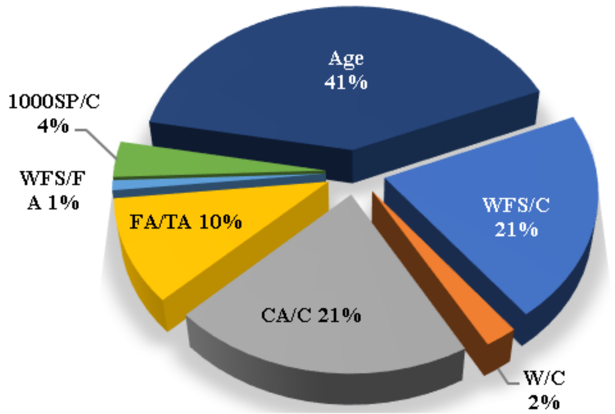


a) With respect to CS_WFS

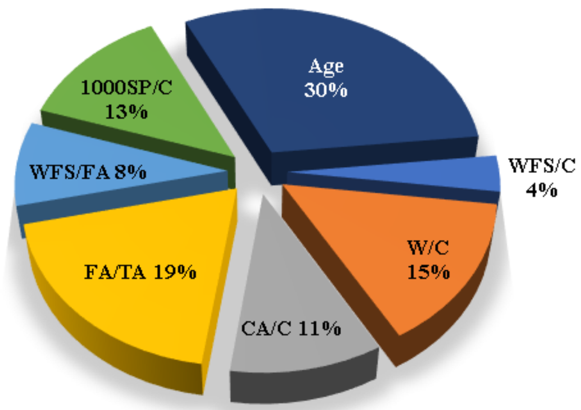


b) With respect to E_WFS

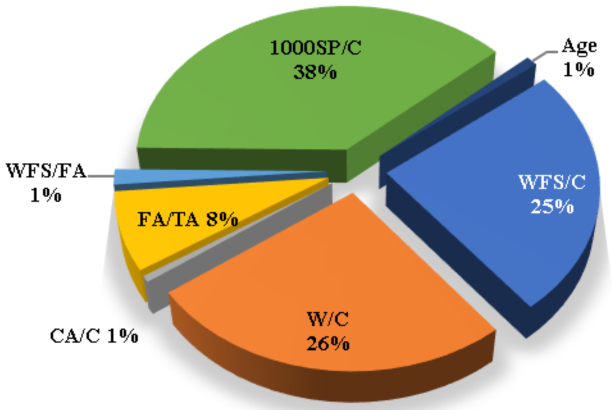


c) With respect to STS_WFS

**Figure 2. Sensitivity analysis**

## 3.3. Research Program

Five different ML techniques were used to predict the CS_WFS, E_WFS and STS_WFS of the waste foundry sand concrete using the collected database. These techniques are "Group Methods Data Handling Neural Network (GMDH-NN)", "Support vector machine (SVM), "K-Nearest Neighbors (KNN)", "Tree Decision (Tree)" and "Random Forest (RF)". (GMDH-NN) model was created using GMDH Shell 3.0 software, while (SVM), (KNN), (Tree) and (RF) models were created using "Orange Data Mining" software version 3.36. The considered data flow diagram is shown in Figure 3. The following section discusses the results of each model. The Accuracies of developed models were evaluated by comparing SSE, MAE, MSE, RMSE, Error %, Accuracy % and $R^2$ between predicted and calculated shear strength parameters values. The definition of each used measurement is presented in Equations 2 to 7.

$$MAE = \frac{1}{N}\sum_{i=1}^{N}|y_i - \hat{y}| \tag{2}$$

$$MSE = \frac{1}{N}\sum_{i=1}^{N}(y_i - \hat{y})^2 \tag{3}$$

$$RMSE = \sqrt{MSE} \tag{4}$$

$$Error\ \% = \frac{RMSE}{\hat{y}} \tag{5}$$

$$Accurcy\ \% = 1 - Error\ \% \tag{6}$$

$$R^2 = 1 - \frac{\sum(y_i-\hat{y})^2}{\sum(y_i-\bar{y})^2} \tag{7}$$

where: N is Total number of observations or data points, $y_i$ is the actual (observed) value of the target variable for the $i^{th}$ observation, $\hat{y}$: The predicted value of the target variable for the $i^{th}$ observation, generated by the model, $\bar{y}$: The mean (average) of all actual values in the dataset, and R: coefficient of determination.

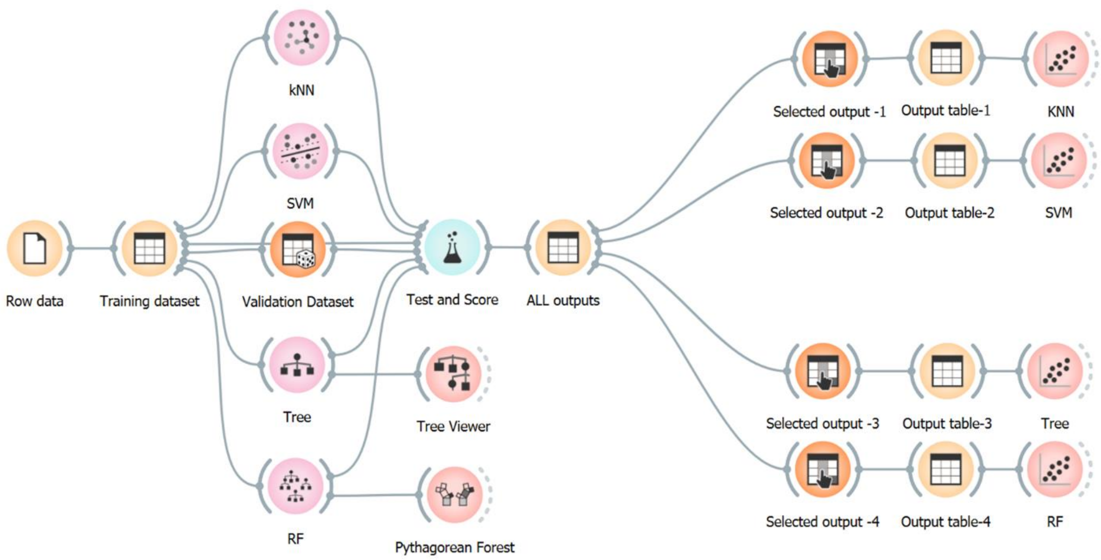


**Figure 3. The data flow considered in Orange software**

### 3.4. Theory of the Machine Learning Framework

#### 3.4.1. Group Methods Data Handling Neural Network (GMDH-NN)

The Group Method of Data Handling (GMDH) is a self-organizing computational approach used for modeling complex systems [26]. It is based on neural networks and is particularly effective for tasks involving prediction, optimization, and system identification. Self-Organizing Architecture: GMDH builds a neural network structure iteratively by selecting and combining input features and their transformations as shown in Figure 4. The model evolves layer by layer, with each layer comprising polynomial neurons. Polynomial Neurons: GMDH uses polynomial functions (e.g., quadratic or linear forms) to approximate the relationships between inputs and outputs [26]. Each neuron generates multiple models based on input combinations.

A selection criterion (e.g., minimum error or Akaike Information Criterion) determines which models advance to the next layer. The algorithm evaluates all possible combinations of inputs and retains only the most relevant ones. This reduces overfitting and improves interpretability. How GMDH-NN Works: Split data into training and validation sets. Inputs may include direct variables or their transformations (e.g., polynomial terms). At each layer, neurons are created using all possible pairs of inputs. Polynomial functions approximate relationships between inputs and the target variable. Evaluate each neuron based on the validation set. Retain only the top-performing neurons for the next layer. The process stops when adding new layers no longer improves performance or leads to overfitting [27]. The best-performing neurons across all layers are combined to form the final predictive model. GMDH-NN for Concrete Strength Prediction: Inputs: Mix proportions: W/C, WFS/C, CA/C, FA/TA, 1000SP/C, etc. Curing conditions: Curing Age (days). Outputs: Compressive strength, tensile strength, or flexural strength. Advantages in Concrete Strength Prediction: Nonlinear Relationships: GMDH-NN can capture complex, nonlinear dependencies between input parameters and strength properties. Feature Selection: Automatically identifies the most influential factors (e.g., W/C ratio or curing age). Scalability: Effective for datasets with many features or limited size.

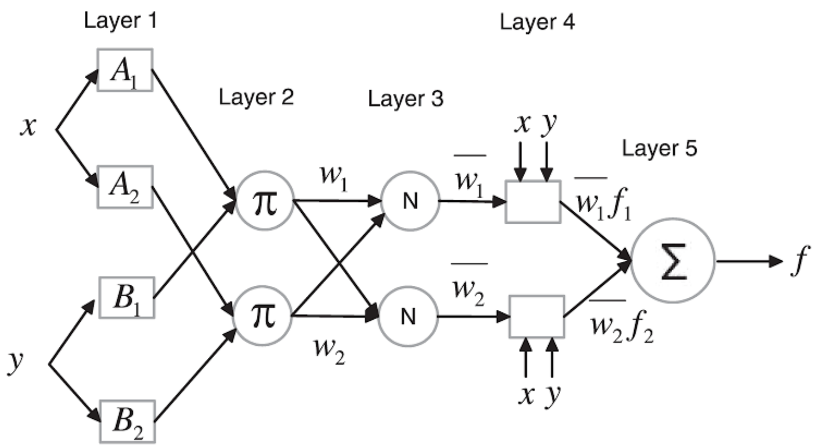


**Figure 4. The theoretical network of the GMDH-NN**

#### 3.4.2. Support vector machine (SVM)

Support Vector Machines (SVMs) are supervised learning algorithms used for both classification and regression tasks. They are particularly effective in high-dimensional spaces and are widely used for non-linear decision-making. Hyperplane: SVM aims to find the optimal hyperplane that best separates the data into different categories (classification) or predicts the output variable (regression) (see Figure 5). Support Vectors: The data points closest to the hyperplane, which define its position and orientation [28]. These are the critical points for the model. Margin: The distance between the hyperplane and the nearest data points on either side. SVM maximizes this margin to create a robust model. Kernel Trick: For non-linear data, SVM transforms input features into a higher-dimensional space using kernels. Common kernels include: Linear Kernel: Works for linearly separable data. Polynomial Kernel: Maps data into polynomial feature space. Radial Basis Function (RBF) Kernel: Handles non-linear separations effectively. Sigmoid Kernel: Similar to a neural network's activation function. SVM for Regression (SVR): In Support Vector Regression (SVR), the goal is to predict continuous values while maintaining a margin of tolerance $\epsilon$ around the hyperplane. The model tries to fit data points within a tube of width $\epsilon$ (controlled by the hyperparameter $\epsilon$). Points outside the tube are penalized based on their distance from the margin [28]. SVM for Concrete Strength Prediction Input Features: Mix Proportions: W/C, WFS/C, CA/C, FA/TA, 1000SP/C, etc. Curing Age: Number of days. Target Variables: Compressive Strength, Tensile Strength, or Flexural Strength.

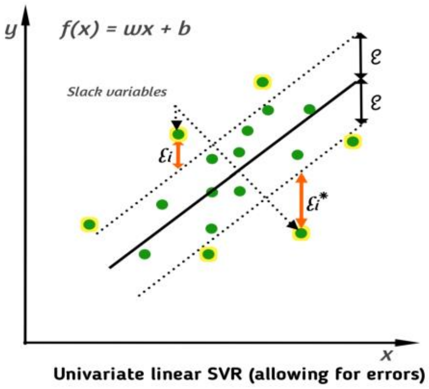


**Figure 5. The theoretical network of the SVM**

Considering dataset of labeled instances ($x_i$,$y_i$)) where xi∈Rn and yi∈{−1,1}, the decision boundary becomes a hyperplane w·x+b=0, where w = weight vector perpendicular to the hyperplane, and b= bias term. The optimization problem to maximize the margin is formulated as:

$$\min_{w,b} \frac{1}{2} ||w||^2 \quad (8)$$

Subject to the constraints:

$$y_i(w.x_i + b) \geq 1 \quad \forall i \quad (9)$$

In the case of non-linearly separable data, SVM applies the kernel functions to project data into a higher-dimensional space, where a linear separation is possible. Common kernels include the linear, polynomial, and radial basis function (RBF) kernels. The decision function for classification is then:

$$f(x) = sign(\sum_{i=1}^{n} \alpha_i y_i K(x, x_i) + b) \quad (10)$$

where $\alpha_i$ is Lagrange multipliers, and K(x,$x_i$) is chosen kernel function.

### 3.4.3. K-Nearest Neighbors (KNN)

K-Nearest Neighbors (KNN) is a simple, yet powerful supervised learning algorithm (see illustration in Figure 6) used for both regression and classification tasks. It makes predictions based on the similarity of input data points to their nearest neighbors in the feature space. Non-parametric: KNN does not assume any specific form for the underlying data distribution [23]. Lazy Learning: It does not build an explicit model during training; predictions are made on-the-fly. Sensitive to Scaling: Input features need to be scaled to ensure fair distance calculations. Figure 6 shows the illustration of the K-nearest neighbours.

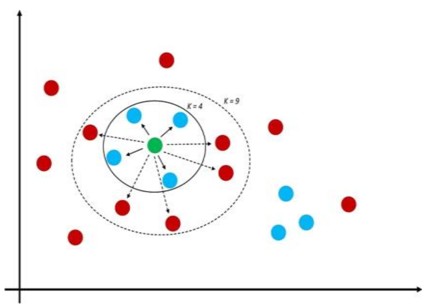

**Figure 6. Illustration of the K-nearest neighbours**

It operates by estimating the distance between the query instance and all other points in the dataset, commonly using Euclidean distance for continuous variables:

$$d(x, x') = \sqrt{\sum_{i=1}^{n} (x_i - x_i')^2} \quad (11)$$

where x and x′ are two instances in n-dimensional space.

### 3.4.4. Tree Decision (Tree)

A decision tree is a predictive modeling tool used for classification and regression tasks. It uses a tree-like structure to make decisions based on input features, splitting data at nodes according to the feature that provides the most information gain or minimizes a specific error metric [26, 29]. Below is a detailed overview of decision trees, including their structure, key concepts, an example of implementation, and how they can be applied to concrete strength prediction. Structure of a Decision Tree includes: Root Node: The starting point where the first decision is made based on a feature [27]. Internal Nodes: Represent decision points that split the dataset based on feature values. Branches: Paths that connect nodes, representing possible outcomes of a decision. Leaf Nodes: Terminal points of the tree, where predictions or classifications are made (see illustration in Figure 7). For example, considering a dataset D with classes C, the tree grows by selecting features that maximize the information gain or minimize the impurity. Hence, information gain IG for a split on feature X is respected as:

$$IG(D.X) = H(D) - \sum_{v \in values(X)} \frac{|D_v|}{|D|} H(D_v) \tag{12}$$

where H(D) is the entropy or impurity of dataset D, and Dv is the subset of D for each value v of feature X.

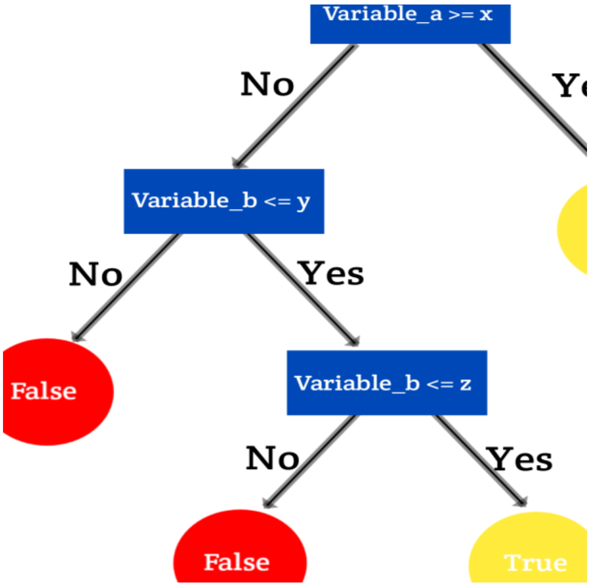


**Figure 7. The theoretical network of the decision Tree**

### 3.4.5. Random Forest (RF)

Using Random Forest (RF) for predicting the strength of waste foundry sand (WFS) cement concrete is a powerful approach due to its ability to handle complex, non-linear relationships and interactions between multiple variables. Random Forest (RF) is a powerful machine-learning algorithm commonly used for regression and classification tasks [20]. It operates by constructing a multitude of decision trees during training and outputs either the average prediction (for regression) or the majority vote (for classification) from all the trees [23]. Ensemble Learning: RF combines the predictions of multiple decision trees, making it more robust and accurate [26, 29]. Bootstrap Aggregation (Bagging): Each tree is trained on a random subset (sampled with replacement) of the dataset. This reduces overfitting by diversifying the individual trees. Feature Randomness: At each split in a tree, only a random subset of features is considered. This further decorrelates the trees and enhances performance. Non-Linear Relationships: RF can model complex, non-linear interactions between variables. Feature Importance: RF provides insights into which features most influence the target variable. Robustness: Resistant to overfitting, especially when there are sufficient trees in the forest [23]. Interpretability: While not as interpretable as simple models like linear regression, RF provides feature importance scores and partial dependence plots (see tree illustration in Figure 8).

For a training dataset D with n samples, for instance, Random Forest will construct m decision trees $T_1, T_2, \ldots, T_m$. Thus, each of the trees is trained on a bootstrap sample $D_i$ (random sample with replacement) from D, and at each node, a random subset of k features is selected to find the best split. For classification, the output is determined by a majority vote across all trees

$$\hat{y} = mode(T_1(x), T_2(x), \ldots, T_m(x)) \tag{13}$$

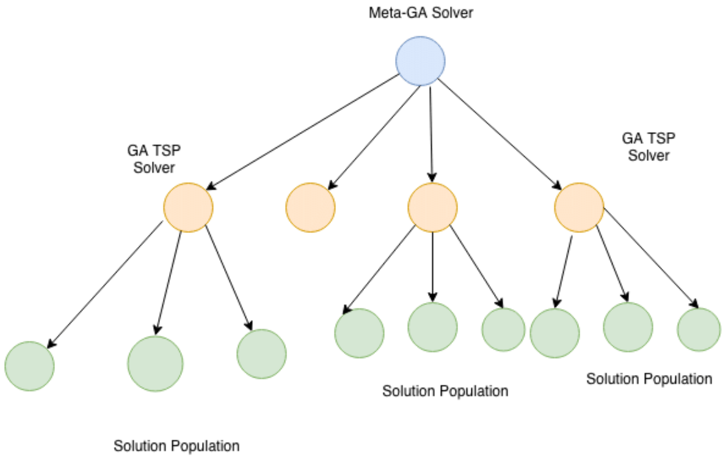


**Figure 8. The theoretical network of the RF**

For regression, the output is the average prediction from all trees:

$$\hat{y} = \frac{1}{m}\sum_{i=1}^{m} T_i(x) \tag{14}$$

# 4. Results Presentation and Discussion

## 4.1. GMDH-NN WFS Cement Concrete Strength Models

The GMDH-NN model developed for predicting the strength properties of waste foundry sand (WFS) cement concrete was trained and tested using a 75/25 split. The model utilized the following hyperparameters: 50 variables dropped after ranking, RMSE as the validation criterion, correlation-based variable ranking, a custom neuron function, a maximum of 3 layers, an initial layer width of 1000 neurons, a maximum power of a variable of 3, a minimum power of -3, a maximum total power in a term of 3, and a maximum of 3 variables per term, as illustrated in Figure 9.

For the **compressive strength model**, the GMDH-NN achieved:

- $R^2$ = 0.77, indicating that 77% of the variance in compressive strength is explained by the model.
- Accuracy = 0.885, suggesting acceptable predictive performance for practical applications, although with room for improvement.
- Error = 0.115, reflecting an average deviation of 11.5% from actual values.
- RMSE = 3.75, MSE = 14.35, MAE = 2.85, and SSE = 2820.5.

**Implications:** The model demonstrates solid performance given the complexity of compressive strength prediction. Some underperformance may be due to nonlinearities or interactions not fully captured by the GMDH-NN configuration.

For the **elastic modulus model**, the GMDH-NN achieved:

- $R^2$ = 0.825, demonstrating stronger predictive capability than the compressive strength model.
- Accuracy = 0.915, with Error = 0.09, indicating reliable predictions with only a 9% average deviation from actual values.
- RMSE = 2.8, MSE = 7.65, MAE = 2.25, and SSE = 600.5.

**Implications:** The elastic modulus model benefits significantly from the GMDH-NN's ability to capture correlations and interactions among variables. Its precise predictions make it highly suitable for practical applications.

For the **splitting tensile strength model**, the GMDH-NN achieved:

- $R^2$ = 0.75, comparable to the compressive strength model but slightly lower than for elastic modulus.
- Accuracy = 0.885, with Error = 0.115.
- RMSE = 0.4, MSE = 0.15, MAE = 0.3, and SSE = 17.

**Implications:** The splitting tensile strength model provides satisfactory predictions, although the relatively lower $R^2$ suggests there is room for improvement. While the model captures most of the variance, further feature engineering or hyperparameter tuning could enhance accuracy.

**Strengths of the GMDH-NN Model:**

- **Self-Organizing Capability:** Dynamically selects relevant input variables and polynomial terms, reducing the risk of overfitting.
- **Versatility:** Successfully models compressive strength, elastic modulus, and splitting tensile strength with consistent accuracy.
- **Nonlinear Feature Handling:** Effectively captures complex relationships between mix proportions, curing age, and strength properties.

While the $R^2$ values are satisfactory, further improvements could be achieved by:

- Incorporating additional features, such as curing temperature or specific admixtures.
- Exploring higher initial layer widths or deeper architectures to capture more complex interactions.
- Fine-tuning hyperparameters, such as adjusting power ranges or refining neuron functions.
- Using alternative selection criteria, like cross-validation instead of relying solely on RMSE.
- Expanding the dataset to enhance the model's generalizability and robustness.
- Benchmarking against other machine learning techniques (e.g., Random Forest, SVM) to assess whether GMDH-NN offers the optimal balance of accuracy and complexity.

Overall, the GMDH-NN model demonstrates strong predictive performance for compressive strength, elastic modulus, and splitting tensile strength of WFS cement concrete. Among the three, the elastic modulus model stands out as the best performer ($R^2$ = 0.825, Accuracy = 0.915), though all models are suitable for practical applications with acceptable error margins. Further refinements in feature engineering, model parameters, and dataset size could lead to even greater predictive accuracy.

Equations 15, 16, and 17 provide the closed-form solutions for the compressive strength, elastic modulus, and splitting tensile strength models, respectively.

CS_WFS = 1408.58 + "WFS/C"*"1000SP/C"*Age*0.00552301 + "W/C"*Age*23.6066 + "W/C"*Age^2*(-0.000768451) + "W/C"*Age^(-1)*(-336.072) + "W/C"*Age^(-2)*1683.95 + "W/C"^2*(-11662.1) + "W/C"^2*"CA/C"*3674.33 + "W/C"^2*"CA/C"^(-1)*14945.6 + "W/C"^2*"FA/TA"*(-995.659) + "W/C"^2*"FA/TA"^(-1)*32.7605 + "W/C"^2*"WFS/FA"*211.343 + "W/C"^2*"1000SP/C"*(-119.233) + "W/C"^2*Age*(-26.739) + "W/C"^3*(-2781.21) + "W/C"^(-1)*"CA/C"*271.437 + "W/C"^(-1)*"CA/C"*"FA/TA"^(-1)*42.5554 + "W/C"^(-1)*"CA/C"*"1000SP/C"*4.68603 + "W/C"^(-1)*"CA/C"*Age*(-0.433006) + "W/C"^(-1)*"CA/C"*Age^(-1)*5.82337 + "W/C"^(-1)*"CA/C"^2*(-8.33253) + "W/C"^(-1)*"CA/C"^(-1)*"FA/TA"*(-1545.91) + "W/C"^(-1)*"CA/C"^(-1)*"1000SP/C"*88.3044 + "W/C"^(-1)*"CA/C"^(-1)*Age*(-0.0695051) + "W/C"^(-1)*"FA/TA"*722.621 + "W/C"^(-1)*"FA/TA"*"1000SP/C"*38.8956 + "W/C"^(-1)*"FA/TA"*Age*(-0.318163) + "W/C"^(-1)*"FA/TA"^(-1)*(-76.7526) + "W/C"^(-1)*"FA/TA"^(-1)*"WFS/FA"*3.25934 + "W/C"^(-1)*"FA/TA"^(-1)*"1000SP/C"*3.99224 + "W/C"^(-1)*"FA/TA"^(-1)*Age*(-0.0450544) + "W/C"^(-1)*"WFS/FA"*Age*0.0218961 + "W/C"^(-1)*"WFS/FA"^2*(-6.00962) + "W/C"^(-1)*"1000SP/C"*(-130.049) + "W/C"^(-1)*"1000SP/C"*Age*(-0.00135914) + "W/C"^(-1)*"1000SP/C"*Age^(-1)*(-5.99298) + "W/C"^(-1)*Age*(-5.07361) + "W/C"^(-1)*Age^2*4.94843e-05 + "W/C"^(-2)*(-116.491) + "W/C"^(-2)*"1000SP/C"*8.48573 + "W/C"^(-2)*Age*1.41566 + "CA/C"*(-1024.01) + "CA/C"*"FA/TA"*"1000SP/C"*(-27.8227) + "CA/C"*"FA/TA"*Age*0.00217005 + "CA/C"*"FA/TA"^(-1)*"1000SP/C"*(-2.48045) + "CA/C"*"FA/TA"^(-1)*Age*0.0196678 + "CA/C"*"WFS/FA"*(-52.1479) + "CA/C"*"WFS/FA"*"1000SP/C"*(-0.414378) + "CA/C"*"WFS/FA"*Age*(-0.0347902) + "CA/C"*"1000SP/C"*86.188 + "CA/C"*"1000SP/C"*Age^(-1)*4.52011 + "CA/C"*"1000SP/C"^2*(-0.0429631) + "CA/C"*Age*0.796254 + "CA/C"*Age^2*4.37538e-05 + "CA/C"*Age^(-2)*(-184.864) + "CA/C"^2*"FA/TA"*(-30.124) + "CA/C"^2*"FA/TA"^(-1)*(-12.9877) + "CA/C"^2*"WFS/FA"*9.36123 + "CA/C"^2*"1000SP/C"*(-9.76699) (15)

E_WFS = 19.6635 + "W/C"^(-1)*"CA/C"*(-9.48673) + "W/C"^(-1)*"FA/TA"^2*(-198.68) + "W/C"^(-2)*12.8252 + "CA/C"*"1000SP/C"*(-29.8099) + "CA/C"*"1000SP/C"^2*0.0246579 + "CA/C"^2*26.3164 + "CA/C"^2*"FA/TA"*10.461 + "CA/C"^2*"1000SP/C"*7.43021 + "CA/C"^3*(-7.58171) + "CA/C"^(-1)*"FA/TA"*(-489.077) + "CA/C"^(-1)*"FA/TA"*"WFS/FA"*(-77.1434) + "CA/C"^(-1)*"FA/TA"*"1000SP/C"*116.25 + "CA/C"^(-1)*"FA/TA"^2*1359.21 + "CA/C"^(-1)*"FA/TA"^(-1)*"1000SP/C"*6.77477 (16)

STS_WFS = 10.9142 + "WFS/C"*"CA/C"^(-2)*3.14175 + "W/C"^(-2)*Age*(-0.00385172) + "W/C"^(-2)*Age^(-1)*(-1.718) + "W/C"^(-3)*0.0710875 + "CA/C"*(-2.00363) + "CA/C"*"FA/TA"*"WFS/FA"*1.01286 + "CA/C"*"FA/TA"*"1000SP/C"*18.3634 + "CA/C"*"FA/TA"*Age*0.0755048 + "CA/C"*"FA/TA"*Age^(-1)*1.49366 + "CA/C"*"FA/TA"^2*1.20013 + "CA/C"*"FA/TA"^(-1)*"1000SP/C"*(-0.0787705) + "CA/C"*"FA/TA"^(-1)*Age*(-0.00699899) + "CA/C"*"FA/TA"^(-1)*Age^(-1)*(-0.120925) + "CA/C"*"FA/TA"^(-2)*0.0137339 + "CA/C"*"WFS/FA"*"1000SP/C"*(-0.157937) + "CA/C"*"WFS/FA"*Age*0.0257611 + "CA/C"*"WFS/FA"*Age^(-1)*1.66632 + "CA/C"*"1000SP/C"*(-17.0813) + "CA/C"*"1000SP/C"*Age*3.47694e-05 + "CA/C"*"1000SP/C"*Age^(-1)*0.103497 + "CA/C"*"1000SP/C"^2*0.0166741 + "CA/C"*Age*0.0534488 + "CA/C"*Age^2*(-2.23536e-05) + "CA/C"^2*(-0.277902) + "CA/C"^2*"FA/TA"*0.489598 + "CA/C"^2*"1000SP/C"*2.32653 + "CA/C"^2*Age*(-0.00232576) + "CA/C"^(-1)*"FA/TA"*"1000SP/C"*210.071 + "CA/C"^(-1)*"FA/TA"*Age*0.357452 + "CA/C"^(-1)*"FA/TA"^(-1)*"WFS/FA"*(-0.449399) + "CA/C"^(-1)*"FA/TA"^(-1)*"1000SP/C"*0.718041 + "CA/C"^(-1)*"FA/TA"^(-1)*Age*0.0360948 + "CA/C"^(-1)*"FA/TA"^(-1)*Age^(-1)*(-4.00645) + "CA/C"^(-1)*"WFS/FA"*Age*(-0.185519) + "CA/C"^(-1)*"1000SP/C"*234.101 + "CA/C"^(-1)*"1000SP/C"^2*(-0.504111) + "CA/C"^(-1)*Age*(-0.359478) + "CA/C"^(-1)*Age^2*0.000193364 + "CA/C"^(-2)*(-14.616) + "CA/C"^(-2)*"1000SP/C"*(-404.023) + "CA/C"^(-2)*Age*0.598915 + "FA/TA"*"WFS/FA"*Age*(-0.0796514) + "FA/TA"*"1000SP/C"*(-132.347) + "FA/TA"*"1000SP/C"^2*0.260353 + "FA/TA"*Age*(-0.478727) + "FA/TA"*Age^(-2)*20.3695 (17)

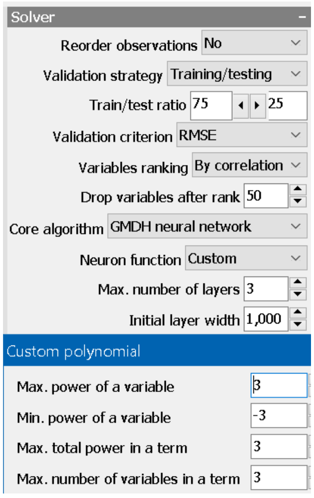


**Figure 9. The considered hyper-parameters of (GMDH-NN) model**

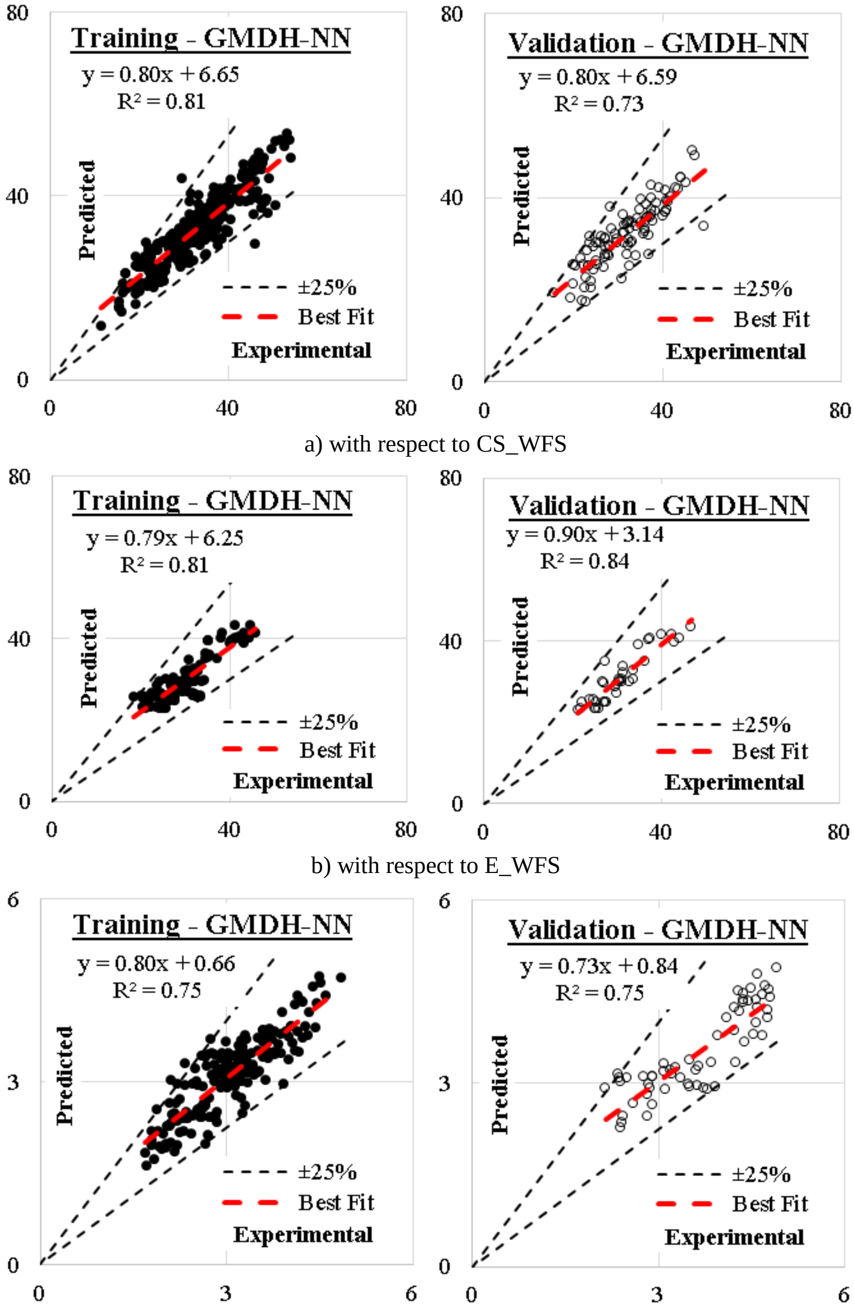


a) with respect to CS_WFS

b) with respect to E_WFS

c) with respect to STS_WFS

**Figure 10. Relation between predicted and calculated strength using (GMDH-NN)**

### 4.2. KNN WFS Cement Concrete Strength Models

The kNN model developed for predicting the strength properties of waste foundry sand (WFS) cement concrete was configured with the following hyperparameters: one neighbor, Euclidean distance metric, and distance-based weighting, as shown in Figure 11.

For the **compressive strength model**, the kNN achieved:

- $R^2 = 0.96$, indicating that 96% of the variance in compressive strength is explained by the model.
- Accuracy = 0.955, demonstrating high reliability, with an average deviation of only 4.5% from the actual values.
- RMSE = 1.5, MSE = 2.25, MAE = 1.3, and SSE = 425, all suggesting minimal prediction errors.

**Implications:** The kNN model effectively captures the nonlinear relationships present in the compressive strength data. Utilizing a single neighbor combined with distance-based weighting helps the model avoid overfitting while maintaining high precision.

For the **elastic modulus model**, the kNN achieved:

- $R^2 = 0.96$, matching the performance of the compressive strength model.
- Accuracy = 0.95, with an Error of 0.05, indicating excellent predictive capability, though slightly lower than that of the compressive strength model.
- RMSE = 1.5, MSE = 2.15, MAE = 1.2, and SSE = 156.5, confirming low prediction errors.

**Implications:** The model accurately captures the factors affecting elastic modulus and delivers near-perfect predictions. The Euclidean metric and distance-based weighting scheme effectively preserve precision in elastic modulus estimations.

For the **splitting tensile strength model**, the kNN achieved:

- $R^2 = 0.96$, consistent with the other models.
- Accuracy = 0.955, with an Error of 0.045, highlighting the model's strong reliability.
- RMSE = 0.15, MSE = 0.0, MAE = 0.1, and SSE = 3, indicating extremely low errors, which is consistent with the smaller scale of tensile strength values.

**Implications:** The kNN model performs exceptionally well in predicting splitting tensile strength, with negligible errors for practical applications. The high $R^2$ and minimal SSE suggest that the model successfully captures critical interactions influencing tensile strength.

**Strengths of the kNN Model:**

- **High Accuracy:** $R^2$ values of 0.96 across all three strength properties demonstrate excellent predictive capability.
- **Low Errors:** Metrics such as RMSE, MSE, MAE, and SSE are all minimal, highlighting the model's precision.
- **Simplicity:** The kNN algorithm is easy to implement and requires minimal parameter tuning.
- **Effective Weighting:** Distance-based weighting ensures that closer, more relevant data points exert greater influence on predictions, effectively capturing complex relationships in the data.

**Considerations for Improvement:**

- Using k = 1 can make the model sensitive to noise or outliers. Increasing k slightly (e.g., to 3 or 5) could improve stability without significantly compromising accuracy.
- For larger datasets, kNN can become computationally expensive due to distance calculations for each prediction. Alternative methods like Random Forests may offer better scalability.
- kNN models may struggle to generalize well to unseen data if the dataset is small. Applying cross-validation or expanding the training set can help mitigate this limitation.

While the GMDH-NN model performed well ($R^2$ ranging from 0.75 to 0.825), the kNN model significantly outperforms it in terms of $R^2$, accuracy, and error metrics. In particular, kNN achieves superior generalization and precision, especially for predicting compressive strength and elastic modulus. Compared to Random Forests, kNN delivers comparable or even better performance in this study, although Random Forests may be more robust when dealing with noisy data or large feature sets.

Overall, the kNN model demonstrates exceptional performance in predicting the compressive strength, elastic modulus, and splitting tensile strength of WFS cement concrete. With high $R^2$ values, accuracy exceeding 95%, and minimal errors, it serves as a reliable and precise tool for these applications. Further improvements could be achieved by fine-tuning the number of neighbors and exploring alternative distance metrics to enhance the model's robustness and scalability (see Figure 12 for detailed results).

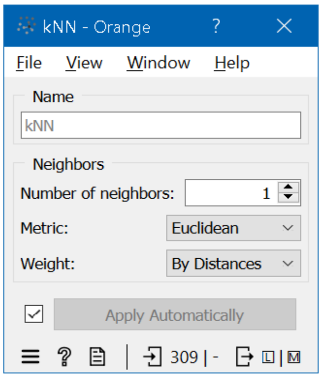


**Figure 11. The considered hyper-parameters of (KNN) model**

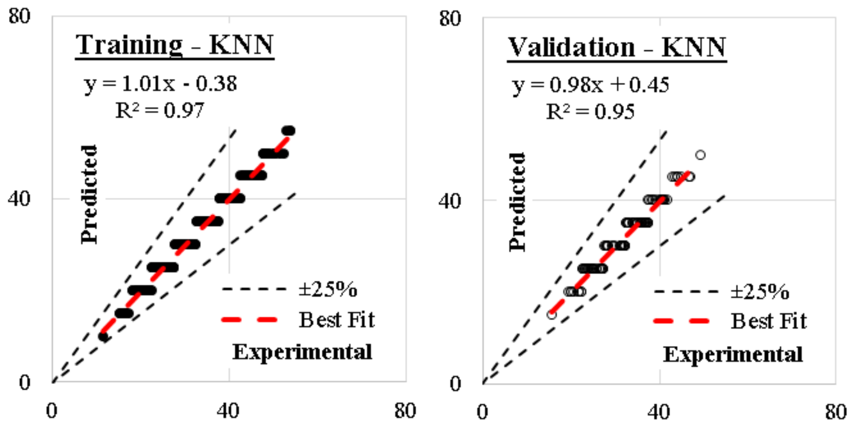


a) With respect to CS_WFS

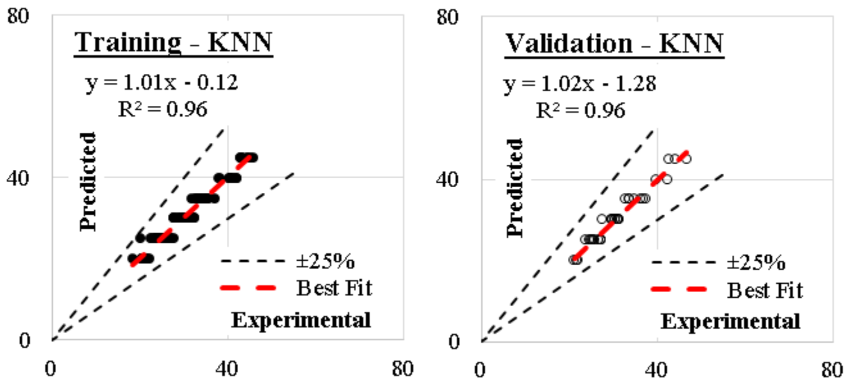


b) With respect to E_WFS

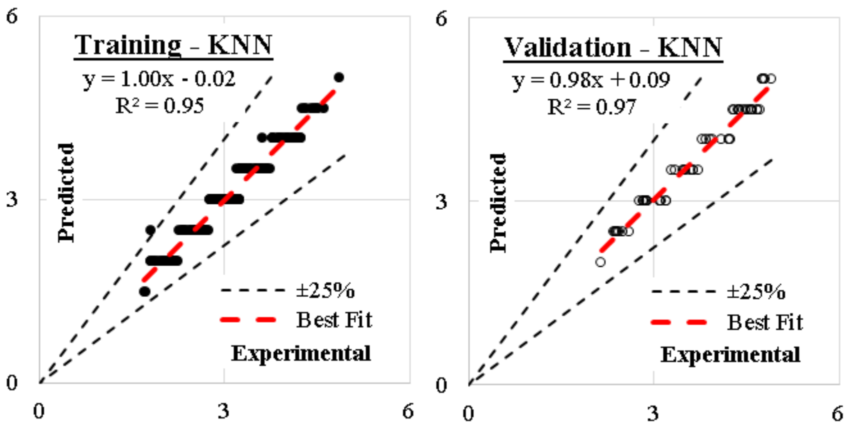


c) With respect to STS_WFS

**Figure 12. Relation between predicted and calculated strength using (KNN)**

### 4.3. SVM WFS Cement Concrete Strength Models

The Support Vector Machine (SVM) model developed for predicting the strength properties of waste foundry sand (WFS) cement concrete was configured with the following hyperparameters: cost (C) of 100.00, regression loss epsilon of 0.10, a polynomial kernel, and a numerical tolerance of 1.0000, as shown in Figure 13.

For the **compressive strength model**, the SVM achieved:

- $R^2 = 0.96$, indicating that 96% of the variance in compressive strength is explained by the model.
- Accuracy = 0.93, with an average error of 5% between predicted and actual values.
- RMSE = 1.55, MSE = 2.5, MAE = 1.35, and SSE = 484.5, suggesting minimal prediction errors.

**Implications:** The model effectively captures complex nonlinear relationships affecting compressive strength. The high C value prioritizes precision in fitting the training data, though it may reduce generalization capacity.

For the **elastic modulus model**, the SVM achieved:

- $R^2 = 0.955$, slightly lower than the compressive strength model but still excellent.
- Accuracy = 0.93, with an Error of 0.05, indicating robust predictive capability.
- RMSE = 1.55, MSE = 2.45, MAE = 1.25, and SSE = 188, reflecting low prediction errors.

**Implications:** The SVM handles elastic modulus prediction with high reliability, capturing nonlinear relationships effectively. The polynomial kernel contributes to strong generalization for elastic modulus dependencies.

For the **splitting tensile strength model**, the SVM achieved:

- $R^2 = 0.935$, slightly lower than the other models but still demonstrating strong performance.
- Accuracy = 0.92, with an Error of 0.05, highlighting consistent and reliable predictions.
- RMSE = 0.2, MSE = 0.05, MAE = 0.15, and SSE = 5, indicating very small prediction errors, consistent with the smaller magnitude of tensile strength values.

**Implications:** The model predicts splitting tensile strength with high accuracy, although its performance is slightly lower than for compressive strength and elastic modulus. The minimal SSE confirms negligible cumulative error across the dataset.

**Strengths of the SVM Model:**

- **High Predictive Performance:** $R^2$ values above 0.93 across all models reflect the SVM's capability to model nonlinear relationships accurately.
- **Robustness:** Similar RMSE, MAE, and accuracy metrics across different strength properties indicate consistent model behavior.
- **Polynomial Kernel Effectiveness:** Captures complex interactions between input variables, enhancing prediction precision.

**Considerations for Improvement:**

- The high C value (100.00) may increase the risk of overfitting, especially with smaller or noisier datasets. Reducing C (e.g., to 10 or 50) might improve generalization without sacrificing much accuracy.
- Exploring alternative kernels, such as the radial basis function (RBF), could further enhance performance for specific strength properties.
- SVMs with polynomial kernels and high C values can become computationally intensive for large datasets. Simplifying the kernel choice or adjusting numerical tolerance could reduce training time.
- While the model achieves high accuracy (93–95%), slight improvements may be possible through enhanced feature engineering or incorporating additional variables (e.g., curing conditions, admixtures).

In comparison, the SVM model achieves similar $R^2$ values to kNN (approximately 0.96) but slightly lower accuracy (93–95% vs. 95–96% for kNN). Although SVM offers greater flexibility in handling nonlinear relationships, it is more computationally demanding. Nevertheless, SVM significantly outperforms the GMDH-NN model ($R^2 = 0.75$–$0.825$) across all metrics, making it a superior choice for precision and reliability. SVM also offers comparable performance to Random Forests, with the polynomial kernel potentially better capturing specific nonlinearities in the data, depending on the strength property in question.

Overall, the SVM model demonstrates excellent predictive performance for the compressive strength, elastic modulus, and splitting tensile strength of WFS cement concrete. With $R^2$ values exceeding 0.93 and consistently high accuracy, it serves as a reliable and precise tool for these applications. Fine-tuning the model's hyperparameters and exploring alternative kernels could further optimize its performance (see Figure 14 for detailed results).

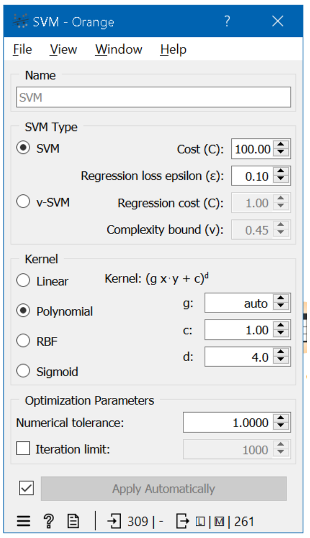


**Figure 13. The considered hyper-parameters of (SVM) model**

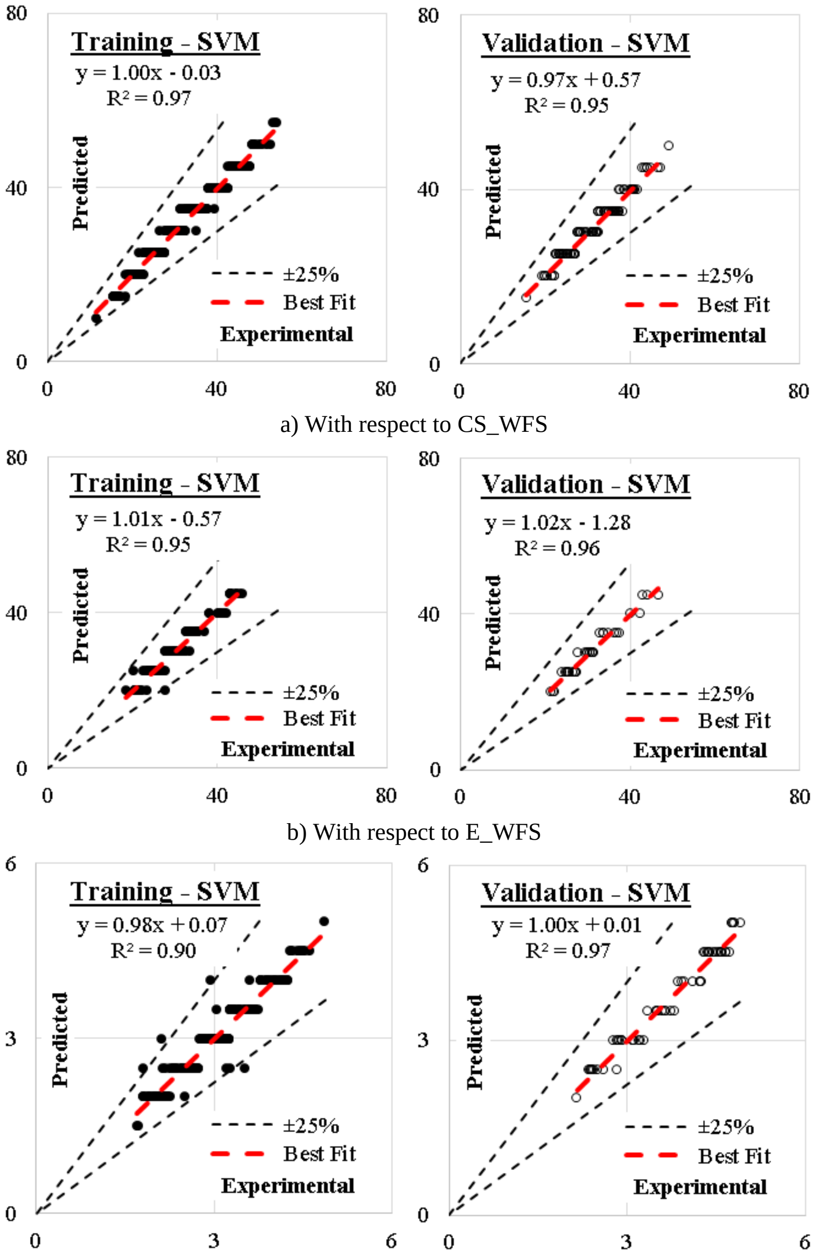


**Figure 14. Relation between predicted and calculated strength using (SVM)**

### 4.4. Tree WFS Cement Concrete Strength Models

The Decision Tree model developed for predicting the strength properties of waste foundry sand (WFS) cement concrete was configured with the following hyperparameters: a minimum of 1 instance in each leaf, prohibition of splitting subsets smaller than 1, a maximum tree depth of 8, and a stopping criterion requiring that splitting ceases when 95% of a subset belongs to the same class or range, as illustrated in Figures 15 and 16.

For the **compressive strength model**, the Decision Tree achieved:

- $R^2 = 0.87$, indicating that 87% of the variance in compressive strength is explained by the model.
- Accuracy = 0.91, which is reasonable but lower than that achieved by other models like SVM or kNN.
- RMSE = 2.95, MSE = 8.75, MAE = 1.95, and SSE = 1524.5, reflecting moderate prediction errors.

**Implications:** The model shows some difficulty fully capturing the complex nonlinear relationships governing compressive strength. While the limited tree depth of 8 helps avoid overfitting, it also constrains the model's capacity for precision.

For the **elastic modulus model**, the Decision Tree achieved:

- $R^2 = 0.96$, demonstrating excellent predictive performance.
- Accuracy = 0.95, with an Error of 0.05, indicating reliable predictions consistent with high-performing models like kNN and SVM.
- RMSE = 1.55, MSE = 2.35, MAE = 1.25, and SSE = 164, confirming low prediction errors.

**Implications:** The model handles elastic modulus predictions very effectively. The stopping criteria and controlled tree depth help maintain a good balance between model complexity and predictive accuracy for this property.

For the **splitting tensile strength model**, the Decision Tree achieved:

- $R^2 = 0.845$, slightly lower than for the compressive strength model but still acceptable.
- Accuracy = 0.915, with an Error of 0.085, indicating moderate reliability.
- RMSE = 0.3, MSE = 0.05, MAE = 0.15, and SSE = 14.5, reflecting minimal prediction errors, consistent with the smaller magnitude of tensile strength values.

**Implications:** The model performs well for splitting tensile strength, though further hyperparameter tuning may enhance its performance.

**Strengths of the Decision Tree Model:**

- **Interpretability:** Decision Trees are inherently transparent, allowing clear identification of how input variables influence predictions.
- **Strong Performance for Elastic Modulus:** The model performs exceptionally well for elastic modulus, achieving $R^2 = 0.96$ with minimal errors.
- **Controlled Complexity:** The imposed limits on tree depth and subset splitting help prevent overfitting while maintaining reasonable accuracy.

**Limitations and Considerations:**

- **Weaker Performance for Compressive and Tensile Strength:** While the $R^2$ values for compressive (0.87) and tensile strength (0.845) are reasonable, they fall short of the performance achieved by SVM and kNN. Increasing the maximum tree depth (e.g., to 10) or relaxing the stopping criterion (e.g., majority at 90%) could potentially improve predictions.
- **High Sensitivity to Hyperparameters:** The model's performance heavily depends on parameters like tree depth and leaf size. Techniques such as cross-validation and grid search can be valuable for optimization.
- **Risk of Overfitting with Small Leaves:** Setting the minimum leaf size to 1 instance increases the risk of fitting noise, especially in smaller datasets. Raising this to 2–5 instances may enhance generalization.

Compared to kNN ($R^2 = 0.96$), the Decision Tree underperforms in predicting compressive and tensile strength but matches kNN's performance for elastic modulus. SVM consistently outperforms the Decision Tree across all properties, offering higher $R^2$ values, greater accuracy, and lower RMSE. Random Forests typically surpass single decision trees by aggregating multiple trees, which reduces variance and increases robustness. If computational resources allow, transitioning to Random Forests would be a superior option.

Overall, the Decision Tree model performs well for elastic modulus predictions ($R^2 = 0.96$) and reasonably for compressive strength ($R^2 = 0.87$) and splitting tensile strength ($R^2 = 0.845$). However, it lags behind advanced models like SVM and kNN in terms of predictive accuracy and power. Fine-tuning hyperparameters or moving toward ensemble methods like Random Forests could significantly improve performance (see Figure 17 for detailed results).

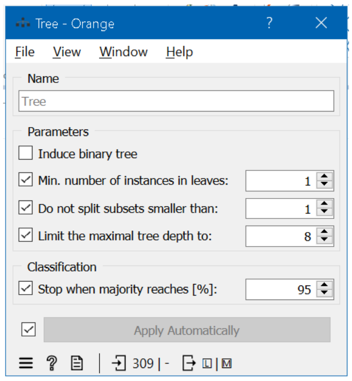


**Figure 15. The considered hyper-parameters of (Tree) model**

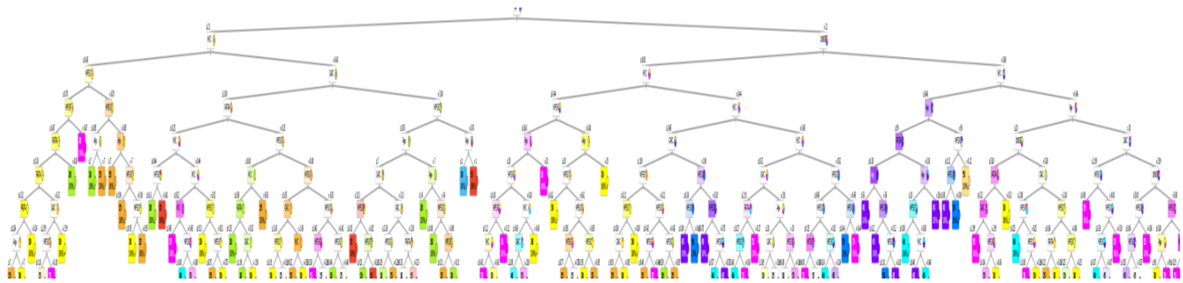

a) With respect to CS_WFS

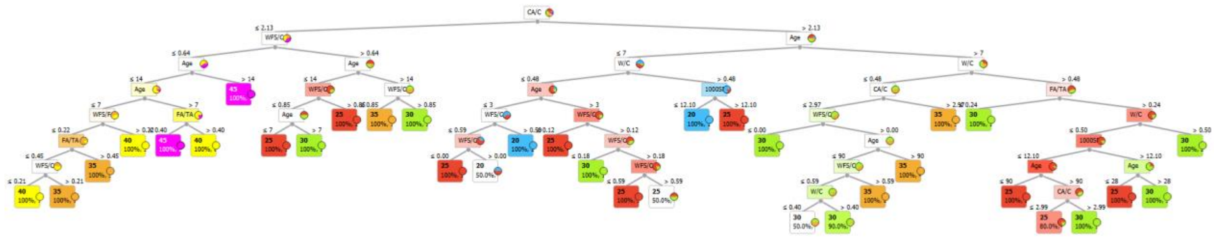

b) With respect to E_WFS

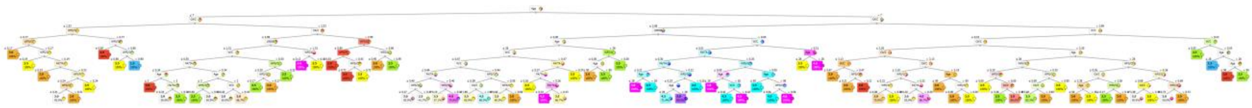

c) With respect to STS_WFS

**Figure 16. The layout of the developed (Tree) model**

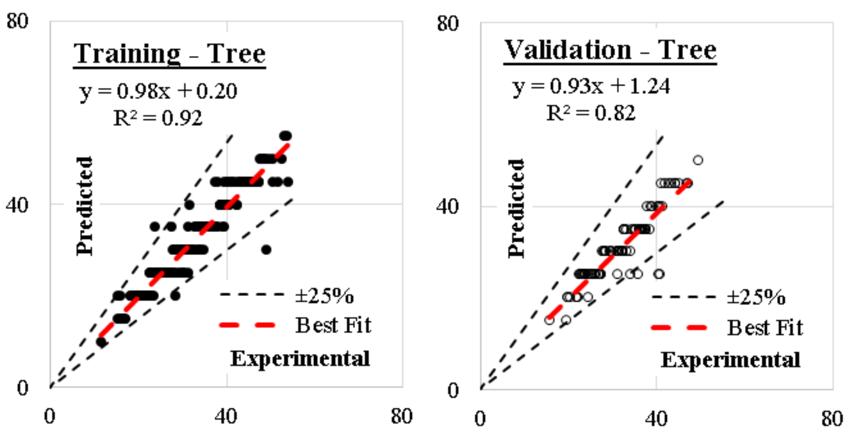


a) With respect to CS_WFS

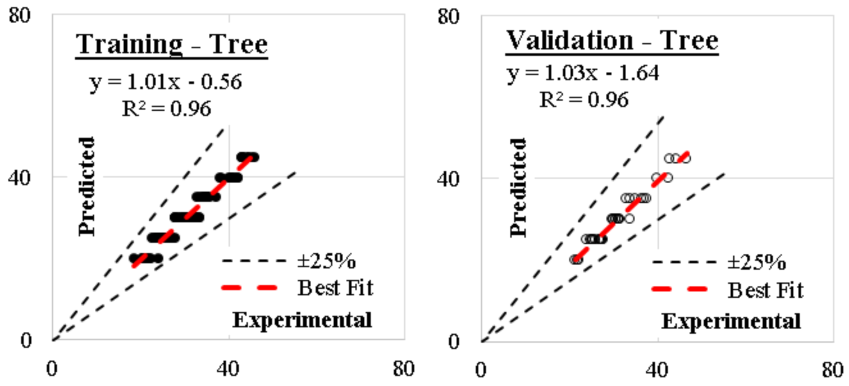


b) With respect to E_WFS

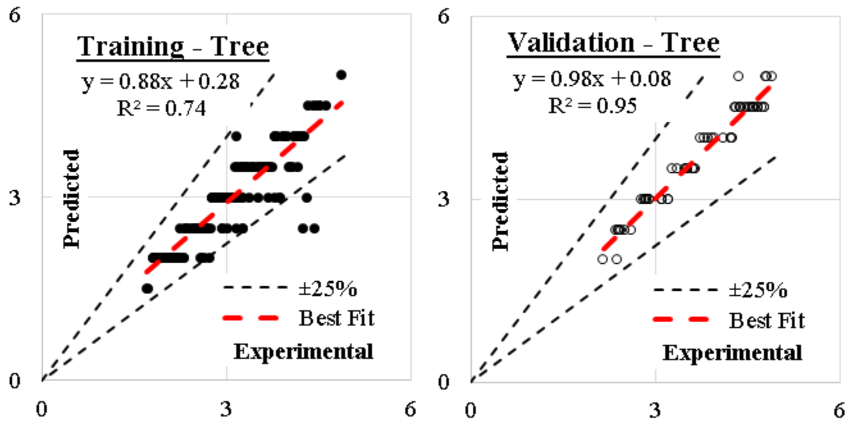


c) With respect to STS_WFS

**Figure 17. Relation between predicted and calculated strength using (Tree)**

### 4.5. RF WFS Cement Concrete Strength Models

The Random Forest (RF) model developed for predicting the strength properties of waste foundry sand (WFS) cement concrete was configured with the following hyperparameters: eight trees, two attributes considered at each split, a maximum tree depth of eight, and a minimum subset size of two for splitting, as shown in Figures 18 and 19.

For the **compressive strength model**, the RF achieved:

- $R^2$ = 0.94, indicating that 94% of the variance in compressive strength is explained by the model.
- Accuracy = 0.94, with an Error of 0.06, reflecting high reliability and low prediction errors.
- RMSE = 2.0, MSE = 8.05, MAE = 1.55, and SSE = 945, suggesting precise predictions with minimal deviations.

**Implications:** The RF model effectively balances bias and variance, capturing the nonlinear relationships influencing compressive strength. Increasing the number of trees could potentially enhance performance further.

For the **elastic modulus model**, the RF achieved:

- $R^2$ = 0.935, demonstrating strong predictive capability and explaining 93.5% of the variance.
- Accuracy = 0.94, with an Error of 0.06, indicating consistently reliable predictions.
- RMSE = 1.85, MSE = 2.5, MAE = 1.35, and SSE = 216.5, confirming low prediction errors, slightly lower than those for compressive strength.

**Implications:** The RF model captures elastic modulus behavior well and performs comparably to SVM and kNN. Limiting tree depth helps prevent overfitting while maintaining strong accuracy.

For the **splitting tensile strength model**, the RF achieved:

- $R^2$ = 0.92, indicating slightly lower predictive performance compared to compressive strength and elastic modulus.
- Accuracy = 0.94, with an Error of 0.06, showing reliable predictions with minimal error.
- RMSE = 0.05, MAE = 0.15, and SSE = 6, reflecting very low prediction errors consistent with the smaller range of tensile strength values.

**Implications:** The RF model performs well for splitting tensile strength but slightly less effectively than for the other two properties.

**Strengths of the RF Model:**

- **High Predictive Performance:** $R^2$ values ranging from 0.92 to 0.94 demonstrate RF's strong ability to model complex, nonlinear relationships in concrete strength properties.
- **Low Errors:** Consistently low RMSE, MAE, and SSE values confirm the model's reliability and precision.
- **Good Generalization:** Limiting tree depth and the number of attributes per split improves generalization without sacrificing accuracy.
- **Variance Reduction:** Combining multiple decision trees reduces prediction variance, enhancing model stability.

**Considerations for Improvement:**

- Using only eight trees may limit ensemble diversity and predictive power. Increasing the number of trees to 50–100 could further stabilize and improve predictions.
- While a tree depth of eight balances bias and variance, experimenting with deeper trees (e.g., depth = 10) might improve performance for splitting tensile strength.
- Conducting feature importance analysis could identify key variables, allowing for more targeted and efficient modeling.
- RF models with larger ensembles and deeper trees can increase training time, requiring sufficient computational resources.

In comparison, RF achieves comparable $R^2$ values (0.92–0.94) but often exhibits lower errors and better robustness due to ensemble averaging. Although SVM slightly outperforms RF for elastic modulus prediction ($R^2$ = 0.955), the two models perform similarly for compressive and tensile strength. RF consistently surpasses standalone decision trees by reducing variance and enhancing generalization. It significantly outperforms the GMDH-NN model ($R^2$ = 0.75–0.825), making it a stronger choice for modeling concrete strength properties.

Overall, the RF model demonstrates excellent performance in predicting the compressive strength, elastic modulus, and splitting tensile strength of WFS cement concrete. With $R^2$ values exceeding 0.92 and consistently low error metrics across all properties, it stands as a robust and reliable tool for this application. Nonetheless, increasing the number of trees and fine-tuning the tree depth could further enhance its predictive capabilities (see Figure 20 for detailed results).

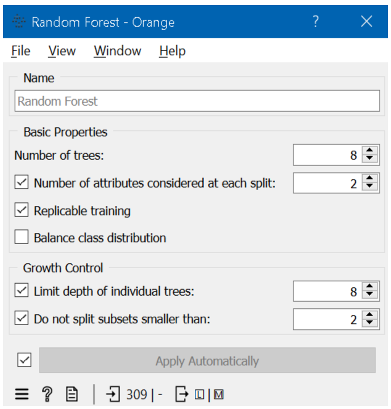


**Figure 18. The considered hyper-parameters of (RF) model**

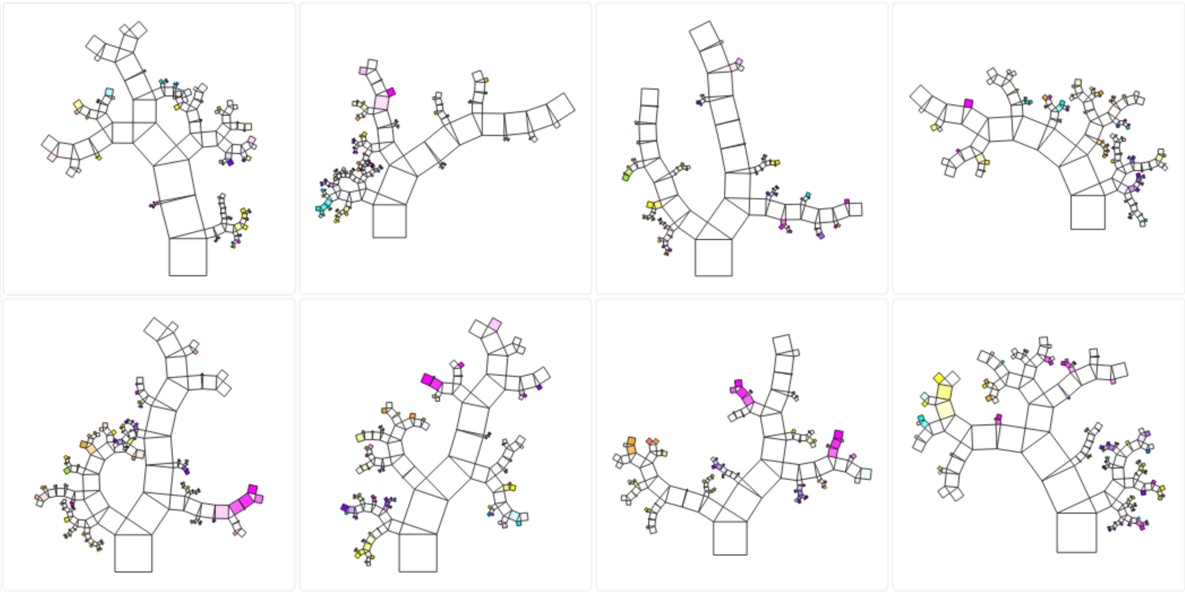

a) With respect to CS_WFS

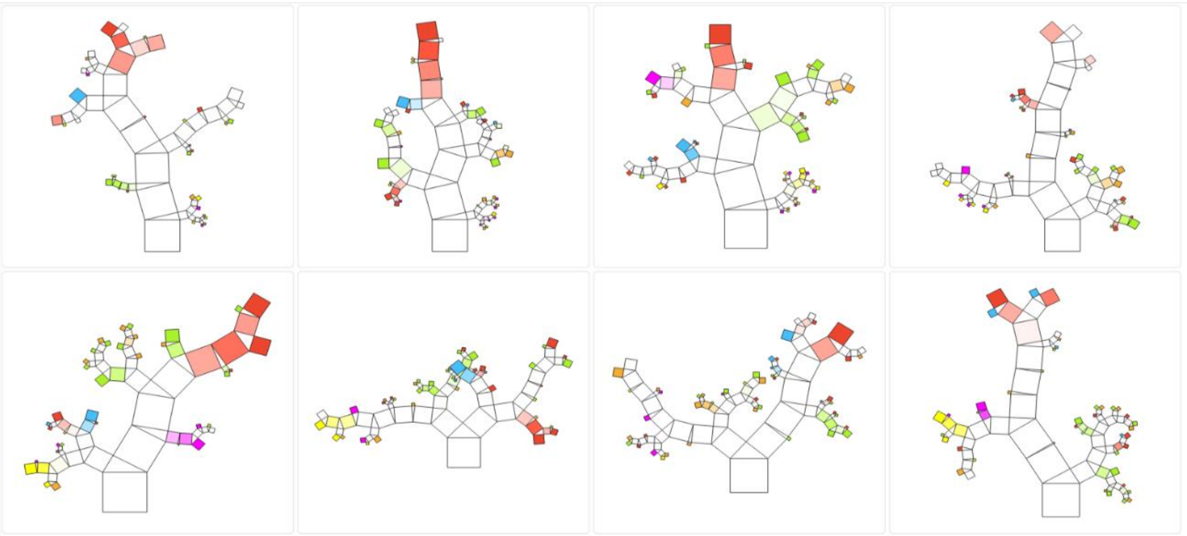

b) With respect to E_WFS

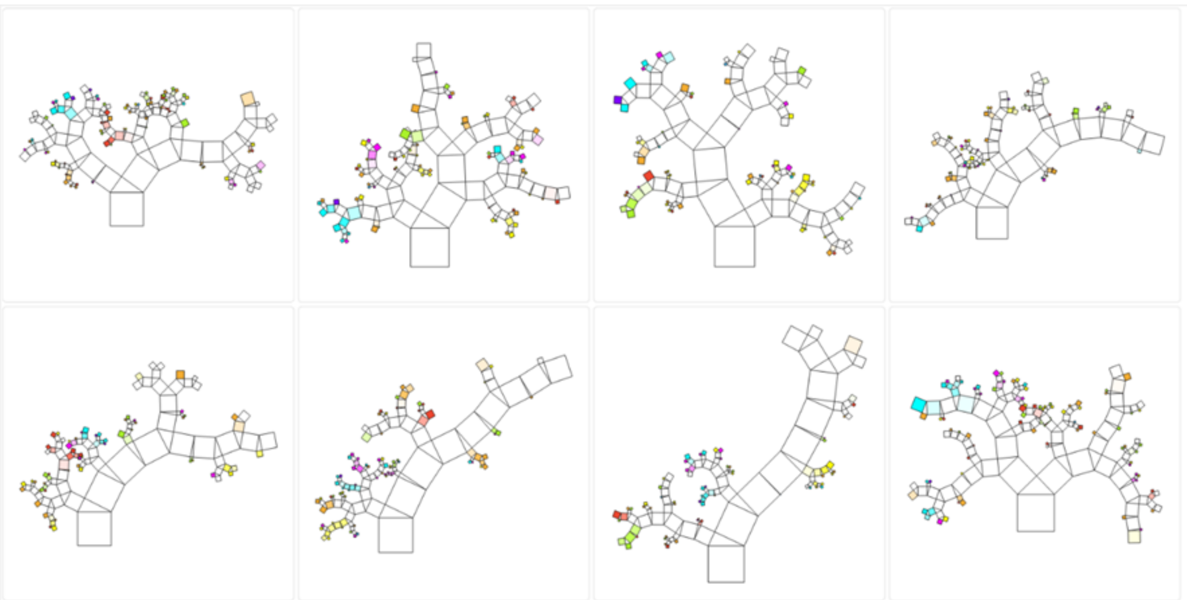

c) With respect to STS_WFS

**Figure 19. Pythagorean Forest diagram for the developed (RF) models**

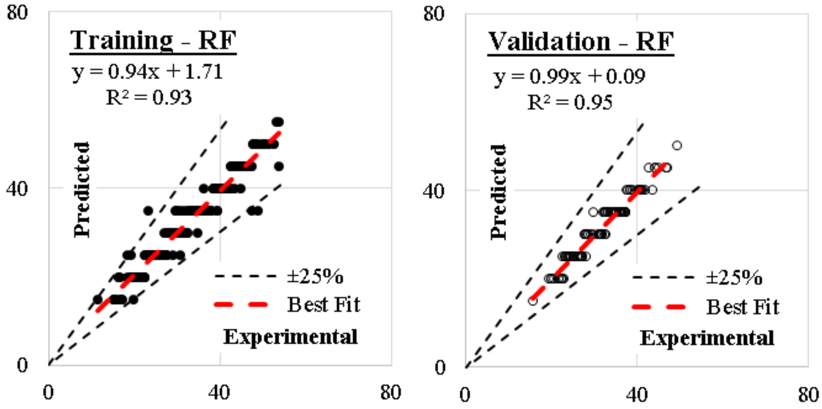


a) With respect to CS_WFS

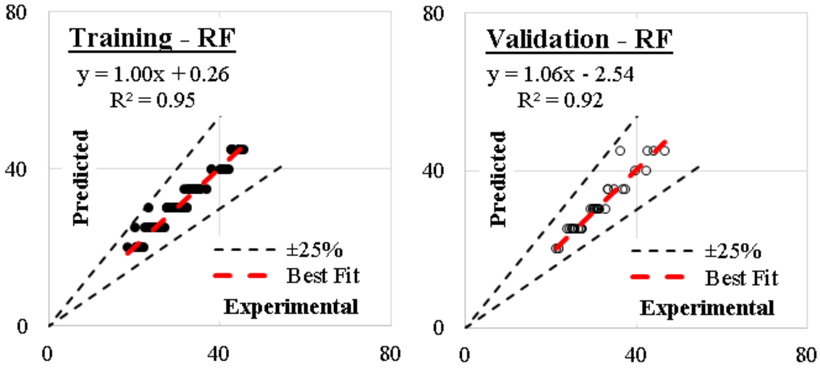


b) With respect to E_WFS

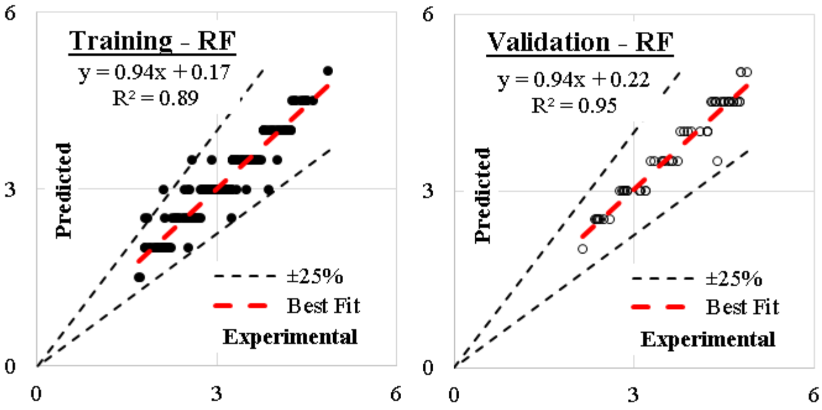


c) With respect to STS_WFS

**Figure 20. Relation between predicted and calculated strength using (RF)**

Overall, the predictive models developed for WFS cement concrete—such as Random Forest (RF), Support Vector Machine (SVM), and k-Nearest Neighbors (kNN)—demonstrate significant potential for driving the industrial adoption of sustainable, green concrete. Quantitative comparisons revealed that kNN, SVM, and RF consistently outperformed other models across all strength parameters. For instance, during the validation phase for compressive strength prediction, kNN and SVM achieved RMSE values of 1.6 MPa and $R^2$ values of 0.95, significantly surpassing the performance of the GMDH-NN and Decision Tree models. Similarly, for elastic modulus and splitting tensile strength, these top-performing models recorded lower MAE and RMSE values, with $R^2$ values reaching up to 0.97 in validation datasets. These statistical metrics provide a robust foundation for concluding the superior performance of kNN, SVM, and RF in predicting the mechanical behavior of concrete containing waste foundry sand. The use of multiple quantitative indicators enhances the reliability of model evaluations and reinforces the study's findings.

These predictive models play a crucial role in optimizing material compositions, improving performance, and minimizing environmental impacts. Below is an analysis of their industrial applications:

- **High Accuracy in Predicting Critical Properties:** The models reliably predict key properties such as compressive strength, elastic modulus, and splitting tensile strength, enabling precise material optimization.
- **Tailoring Material Composition:** They help adjust WFS content, cement ratios, and additives to meet specific structural and environmental requirements. Identifying optimal WFS proportions reduces dependence on costly virgin materials like cement and fine aggregates.

- **Sustainability and Cost Savings:** Sustainable utilization of WFS decreases waste disposal costs for foundries and promotes the circular economy by integrating industrial by-products into construction materials. Optimizing WFS content also lowers cement consumption, reducing $CO_2$ emissions from cement production and aiding compliance with green building standards like LEED or BREEAM.
- **Integration into Industrial Processes:** The models can be embedded into production systems to predict concrete properties using real-time input data, ensuring consistent quality and detecting suboptimal mix designs before production.
- **Standardization and Benchmarking:** Reliable predictions provide benchmarks for incorporating WFS concrete into construction standards and codes, promoting wider industry acceptance.
- **Enhanced Manufacturing Efficiency:** Predictive modeling supports the production of precast elements—such as blocks, panels, and tiles—with consistent strength and durability. It streamlines production by minimizing trial-and-error in mix design and is applicable to road pavements, bridges, and industrial flooring where sustainable materials are increasingly prioritized.
- **Structural Reliability:** Accurate predictions of mechanical properties help ensure compliance with structural requirements. Early identification of unsuitable mix designs reduces the risk of structural failures and enables simulations of different production scales, helping manufacturers evaluate feasibility before scaling operations.
- **Operational Efficiency and Cost Reduction:** Automating mix design and testing shortens production timelines and reduces effort. Optimized material usage and reduced waste contribute to lower manufacturing costs, supporting green construction practices and enabling producers to offer innovative, eco-friendly products aligned with global sustainability goals.

Despite these benefits, certain challenges remain. The composition of WFS varies significantly depending on its source, affecting consistency. Moreover, adopting alternative materials like WFS may face resistance due to a lack of standardized guidelines and industry familiarity. The adoption of predictive models for WFS cement concrete represents a significant advancement toward sustainable industrial practices. These models provide a solid foundation for optimizing material use, ensuring product quality, and achieving environmental targets. Industries leveraging these tools can produce eco-friendly, high-performance concrete while effectively managing waste and reducing their carbon footprint. A summary of the models is presented in Table 2, and a Taylor chart comparing the models is shown in Figure 21.

**Table 2. Performance measurements of developed models**

| Compressive Strength | | | | | | | | |
|---|---|---|---|---|---|---|---|---|
| **Model** | **Dataset** | **SSE** | **MAE** | **MSE** | **RMSE** | **Error** | **Accuracy** | **$R^2$** |
| - | - | - | **MPa** | **MPa** | **MPa** | **%** | **%** | - |
| GMDH-NN | Training | 4214 | 2.8 | 14.0 | 3.7 | 0.11 | 0.89 | 0.81 |
| | Validation | 1427 | 2.9 | 14.7 | 3.8 | 0.12 | 0.88 | 0.73 |
| KNN | Training | 610 | 1.2 | 2.0 | 1.4 | 0.04 | 0.96 | 0.97 |
| | Validation | 240 | 1.4 | 2.5 | 1.6 | 0.05 | 0.95 | 0.95 |
| SVM | Training | 718 | 1.3 | 2.4 | 1.5 | 0.05 | 0.95 | 0.97 |
| | Validation | 251 | 1.4 | 2.6 | 1.6 | 0.05 | 0.91 | 0.95 |
| Tree | Training | 1999 | 1.8 | 6.7 | 2.6 | 0.08 | 0.92 | 0.92 |
| | Validation | 1050 | 2.1 | 10.8 | 3.3 | 0.10 | 0.90 | 0.82 |
| RF | Training | 1593 | 1.6 | 5.3 | 2.3 | 0.07 | 0.93 | 0.93 |
| | Validation | 297 | 1.5 | 10.8 | 1.7 | 0.05 | 0.95 | 0.95 |
| **Elastic Modulus** | | | | | | | | |
| **Model** | **Dataset** | **SSE** | **MAE** | **MSE** | **RMSE** | **Error** | **Accuracy** | **$R^2$** |
| - | - | - | **GPa** | **GPa** | **GPa** | **%** | **%** | - |
| GMDH-NN | Training | 965 | 2.4 | 8.8 | 3.0 | 0.10 | 0.90 | 0.81 |
| | Validation | 236 | 2.1 | 6.5 | 2.6 | 0.08 | 0.92 | 0.84 |
| KNN | Training | 235 | 1.2 | 2.1 | 1.5 | 0.05 | 0.95 | 0.96 |
| | Validation | 78 | 1.2 | 2.2 | 1.5 | 0.05 | 0.95 | 0.96 |
| SVM | Training | 298 | 1.3 | 2.7 | 1.6 | 0.05 | 0.95 | 0.95 |
| | Validation | 78 | 1.2 | 2.2 | 1.5 | 0.05 | 0.91 | 0.96 |
| Tree | Training | 239 | 1.2 | 2.2 | 1.5 | 0.05 | 0.95 | 0.96 |
| | Validation | 89 | 1.3 | 2.5 | 1.6 | 0.05 | 0.95 | 0.96 |
| RF | Training | 275 | 1.2 | 2.5 | 1.6 | 0.05 | 0.95 | 0.95 |
| | Validation | 158 | 1.5 | 2.5 | 2.1 | 0.07 | 0.93 | 0.92 |

| Split Tensile Strength | | | | | | | | |
|---|---|---|---|---|---|---|---|---|
| **Model** | **Dataset** | **SSE** | **MAE** | **MSE** | **RMSE** | **Error** | **Accuracy** | **$R^2$** |
| - | - | - | **MPa** | **MPa** | **MPa** | **%** | **%** | |
| GMDH-NN | Training | 23 | 0.3 | 0.1 | 0.4 | 0.11 | 0.89 | 0.75 |
| | Validation | 11 | 0.3 | 0.2 | 0.4 | 0.12 | 0.88 | 0.75 |
| KNN | Training | 5 | 0.1 | 0.0 | 0.2 | 0.05 | 0.95 | 0.95 |
| | Validation | 1 | 0.1 | 0.0 | 0.1 | 0.04 | 0.96 | 0.97 |
| SVM | Training | 9 | 0.2 | 0.1 | 0.2 | 0.07 | 0.93 | 0.90 |
| | Validation | 1 | 0.1 | 0.0 | 0.2 | 0.04 | 0.91 | 0.97 |
| Tree | Training | 27 | 0.2 | 0.1 | 0.4 | 0.12 | 0.88 | 0.74 |
| | Validation | 2 | 0.1 | 0.0 | 0.2 | 0.05 | 0.95 | 0.95 |
| RF | Training | 10 | 0.2 | 0.1 | 0.2 | 0.07 | 0.93 | 0.89 |
| | Validation | 2 | 0.1 | 0.0 | 0.2 | 0.05 | 0.95 | 0.95 |

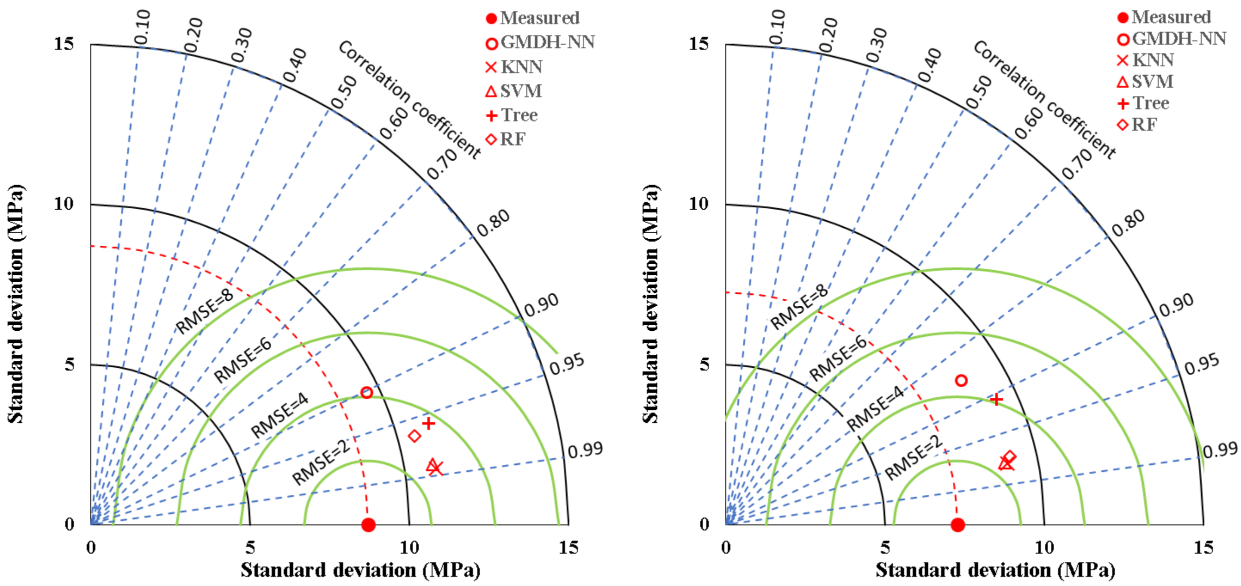


Training Validation

a) With respect to CS_WFS

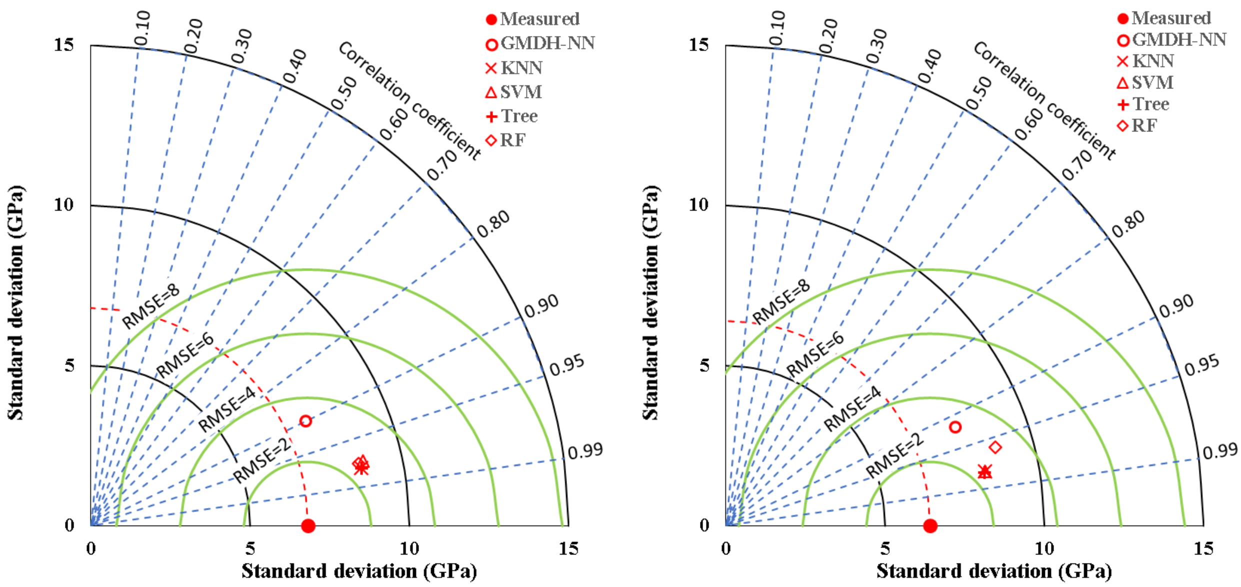


Training Validation

b) With respect to E_WFS

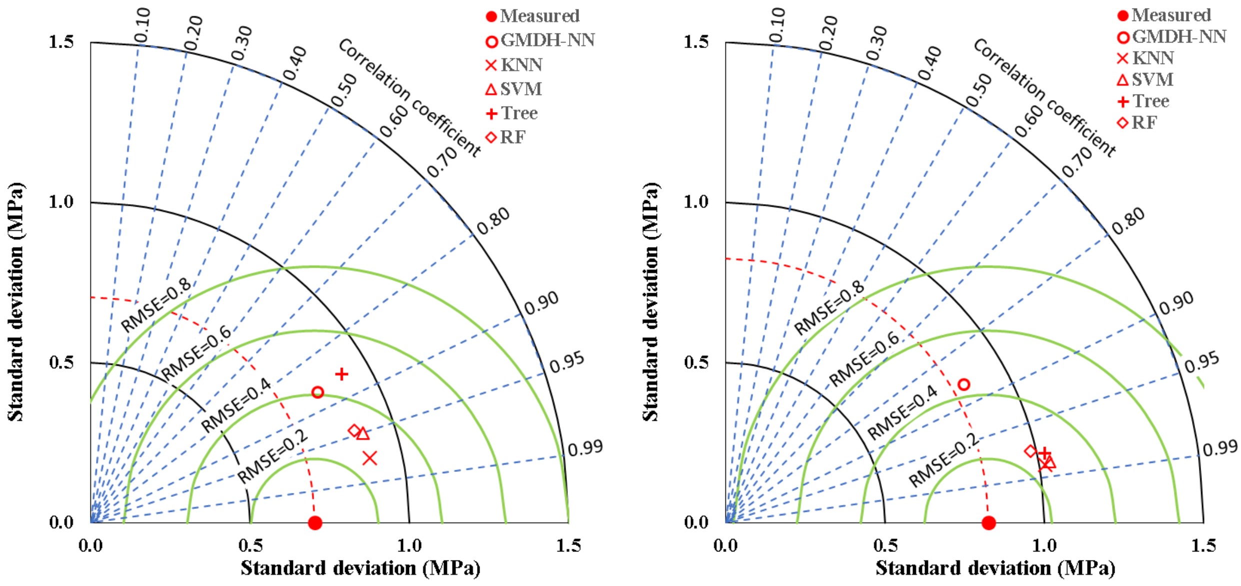


Training Validation

c) With respect to STS_WFS

**Figure 21. Comparing the accuracies of the developed models using Taylor charts**

The results presented in this study indicate that the applied machine learning models exhibit strong predictive performance across all three key mechanical properties—compressive strength, elastic modulus, and splitting tensile strength—when compared to models reported in existing literature. For instance, in the case of compressive strength prediction, the KNN and SVM models achieved $R^2$ values of 0.97 and 0.95, respectively, in both training and validation datasets, surpassing those reported by Behnood & Golafshani (2021) [13] and ALYousef et al. (2023) [18], whose models typically achieved $R^2$ values above 0.90 but focused only on individual parameters. Similarly, the present study's prediction of elastic modulus with models like KNN and Tree also yielded high $R^2$ values of up to 0.96 in validation, which are on par or better than those of prior works such as Iqbal et al. (2021) [14], who did not simultaneously predict multiple properties. For splitting tensile strength, KNN and SVM models again outperformed previously published models, with validation $R^2$ values reaching as high as 0.97 and accuracy above 95%. In terms of materials for concrete sustainability, this research strengthens the case for using waste foundry sand (WFS) as a viable partial replacement for fine aggregates by integrating multiple strength predictions into one framework. Unlike past studies that focused on a single property or lacked generalizability due to narrow modeling scope, the current models allow for more comprehensive material design and performance evaluation. The ability to reliably predict compressive, tensile, and elastic properties enables engineers to make informed decisions regarding WFS content in structural and non-structural applications, aligning with sustainable design goals. From a design perspective, this integrated modeling approach offers practical advantages over literature-reported single-objective models by allowing holistic optimization of concrete mixtures incorporating WFS. The accurate performance of all five ML models across multiple strength properties not only promotes confidence in WFS usage but also facilitates its practical implementation in green concrete applications, contributing directly to environmental and structural sustainability.

## 5. Conclusions

In this research paper, advanced machine learning models have been presented for the soft computing of the optimal waste foundry sand (WFS) content in concrete, focusing on strength properties to support sustainable green structures. Machine learning techniques such as **Group Method of Data Handling Neural Network (GMDH-NN), Support Vector Machine (SVM), k-Nearest Neighbors (kNN), Decision Tree (Tree),** and **Random Forest (RF)** were applied to a database comprising 397 records for compressive strength, 146 records for elastic modulus, and 242 records for split tensile strength.

Each record includes the following input parameters: C — Cement content (kg/m³), WFS — Waste foundry sand content (kg/m³), W — Water content (kg/m³), SP — Super-plasticizer content (kg/m³), CA — Coarse aggregates content (kg/m³), FA — Fine aggregates content (kg/m³), TA — Total aggregates content (kg/m³), and Age — The concrete age at testing (days). The output parameters are CS_WFS — Compressive strength of WFS concrete (MPa), E_WFS — Elastic modulus of WFS concrete (GPa), and STS_WFS — Split tensile strength of WFS concrete (MPa).

A 75/25 partitioning pattern for training and testing the database was employed following established guidelines. Finally, a sensitivity analysis was conducted. At the conclusion of the model evaluations, the following findings were established:

- There was internal consistency between the input and output parameters for all three strength properties, as confirmed by the preliminary Pearson analysis.
- kNN, SVM, and RF demonstrated superior performance and consistently outperformed the other models across all three strength properties of WFS cement concrete. Consequently, these models were selected as the primary tools for predicting compressive strength, elastic modulus, and splitting tensile strength in WFS cement concrete.
- Sensitivity analyses revealed that **Age, WFS/C, and CA/C** are the most influential factors for compressive strength; **Age, FA/TA, and W/C** are most impactful for elastic modulus; and **1000SP/C, WFS/C, and W/C** are the key factors influencing the splitting tensile strength of WFS cement concrete.
- Overall, these machine learning models provide a solid foundation for optimizing material usage, ensuring quality, and achieving environmental sustainability goals. Industries that adopt these tools can produce eco-friendly, high-performance concrete while simultaneously addressing waste management challenges and reducing their carbon footprint.

### 5.1. Research Limitations

Despite the encouraging results and valuable insights provided by this study, several limitations should be acknowledged to contextualize the scope and applicability of the findings. The most significant constraint is the relatively small dataset size for each strength category, which may limit the generalizability of the models to broader or more diverse concrete compositions. Additionally, the dataset reflects controlled laboratory conditions with limited environmental variability, which does not fully account for real-world factors such as fluctuating temperatures, varied mixing practices, and diverse curing environments commonly encountered in field applications. The absence of external validation using independent datasets also restricts the evaluation of the models' robustness beyond the collected data. Furthermore, while a train/test split of 75/25 was used to ensure a fair evaluation, the lack of k-fold cross-validation may limit the assessment of model performance across different data subsets. These limitations suggest that while the models show strong predictive potential, further work involving larger, more diverse datasets and real-world field validation is needed to strengthen their practical reliability and generalizability in sustainable concrete production.

### 5.2. Research Practical Application

The outcomes of this research offer significant practical relevance for the construction industry, particularly in advancing sustainable concrete production. By accurately predicting the compressive strength, elastic modulus, and splitting tensile strength of concrete incorporating waste foundry sand (WFS) through advanced machine learning models, this study provides a data-driven approach for optimizing material proportions and enhancing concrete performance. The models can assist engineers and material scientists in designing eco-friendly concrete mixes that reduce reliance on natural fine aggregates and promote the reuse of industrial byproducts. Construction firms can integrate these predictive tools into quality control systems to ensure consistency and performance while minimizing material wastage. Additionally, the application of such models supports regulatory compliance in green building standards and aids in achieving sustainability targets by lowering the environmental impact of concrete production through reduced landfill disposal and improved resource efficiency.

## 6. Declarations

### 6.1. Author Contributions

Conceptualization, N.U., K.M.V.V., and A.M.B.C.; methodology, N.U., M.M.C., and B.G.V.V.; software, M.M.C. and B.G.V.V.; validation, N.U., K.M.V.V., and A.M.B.C.; formal analysis, N.U.; investigation, N.U., K.M.V.V., A.M.B.C., M.M.C., and B.G.V.V.; data curation, N.U. and K.M.V.V.; writing—original draft preparation, N.U., K.M.V.V., A.M.B.C., M.M.C., and B.G.V.V.; writing—review and editing, N.U., K.M.V.V., A.M.B.C., M.M.C., and B.G.V.V.; visualization, N.U.; supervision, N.U. All authors have read and agreed to the published version of the manuscript.

### 6.2. Data Availability Statement

The data presented in this study are available on request from the corresponding author.

### 6.3. Funding

The authors received no financial support for the research, authorship, and/or publication of this article.

### 6.4. Conflicts of Interest

The authors declare no conflict of interest.

## 7. References


[1] Ahmadi, A. A., Arabbeiki, M., Ali, H. M., Goodarzi, M., & Safaei, M. R. (2020). Configuration and optimization of a minichannel using water–alumina nanofluid by non-dominated sorting genetic algorithm and response surface method. Nanomaterials, 10(5), 901. doi:10.3390/nano10050901.

[2] Chen, W., Jin, R., Xu, Y., Wanatowski, D., Li, B., Yan, L., Pan, Z., & Yang, Y. (2019). Adopting recycled aggregates as sustainable construction materials: A review of the scientific literature. Construction and Building Materials, 218, 483–496. doi:10.1016/j.conbuildmat.2019.05.130.

[3] Kurt, Z., Yilmaz, Y., Cakmak, T., & Ustabaş, I. (2023). A novel framework for strength prediction of geopolymer mortar: Renovative precursor effect. Journal of Building Engineering, 76, 107041. doi:10.1016/j.jobe.2023.107041.

[4] Lee, C. Y., Shon, J. G., & Park, J. S. (2022). An edge detection–based eGAN model for connectivity in ambient intelligence environments. Journal of Ambient Intelligence and Humanized Computing, 13(10), 4591–4600. doi:10.1007/s12652-021-03261-2.

[5] Raut, S. P., Ralegaonkar, R. V., & Mandavgane, S. A. (2011). Development of sustainable construction material using industrial and agricultural solid waste: A review of waste-create bricks. Construction and Building Materials, 25(10), 4037–4042. doi:10.1016/j.conbuildmat.2011.04.038.

[6] Khan, M. I., & Siddique, R. (2011). Utilization of silica fume in concrete: Review of durability properties. Resources, Conservation and Recycling, 57, 30–35. doi:10.1016/j.resconrec.2011.09.016.

[7] Hemalatha, T., & Ramaswamy, A. (2017). A review on fly ash characteristics – Towards promoting high volume utilization in developing sustainable concrete. Journal of Cleaner Production, 147, 546–559. doi:10.1016/j.jclepro.2017.01.114.

[8] Behnood, A., Behnood, V., Modiri Gharehveran, M., & Alyamac, K. E. (2017). Prediction of the compressive strength of normal and high-performance concretes using M5P model tree algorithm. Construction and Building Materials, 142, 199–207. doi:10.1016/j.conbuildmat.2017.03.061.

[9] Thomas, B. S. (2018). Green concrete partially comprised of rice husk ash as a supplementary cementitious material – A comprehensive review. Renewable and Sustainable Energy Reviews, 82, 3913–3923. doi:10.1016/j.rser.2017.10.081.

[10] Özbay, E., Erdemir, M., & Durmuş, H. I. (2016). Utilization and efficiency of ground granulated blast furnace slag on concrete properties - A review. Construction and Building Materials, 105, 423–434. doi:10.1016/j.conbuildmat.2015.12.153.

[11] Javed, M. F., Khan, M., Fawad, M., Alabduljabbar, H., Najeh, T., & Gamil, Y. (2024). Comparative analysis of various machine-learning algorithms to predict strength properties of sustainable green concrete containing waste foundry sand. Scientific Reports, 14(1), 14617. doi:10.1038/s41598-024-65255-2.

[12] Shah, M. I., Amin, M. N., Khan, K., Niazi, M. S. K., Aslam, F., Alyousef, R., Javed, M. F., & Mosavi, A. (2021). Performance evaluation of soft computing for modeling the strength properties of waste substitute green concrete. Sustainability (Switzerland), 13(5), 1–21. doi:10.3390/su13052867.

[13] Behnood, A., & Mohammadi Golafshani, E. (2021). Predicting the dynamic modulus of asphalt mixture using machine-learning techniques: An application of multi biogeography-based programming. Construction and Building Materials, 266, 120983. doi:10.1016/j.conbuildmat.2020.120983.

[14] Iqbal, M. F., Javed, M. F., Rauf, M., Azim, I., Ashraf, M., Yang, J., & Liu, Q. feng. (2021). Sustainable utilization of foundry waste: Forecasting mechanical properties of foundry sand based concrete using multi-expression programming. Science of the Total Environment, 780, 146524. doi:10.1016/j.scitotenv.2021.146524.

[15] Ghanizadeh, A. R., Tavana Amlashi, A., & Dessouky, S. (2023). A novel hybrid adaptive boosting approach for evaluating properties of sustainable materials: A case of concrete containing waste foundry sand. Journal of Building Engineering, 72, 106595. doi:10.1016/j.jobe.2023.106595.

[16] Ali, M., Khan, M. I., Masood, F., Alsulami, B. T., Bouallegue, B., Nawaz, R., & Fediuk, R. (2022). Central composite design application in the optimization of the effect of waste foundry sand on concrete properties using RSM. Structures, 46, 1581–1594. doi:10.1016/j.istruc.2022.11.013.

[17] Lahoti, M., Narang, P., Tan, K. H., & Yang, E. H. (2017). Mix design factors and strength prediction of metakaolin-based geopolymer. Ceramics International, 43(14), 11433–11441. doi:10.1016/j.ceramint.2017.06.006.

[18] Alyousef, R., Nassar, R. U. D., Khan, M., Arif, K., Fawad, M., Hassan, A. M., & Ghamry, N. A. (2023). Forecasting the strength characteristics of concrete incorporating waste foundry sand using advance machine algorithms including deep learning. Case Studies in Construction Materials, 19, 2459. doi:10.1016/j.cscm.2023.e02459.

[19] Musolf, A. M., Holzinger, E. R., Malley, J. D., & Bailey-Wilson, J. E. (2022). What makes a good prediction? Feature importance

and beginning to open the black box of machine learning in genetics. Human Genetics, 141(9), 1515–1528. doi:10.1007/s00439-021-02402-z.

[20] Ulloa, N., Zumba Novay, E. G., Albuja, M., & Mayorga, D. (2025). Modeling the Compressive Strength of Metakaolin-Based Self-Healing Geopolymer Concrete Using Machine Learning Models. Civil Engineering Journal (Iran), 11(4), 1596–1623. doi:10.28991/CEJ-2025-011-04-020.

[21] Saridemir, M. (2009). Prediction of compressive strength of concretes containing metakaolin and silica fume by artificial neural networks. Advances in Engineering Software, 40(5), 350–355. doi:10.1016/j.advengsoft.2008.05.002.

[22] Sharifi, Y., & Hosseinpour, M. (2020). A predictive model based ann for compressive strength assessment of the mortars containing metakaolin. Journal of Soft Computing in Civil Engineering, 4(2), 1–12. doi:10.22115/SCCE.2020.214444.1157.

[23] Zou, Z. M., Chang, D. H., Liu, H., & Xiao, Y. D. (2021). Current updates in machine learning in the prediction of therapeutic outcome of hepatocellular carcinoma: what should we know? Insights into Imaging, 12(1), 31. doi:10.1186/s13244-021-00977-9.

[24] Ebid, A. E., Deifalla, A. F., & Onyelowe, K. C. (2024). Data Utilization and Partitioning for Machine Learning Applications in Civil Engineering. Sustainable Civil Infrastructures, 87–100. doi:10.1007/978-3-031-70992-0_8.

[25] Hoffman, F. O., & Gardner, R. H. (1983). Evaluation of uncertainties in environmental radiological assessment models. Radiological assessments: a textbook on environmental dose assessment. U.S. Nuclear Regulatory Commission, Report No. NUREG/CR-3332.

[26] Onyelowe, K. C., Kontoni, D. P. N., Ebid, A. M., Dabbaghi, F., Soleymani, A., Jahangir, H., & Nehdi, M. L. (2022). Multi-Objective Optimization of Sustainable Concrete Containing Fly Ash Based on Environmental and Mechanical Considerations. Buildings, 12(7), 948. doi:10.3390/buildings12070948.

[27] Onyelowe, K. C., Ebid, A. M., Riofrio, A., Soleymani, A., Baykara, H., Kontoni, D. P. N., Mahdi, H. A., & Jahangir, H. (2022). Global warming potential-based life cycle assessment and optimization of the compressive strength of fly ash-silica fume concrete; environmental impact consideration. Frontiers in Built Environment, 8, 992552. doi:10.3389/fbuil.2022.992552.

[28] Abdalla, A., & Mohammed, A. S. (2022). Hybrid MARS-, MEP-, and ANN-based prediction for modeling the compressive strength of cement mortar with various sand size and clay mineral metakaolin content. Archives of Civil and Mechanical Engineering, 22(4), 194. doi:10.1007/s43452-022-00519-0.

[29] Ulloa, N., Morales León, M. A., Silva Palmay, L. F., & Mendoza Castillo, M. (2025). Evaluating the compressive strength of industrial wastes-based geopolymer concrete with machine learning models. Construction and Building Materials, 472, 2025. doi:10.1016/j.conbuildmat.2025.140891.

# Appendix I: The Utilized Dataset

**Table A-1. Compressive strength**

| WFS/C | W/C | CA/C | FA/TA | WFS/FA | 1000SP/C | Age | CS_WFS |
|---|---|---|---|---|---|---|---|
| **Training set** | | | | | | | |
| 0.31 | 0.47 | 2.47 | 0.33 | 0.25 | 0 | 28 | 36.74 |
| 0.44 | 0.5 | 3.3 | 0.21 | 0.43 | 15.86 | 56 | 35.36 |
| 0.09 | 0.43 | 2.99 | 0.36 | 0.05 | 0 | 7 | 26.26 |
| 0.29 | 0.5 | 2.99 | 0.26 | 0.25 | 1.51 | 7 | 25.34 |
| 0 | 0.45 | 2.43 | 0.44 | 0 | 0 | 28 | 45.81 |
| 0.72 | 0.47 | 2.91 | 0.26 | 0.67 | 0 | 28 | 34.81 |
| 0.65 | 0.47 | 2.6 | 0.27 | 0.67 | 0 | 28 | 40.36 |
| 0.22 | 0.5 | 2.99 | 0.28 | 0.18 | 1.51 | 7 | 25.59 |
| 0.46 | 0.44 | 2.86 | 0.27 | 0.43 | 0 | 180 | 34.48 |
| 0.18 | 0.5 | 3.38 | 0.33 | 0.11 | 0 | 28 | 29.51 |
| 0.22 | 0.43 | 2.8 | 0.31 | 0.18 | 0 | 28 | 38.50 |
| 0.25 | 0.52 | 4.2 | 0.34 | 0.11 | 6 | 28 | 21.92 |
| 0.18 | 0.4 | 2.53 | 0.28 | 0.18 | 3.67 | 7 | 31.78 |
| 0.18 | 0.5 | 3.38 | 0.33 | 0.11 | 0 | 7 | 23.46 |
| 0.42 | 0.45 | 0.93 | 0.69 | 0.25 | 0 | 28 | 36.68 |
| 0.18 | 0.43 | 2.99 | 0.35 | 0.11 | 0 | 7 | 29.98 |
| 0 | 0.5 | 3.13 | 0.33 | 0 | 0 | 14 | 19.21 |
| 0.77 | 0.44 | 2.86 | 0.21 | 1 | 0 | 90 | 28.10 |
| 0.15 | 0.43 | 2.8 | 0.32 | 0.11 | 0 | 7 | 29.92 |
| 0.4 | 0.4 | 2.5 | 0.2 | 0.66 | 0 | 7 | 27.42 |
| 0.52 | 0.52 | 2.93 | 0.26 | 0.43 | 0 | 7 | 24.04 |
| 0.14 | 0.5 | 2.99 | 0.3 | 0.11 | 1.51 | 7 | 24.03 |
| 0.12 | 0.42 | 2.53 | 0.3 | 0.11 | 3.67 | 90 | 47.31 |
| 1.2 | 0.5 | 4 | 0.13 | 1.5 | 0 | 90 | 27.47 |
| 0.68 | 0.47 | 2.75 | 0.26 | 0.67 | 0 | 28 | 38.37 |
| 1.2 | 0.5 | 4 | 0.13 | 1.5 | 0 | 7 | 15.29 |
| 0.77 | 0.47 | 3.09 | 0.26 | 0.67 | 0 | 28 | 31.14 |
| 1.2 | 0.5 | 4 | 0.13 | 1.5 | 0 | 1 | 11.44 |
| 0.44 | 0.5 | 3.3 | 0.21 | 0.43 | 15.86 | 7 | 22.74 |
| 0.54 | 0.5 | 3.38 | 0.27 | 0.43 | 0 | 90 | 39.24 |
| 0.29 | 0.47 | 2.98 | 0.26 | 0.25 | 0 | 28 | 29.45 |
| 0.9 | 0.42 | 3.51 | 0.38 | 0 | 0 | 28 | 28.64 |
| 0 | 0.5 | 4 | 0.33 | 0 | 0 | 90 | 48.89 |
| 0.07 | 0.43 | 2.8 | 0.33 | 0.05 | 0 | 28 | 33.63 |
| 0.37 | 0.43 | 2.7 | 0.22 | 0.43 | 0 | 28 | 31.52 |
| 0.06 | 0.42 | 2.53 | 0.31 | 0.05 | 3.67 | 7 | 29.00 |
| 0.86 | 0.53 | 3.6 | 0.16 | 1 | 5 | 365 | 51.51 |
| 0 | 0.4 | 2.5 | 0.29 | 0 | 0 | 28 | 36.91 |
| 0.18 | 0.42 | 2.53 | 0.28 | 0.18 | 3.67 | 365 | 53.74 |
| 0.61 | 0.44 | 2.86 | 0.24 | 0.67 | 0 | 90 | 32.18 |
| 0 | 0.44 | 2.86 | 0.35 | 0 | 0 | 28 | 31.74 |
| 0 | 0.5 | 3.3 | 0.3 | 0 | 12.1 | 90 | 32.24 |
| 0 | 0.47 | 2.47 | 0.38 | 0 | 0 | 28 | 33.28 |
| 0.17 | 0.5 | 3.6 | 0.29 | 0.11 | 5 | 28 | 31.14 |
| 1.05 | 0.45 | 3 | 0.12 | 2.33 | 0 | 28 | 44.94 |
| 0.46 | 0.44 | 2.86 | 0.27 | 0.43 | 0 | 7 | 20.55 |
| 0.77 | 0.44 | 2.86 | 0.21 | 1 | 0 | 180 | 27.93 |
| 0.4 | 0.45 | 1.9 | 0.51 | 0.25 | 0 | 7 | 23.12 |
| 0.4 | 0.4 | 2.5 | 0.2 | 0.66 | 0 | 14 | 31.44 |
| 0.23 | 0.5 | 3.13 | 0.28 | 0.23 | 0 | 7 | 18.22 |
| 0.61 | 0.44 | 2.86 | 0.24 | 0.67 | 0 | 7 | 19.75 |
| 0.77 | 0.44 | 2.86 | 0.21 | 1 | 0 | 7 | 16.76 |
| 0.6 | 0.5 | 4 | 0.23 | 0.3 | 0 | 1 | 15.96 |

| | | | | | | | |
|---|---|---|---|---|---|---|---|
| 0.38 | 0.53 | 2.88 | 0.17 | 0.43 | 17.8 | 56 | 39.44 |
| 0.15 | 0.5 | 3.3 | 0.27 | 0.11 | 15.86 | 365 | 35.19 |
| 0.58 | 0.45 | 2.43 | 0.31 | 0.43 | 0 | 7 | 29.05 |
| 0.18 | 0.4 | 2.53 | 0.28 | 0.18 | 3.67 | 90 | 47.66 |
| 0 | 0.44 | 2.86 | 0.35 | 0 | 0 | 7 | 22.25 |
| 0.08 | 0.5 | 3.13 | 0.31 | 0.08 | 0 | 7 | 16.61 |
| 0.86 | 0.53 | 3.6 | 0.16 | 1 | 5 | 28 | 37.08 |
| 0.22 | 0.5 | 2.99 | 0.28 | 0.18 | 1.51 | 28 | 37.29 |
| 0.45 | 0.45 | 3 | 0.21 | 0.43 | 0 | 28 | 47.30 |
| 0.38 | 0.5 | 3.13 | 0.25 | 0.38 | 0 | 7 | 16.27 |
| 0.15 | 0.5 | 3.13 | 0.3 | 0.15 | 0 | 7 | 17.10 |
| 0.63 | 0.45 | 0.93 | 0.69 | 0.43 | 0 | 7 | 23.03 |
| 0.39 | 0.42 | 3.16 | 0.33 | 0.25 | 0 | 14 | 29.83 |
| 0.13 | 0.51 | 2.88 | 0.22 | 0.11 | 17.8 | 56 | 44.45 |
| 0.6 | 0.5 | 4 | 0.23 | 0.3 | 0 | 90 | 36.38 |
| 0.38 | 0.53 | 2.88 | 0.17 | 0.43 | 17.8 | 90 | 40.28 |
| 0.6 | 0.5 | 4 | 0.23 | 0.3 | 0 | 7 | 19.87 |
| 0 | 0.45 | 3 | 0.25 | 0 | 0 | 28 | 45.44 |
| 0.22 | 0.5 | 2.99 | 0.28 | 0.18 | 1.51 | 90 | 41.82 |
| 0.36 | 0.43 | 2.99 | 0.32 | 0.25 | 0 | 28 | 36.70 |
| 0 | 0.42 | 2.53 | 0.33 | 0 | 3.67 | 28 | 39.23 |
| 0 | 0.5 | 2.99 | 0.33 | 0 | 1.51 | 28 | 29.79 |
| 0.77 | 0.45 | 2.43 | 0.26 | 1 | 0 | 28 | 39.77 |
| 0.12 | 0.43 | 2.7 | 0.28 | 0.11 | 0 | 28 | 31.17 |
| 0.35 | 0.52 | 2.93 | 0.3 | 0.25 | 0 | 7 | 25.02 |
| 0.66 | 0.47 | 2.67 | 0.27 | 0.67 | 0 | 28 | 39.78 |
| 0.85 | 0.42 | 3.72 | 0.38 | 0 | 0 | 28 | 24.25 |
| 0.12 | 0.42 | 2.53 | 0.3 | 0.11 | 3.67 | 7 | 30.54 |
| 0.15 | 0.5 | 3.13 | 0.3 | 0.15 | 0 | 21 | 23.51 |
| 0.36 | 0.5 | 3.38 | 0.3 | 0.25 | 0 | 7 | 24.69 |
| 0 | 0.42 | 3.16 | 0.38 | 0 | 0 | 28 | 33.43 |
| 0 | 0.5 | 3.38 | 0.35 | 0 | 0 | 28 | 28.01 |
| 0 | 0.42 | 2.53 | 0.33 | 0 | 3.67 | 365 | 45.97 |
| 0 | 0.44 | 2.86 | 0.35 | 0 | 0 | 90 | 37.42 |
| 0.52 | 0.5 | 3.6 | 0.23 | 0.43 | 5 | 28 | 37.89 |
| 0 | 0.4 | 2.5 | 0.29 | 0 | 0 | 14 | 31.22 |
| 0.12 | 0.42 | 2.53 | 0.3 | 0.11 | 3.67 | 365 | 52.48 |
| 0 | 0.55 | 3 | 0.33 | 0 | 0 | 28 | 34.90 |
| 0.61 | 0.44 | 2.86 | 0.24 | 0.67 | 0 | 28 | 29.28 |
| 0.38 | 0.53 | 2.88 | 0.17 | 0.43 | 17.8 | 7 | 31.37 |
| 0.36 | 0.5 | 3.38 | 0.3 | 0.25 | 0 | 90 | 37.76 |
| 0.18 | 0.42 | 2.53 | 0.28 | 0.18 | 3.67 | 90 | 47.72 |
| 0.12 | 0.42 | 2.53 | 0.3 | 0.11 | 3.67 | 28 | 44.63 |
| 0 | 0.5 | 2.99 | 0.33 | 0 | 1.51 | 365 | 37.08 |
| 0 | 0.43 | 2.8 | 0.34 | 0 | 0 | 28 | 31.30 |
| 0.03 | 0.52 | 4.2 | 0.35 | 0.01 | 6 | 28 | 30.49 |
| 0.25 | 0.4 | 2.53 | 0.26 | 0.25 | 3.67 | 28 | 44.58 |
| 0.72 | 0.5 | 3.38 | 0.24 | 0.67 | 0 | 28 | 30.05 |
| 0.25 | 0.42 | 2.53 | 0.26 | 0.25 | 3.67 | 365 | 53.02 |
| 0.09 | 0.52 | 4.2 | 0.29 | 0.05 | 6 | 7 | 15.30 |
| 0.22 | 0.47 | 2.98 | 0.26 | 0.25 | 0 | 28 | 30.96 |
| 0.18 | 0.42 | 2.53 | 0.28 | 0.18 | 3.67 | 7 | 31.65 |
| 0.15 | 0.44 | 2.86 | 0.33 | 0.11 | 0 | 180 | 36.56 |
| 0.46 | 0.44 | 2.86 | 0.27 | 0.43 | 0 | 28 | 30.69 |
| 0.14 | 0.5 | 2.99 | 0.3 | 0.11 | 1.51 | 28 | 36.01 |
| 0 | 0.52 | 4.2 | 0.38 | 0 | 6 | 28 | 29.01 |
| 0.61 | 0.44 | 2.86 | 0.24 | 0.67 | 0 | 90 | 32.18 |
| 0.29 | 0.47 | 2.98 | 0.3 | 0.11 | 0 | 28 | 34.73 |
| 0.46 | 0.44 | 2.86 | 0.27 | 0.43 | 0 | 90 | 34.36 |

| | | | | | | | |
|---|---|---|---|---|---|---|---|
| 0.58 | 0.45 | 2.43 | 0.31 | 0.43 | 0 | 28 | 45.19 |
| 0.29 | 0.5 | 2.99 | 0.26 | 0.25 | 1.51 | 7 | 25.34 |
| 0 | 0.46 | 2.88 | 0.24 | 0 | 17.8 | 28 | 43.35 |
| 0.35 | 0.52 | 2.93 | 0.3 | 0.25 | 0 | 28 | 34.17 |
| 0.75 | 0.45 | 3 | 0.17 | 1 | 0 | 28 | 46.07 |
| 0.15 | 0.47 | 2.98 | 0.28 | 0.18 | 0 | 28 | 32.16 |
| 0.12 | 0.4 | 2.53 | 0.3 | 0.11 | 3.67 | 90 | 47.19 |
| 0.25 | 0.42 | 2.53 | 0.26 | 0.25 | 3.67 | 28 | 44.52 |
| 0.77 | 0.44 | 2.86 | 0.21 | 1 | 0 | 180 | 27.93 |
| 0.07 | 0.5 | 2.99 | 0.31 | 0.05 | 1.51 | 7 | 22.51 |
| 0 | 0.5 | 3.13 | 0.33 | 0 | 0 | 21 | 21.94 |
| 0.51 | 0.52 | 4.2 | 0.3 | 0.25 | 6 | 7 | 23.18 |
| 0 | 0.45 | 3 | 0.25 | 0 | 0 | 7 | 34.58 |
| 0.25 | 0.52 | 2.88 | 0.2 | 0.25 | 17.8 | 90 | 43.02 |
| 0 | 0.45 | 0.93 | 0.69 | 0 | 0 | 7 | 21.12 |
| 0.51 | 0.54 | 2.88 | 0.1 | 1 | 17.8 | 7 | 29.31 |
| 0 | 0.46 | 2.88 | 0.24 | 0 | 17.8 | 56 | 45.12 |
| 0.36 | 0.5 | 3.38 | 0.3 | 0.25 | 0 | 56 | 35.23 |
| 0.45 | 0.55 | 3 | 0.23 | 0.43 | 0 | 7 | 30.70 |
| 0.72 | 0.5 | 3.38 | 0.24 | 0.67 | 0 | 7 | 24.48 |
| 0.07 | 0.43 | 2.8 | 0.33 | 0.05 | 0 | 7 | 26.80 |
| 0.6 | 0.4 | 2.5 | 0.14 | 1.46 | 0 | 7 | 33.57 |
| 0.08 | 0.5 | 3.13 | 0.31 | 0.08 | 0 | 28 | 25.67 |
| 0.12 | 0.4 | 2.53 | 0.3 | 0.11 | 3.67 | 7 | 30.76 |
| 0.18 | 0.43 | 2.99 | 0.35 | 0.11 | 0 | 28 | 37.01 |
| 0 | 0.45 | 0.93 | 0.69 | 0 | 0 | 28 | 26.45 |
| 0.07 | 0.5 | 2.99 | 0.31 | 0.05 | 1.51 | 365 | 40.56 |
| 0.52 | 0.5 | 3.6 | 0.23 | 0.43 | 5 | 90 | 46.41 |
| 0.77 | 0.44 | 2.86 | 0.21 | 1 | 0 | 90 | 28.10 |
| 0.61 | 0.44 | 2.86 | 0.24 | 0.67 | 0 | 180 | 31.36 |
| 0.63 | 0.45 | 0.93 | 0.69 | 0.43 | 0 | 28 | 27.39 |
| 0.54 | 0.5 | 3.38 | 0.27 | 0.43 | 0 | 7 | 25.45 |
| 0.15 | 0.5 | 3.3 | 0.27 | 0.11 | 15.86 | 28 | 28.43 |
| 0.31 | 0.5 | 3.13 | 0.26 | 0.31 | 0 | 7 | 18.24 |
| 0.06 | 0.4 | 2.53 | 0.31 | 0.05 | 3.67 | 90 | 45.79 |
| 0.54 | 0.5 | 3.38 | 0.27 | 0.43 | 0 | 56 | 36.26 |
| 0 | 0.4 | 2.53 | 0.33 | 0 | 3.67 | 28 | 39.14 |
| 0 | 0.5 | 3.3 | 0.3 | 0 | 12.1 | 7 | 20.60 |
| 0.29 | 0.43 | 2.8 | 0.3 | 0.25 | 0 | 7 | 30.48 |
| 0.38 | 0.5 | 3.13 | 0.25 | 0.38 | 0 | 21 | 21.46 |
| 0 | 0.5 | 3.6 | 0.32 | 0 | 5 | 365 | 44.16 |
| 0.06 | 0.4 | 2.53 | 0.31 | 0.05 | 3.67 | 28 | 42.53 |
| 0 | 0.5 | 2.99 | 0.33 | 0 | 1.51 | 7 | 19.93 |
| 0.15 | 0.5 | 3.13 | 0.3 | 0.15 | 0 | 28 | 26.22 |
| 0 | 0.44 | 2.86 | 0.35 | 0 | 0 | 28 | 31.74 |
| 0.25 | 0.52 | 2.88 | 0.2 | 0.25 | 17.8 | 28 | 39.33 |
| 0.38 | 0.53 | 2.88 | 0.17 | 0.43 | 17.8 | 28 | 35.92 |
| 0.31 | 0.5 | 3.13 | 0.26 | 0.31 | 0 | 21 | 23.94 |
| 0 | 0.5 | 3.38 | 0.35 | 0 | 0 | 7 | 21.75 |
| 0.14 | 0.5 | 2.99 | 0.3 | 0.11 | 1.51 | 90 | 40.98 |
| 0.38 | 0.45 | 2.43 | 0.35 | 0.25 | 0 | 28 | 50.46 |
| 0.25 | 0.52 | 2.88 | 0.2 | 0.25 | 17.8 | 7 | 34.23 |
| 0.21 | 0.45 | 0.93 | 0.69 | 0.11 | 0 | 7 | 28.16 |
| 0.36 | 0.43 | 2.99 | 0.32 | 0.25 | 0 | 7 | 29.99 |
| 0.9 | 0.42 | 3.51 | 0.38 | 0 | 0 | 14 | 25.94 |
| 0.2 | 0.45 | 1.9 | 0.51 | 0.11 | 0 | 28 | 29.71 |
| 0.72 | 0.5 | 3.38 | 0.24 | 0.67 | 0 | 56 | 34.86 |
| 0.77 | 0.45 | 2.43 | 0.26 | 1 | 0 | 7 | 26.04 |
| 0 | 0.4 | 2.53 | 0.33 | 0 | 3.67 | 90 | 42.96 |

| | | | | | | | |
|---|---|---|---|---|---|---|---|
| 0.17 | 0.5 | 3.6 | 0.29 | 0.11 | 5 | 365 | 43.25 |
| 0.75 | 0.45 | 3 | 0.17 | 1 | 0 | 7 | 37.13 |
| 0.69 | 0.51 | 3.6 | 0.19 | 0.67 | 5 | 90 | 44.48 |
| 0.06 | 0.52 | 4.2 | 0.32 | 0.03 | 6 | 28 | 27.26 |
| 0.19 | 0.45 | 2.43 | 0.4 | 0.11 | 0 | 7 | 32.16 |
| 0 | 0.5 | 3.6 | 0.32 | 0 | 5 | 90 | 43.75 |
| 0.17 | 0.52 | 2.93 | 0.33 | 0.11 | 0 | 28 | 33.74 |
| 0 | 0.42 | 3.16 | 0.38 | 0 | 0 | 14 | 29.98 |
| 0 | 0.5 | 4 | 0.33 | 0 | 0 | 1 | 19.25 |
| 0.95 | 0.42 | 3.33 | 0.38 | 0 | 0 | 14 | 28.98 |
| 0.75 | 0.55 | 3 | 0.17 | 1 | 0 | 28 | 33.11 |
| 0.48 | 0.53 | 3.18 | 0.23 | 0.43 | 0 | 28 | 48.14 |
| 1.04 | 0.56 | 3.6 | 0.13 | 1.5 | 5 | 90 | 33.23 |
| 0.15 | 0.5 | 3.3 | 0.27 | 0.11 | 15.86 | 56 | 33.34 |
| 0.07 | 0.5 | 2.99 | 0.31 | 0.05 | 1.51 | 90 | 38.58 |
| 0.77 | 0.44 | 2.86 | 0.21 | 1 | 0 | 7 | 16.76 |
| 0.29 | 0.5 | 2.99 | 0.26 | 0.25 | 1.51 | 90 | 41.10 |
| 0.29 | 0.5 | 2.99 | 0.26 | 0.25 | 1.51 | 28 | 36.08 |
| 0.18 | 0.5 | 3.38 | 0.33 | 0.11 | 0 | 90 | 36.21 |
| 0.56 | 0.53 | 3.18 | 0.22 | 0.54 | 0 | 28 | 48.56 |
| 0.06 | 0.42 | 2.53 | 0.31 | 0.05 | 3.67 | 28 | 42.42 |
| 0.07 | 0.5 | 2.99 | 0.31 | 0.05 | 1.51 | 7 | 22.51 |
| 0.45 | 0.45 | 3 | 0.21 | 0.43 | 0 | 7 | 37.36 |
| 0.52 | 0.52 | 2.93 | 0.26 | 0.43 | 0 | 28 | 32.66 |
| 0 | 0.43 | 2.57 | 0.41 | 0 | 0 | 7 | 22.28 |
| 0.15 | 0.5 | 3.3 | 0.27 | 0.11 | 15.86 | 90 | 33.90 |
| 0.36 | 0.5 | 3.38 | 0.3 | 0.25 | 0 | 28 | 30.48 |
| 0.15 | 0.55 | 3 | 0.3 | 0.11 | 0 | 28 | 36.16 |
| 0.4 | 0.53 | 3.18 | 0.25 | 0.33 | 0 | 28 | 46.80 |
| 0.76 | 0.52 | 4.2 | 0.26 | 0.43 | 6 | 7 | 19.07 |
| 0.29 | 0.5 | 3.3 | 0.24 | 0.25 | 15.86 | 56 | 34.07 |
| 0 | 0.5 | 2.99 | 0.33 | 0 | 1.51 | 90 | 34.88 |
| 0.76 | 0.52 | 4.2 | 0.26 | 0.43 | 6 | 28 | 29.34 |
| 0 | 0.5 | 2.99 | 0.33 | 0 | 1.51 | 28 | 29.79 |
| 0.22 | 0.5 | 2.99 | 0.28 | 0.18 | 1.51 | 365 | 44.84 |
| 0 | 0.4 | 2.53 | 0.33 | 0 | 3.67 | 7 | 27.59 |
| 0 | 0.46 | 2.88 | 0.24 | 0 | 17.8 | 90 | 45.31 |
| 0.77 | 0.44 | 2.86 | 0.21 | 1 | 0 | 28 | 25.12 |
| 1.05 | 0.55 | 3 | 0.1 | 2.33 | 0 | 28 | 35.70 |
| 0.06 | 0.42 | 2.53 | 0.31 | 0.05 | 3.67 | 90 | 45.68 |
| 0.35 | 0.5 | 3.6 | 0.26 | 0.25 | 5 | 90 | 40.04 |
| 0 | 0.5 | 3.38 | 0.35 | 0 | 0 | 90 | 33.47 |
| 0.6 | 0.4 | 2.5 | 0.14 | 1.46 | 0 | 14 | 35.85 |
| 0.13 | 0.51 | 2.88 | 0.22 | 0.11 | 17.8 | 90 | 44.46 |
| 0.06 | 0.52 | 4.2 | 0.32 | 0.03 | 6 | 7 | 19.05 |
| 0.22 | 0.5 | 2.99 | 0.28 | 0.18 | 1.51 | 7 | 25.59 |
| 0 | 0.5 | 3.13 | 0.33 | 0 | 0 | 7 | 16.20 |
| 0.38 | 0.5 | 3.13 | 0.25 | 0.38 | 0 | 14 | 18.95 |
| 0.4 | 0.4 | 2.5 | 0.2 | 0.66 | 0 | 28 | 38.60 |
| 0.31 | 0.44 | 2.86 | 0.3 | 0.25 | 0 | 28 | 32.12 |
| 0.64 | 0.53 | 3.18 | 0.2 | 0.67 | 0 | 28 | 48.05 |
| 0.15 | 0.44 | 2.86 | 0.33 | 0.11 | 0 | 90 | 37.18 |
| 0.27 | 0.43 | 2.99 | 0.34 | 0.18 | 0 | 28 | 39.25 |
| 0.25 | 0.4 | 2.53 | 0.26 | 0.25 | 3.67 | 90 | 46.81 |
| 0 | 0.53 | 3.18 | 0.33 | 0 | 0 | 28 | 36.23 |
| 0.15 | 0.44 | 2.86 | 0.33 | 0.11 | 0 | 28 | 32.62 |
| 0 | 0.45 | 1.9 | 0.51 | 0 | 0 | 7 | 22.28 |
| 0.31 | 0.44 | 2.86 | 0.3 | 0.25 | 0 | 7 | 22.89 |
| 0.25 | 0.4 | 2.53 | 0.26 | 0.25 | 3.67 | 7 | 31.73 |

| | | | | | | | |
|---|---|---|---|---|---|---|---|
| 0.14 | 0.5 | 2.99 | 0.3 | 0.11 | 1.51 | 365 | 43.48 |
| 0.2 | 0.4 | 2.5 | 0.24 | 0.25 | 0 | 14 | 31.41 |
| 0.23 | 0.5 | 3.13 | 0.28 | 0.23 | 0 | 14 | 21.47 |
| 0.18 | 0.4 | 2.53 | 0.28 | 0.18 | 3.67 | 28 | 45.64 |
| 0.29 | 0.5 | 2.99 | 0.26 | 0.25 | 1.51 | 90 | 41.10 |
| 0.14 | 0.5 | 2.99 | 0.3 | 0.11 | 1.51 | 7 | 24.03 |
| 0.45 | 0.55 | 3 | 0.23 | 0.43 | 0 | 28 | 37.93 |
| 0 | 0.42 | 2.53 | 0.33 | 0 | 3.67 | 90 | 43.30 |
| 0.31 | 0.5 | 3.13 | 0.26 | 0.31 | 0 | 14 | 21.24 |
| 0.31 | 0.44 | 2.86 | 0.3 | 0.25 | 0 | 180 | 36.03 |
| 0.06 | 0.4 | 2.53 | 0.31 | 0.05 | 3.67 | 7 | 29.37 |
| 0.22 | 0.5 | 2.99 | 0.28 | 0.18 | 1.51 | 365 | 44.84 |
| 0.62 | 0.43 | 2.7 | 0.16 | 1 | 0 | 28 | 29.39 |
| 1.05 | 0.55 | 3 | 0.1 | 2.33 | 0 | 7 | 29.26 |
| 0.95 | 0.42 | 3.33 | 0.38 | 0 | 0 | 28 | 32.31 |
| 0 | 0.5 | 3.13 | 0.33 | 0 | 0 | 28 | 24.35 |
| 0.31 | 0.44 | 2.86 | 0.3 | 0.25 | 0 | 7 | 22.89 |
| 0.46 | 0.44 | 2.86 | 0.27 | 0.43 | 0 | 180 | 34.48 |
| 0.61 | 0.44 | 2.86 | 0.24 | 0.67 | 0 | 7 | 19.75 |
| 0 | 0.43 | 2.8 | 0.34 | 0 | 0 | 7 | 24.08 |
| 0.31 | 0.44 | 2.86 | 0.3 | 0.25 | 0 | 90 | 36.26 |
| 0.16 | 0.53 | 3.18 | 0.3 | 0.11 | 0 | 28 | 40.22 |
| 0.78 | 0.42 | 3.16 | 0.27 | 0.67 | 0 | 7 | 28.94 |
| 0.95 | 0.42 | 3.33 | 0.38 | 0 | 0 | 7 | 27.22 |
| 0.31 | 0.44 | 2.86 | 0.3 | 0.25 | 0 | 28 | 32.12 |
| 0.18 | 0.5 | 3.38 | 0.33 | 0.11 | 0 | 56 | 34.10 |
| 0.2 | 0.4 | 2.5 | 0.24 | 0.25 | 0 | 28 | 38.59 |
| 0.15 | 0.5 | 3.13 | 0.3 | 0.15 | 0 | 14 | 20.46 |
| 0.15 | 0.44 | 2.86 | 0.33 | 0.11 | 0 | 90 | 37.18 |
| 1.04 | 0.56 | 3.6 | 0.13 | 1.5 | 5 | 365 | 36.20 |
| 0.07 | 0.5 | 2.99 | 0.31 | 0.05 | 1.51 | 28 | 33.84 |
| 0.06 | 0.42 | 2.53 | 0.31 | 0.05 | 3.67 | 365 | 49.66 |
| 0.15 | 0.43 | 2.8 | 0.32 | 0.11 | 0 | 28 | 36.46 |
| 0 | 0.4 | 2.5 | 0.29 | 0 | 0 | 7 | 27.83 |
| 0.29 | 0.5 | 3.3 | 0.24 | 0.25 | 15.86 | 90 | 34.67 |
| 0.69 | 0.52 | 2.93 | 0.22 | 0.67 | 0 | 7 | 23.70 |
| 0 | 0.5 | 2.99 | 0.33 | 0 | 1.51 | 365 | 37.08 |
| 0.32 | 0.53 | 3.18 | 0.27 | 0.25 | 0 | 28 | 44.68 |
| 0.29 | 0.5 | 3.3 | 0.24 | 0.25 | 15.86 | 28 | 28.92 |
| 0.24 | 0.53 | 3.18 | 0.28 | 0.18 | 0 | 28 | 42.41 |
| 0 | 0.5 | 3.3 | 0.3 | 0 | 12.1 | 28 | 26.90 |
| 1.2 | 0.5 | 4 | 0.13 | 1.5 | 0 | 28 | 26.66 |
| 0.6 | 0.5 | 4 | 0.23 | 0.3 | 0 | 28 | 31.36 |
| 0 | 0.5 | 3.38 | 0.35 | 0 | 0 | 56 | 32.18 |
| 0.44 | 0.5 | 3.3 | 0.21 | 0.43 | 15.86 | 90 | 36.45 |
| 0.17 | 0.5 | 3.6 | 0.29 | 0.11 | 5 | 90 | 37.48 |
| 0.22 | 0.47 | 2.98 | 0.28 | 0.18 | 0 | 28 | 31.30 |
| 0.69 | 0.51 | 3.6 | 0.19 | 0.67 | 5 | 365 | 50.30 |
| 0.15 | 0.5 | 3.3 | 0.27 | 0.11 | 15.86 | 7 | 21.82 |
| 0.09 | 0.52 | 4.2 | 0.29 | 0.05 | 6 | 28 | 22.49 |
| 0.22 | 0.5 | 2.99 | 0.28 | 0.18 | 1.51 | 28 | 37.29 |
| 0.51 | 0.54 | 2.88 | 0.1 | 1 | 17.8 | 90 | 37.27 |
| 0.18 | 0.42 | 2.53 | 0.28 | 0.18 | 3.67 | 28 | 45.77 |
| 0.52 | 0.5 | 3.6 | 0.23 | 0.43 | 5 | 365 | 53.81 |
| 0.46 | 0.44 | 2.86 | 0.27 | 0.43 | 0 | 28 | 30.69 |
| 0.15 | 0.45 | 3 | 0.24 | 0.11 | 0 | 28 | 48.80 |

| | | | | | | | |
|---|---|---|---|---|---|---|---|
| 0.07 | 0.5 | 2.99 | 0.31 | 0.05 | 1.51 | 28 | 33.84 |
| 0 | 0.5 | 3.3 | 0.3 | 0 | 12.1 | 365 | 33.70 |
| 0.31 | 0.44 | 2.86 | 0.3 | 0.25 | 0 | 180 | 36.03 |
| 0.29 | 0.5 | 3.3 | 0.24 | 0.25 | 15.86 | 365 | 36.10 |
| 0.9 | 0.42 | 3.51 | 0.38 | 0 | 0 | 7 | 24.51 |
| 0.68 | 0.47 | 2.75 | 0.26 | 0.67 | 0 | 28 | 38.37 |
| 0.31 | 0.44 | 2.86 | 0.3 | 0.25 | 0 | 90 | 36.26 |
| 0.12 | 0.4 | 2.53 | 0.3 | 0.11 | 3.67 | 28 | 44.56 |
| 0.21 | 0.45 | 0.93 | 0.69 | 0.11 | 0 | 28 | 32.14 |
| 0.29 | 0.5 | 3.3 | 0.24 | 0.25 | 15.86 | 7 | 21.89 |
| 0 | 0.52 | 2.93 | 0.37 | 0 | 0 | 28 | 30.89 |
| 0 | 0.44 | 2.86 | 0.35 | 0 | 0 | 180 | 37.17 |
| 0 | 0.52 | 4.2 | 0.38 | 0 | 6 | 7 | 15.43 |
| 1.05 | 0.45 | 3 | 0.12 | 2.33 | 0 | 7 | 36.97 |
| **Validation set** | | | | | | | |
| 0.15 | 0.44 | 2.86 | 0.33 | 0.11 | 0 | 7 | 23.33 |
| 0.85 | 0.42 | 3.72 | 0.38 | 0 | 0 | 7 | 21.82 |
| 0 | 0.44 | 2.86 | 0.35 | 0 | 0 | 7 | 22.25 |
| 0.15 | 0.44 | 2.86 | 0.33 | 0.11 | 0 | 28 | 32.62 |
| 0.44 | 0.5 | 3.3 | 0.21 | 0.43 | 15.86 | 28 | 29.82 |
| 0.77 | 0.47 | 2.47 | 0.24 | 1 | 0 | 28 | 36.39 |
| 0 | 0.46 | 2.88 | 0.24 | 0 | 17.8 | 7 | 40.86 |
| 0.13 | 0.51 | 2.88 | 0.22 | 0.11 | 17.8 | 7 | 36.77 |
| 0.59 | 0.45 | 1.9 | 0.51 | 0.43 | 0 | 28 | 21.78 |
| 0.25 | 0.42 | 2.53 | 0.26 | 0.25 | 3.67 | 7 | 31.28 |
| 0.19 | 0.45 | 2.43 | 0.4 | 0.11 | 0 | 28 | 49.36 |
| 0 | 0.45 | 2.43 | 0.44 | 0 | 0 | 7 | 30.98 |
| 0.86 | 0.53 | 3.6 | 0.16 | 1 | 5 | 90 | 45.11 |
| 0.54 | 0.5 | 3.38 | 0.27 | 0.43 | 0 | 28 | 31.23 |
| 0.46 | 0.44 | 2.86 | 0.27 | 0.43 | 0 | 7 | 20.55 |
| 0.15 | 0.45 | 3 | 0.24 | 0.11 | 0 | 7 | 36.94 |
| 0.72 | 0.5 | 3.38 | 0.24 | 0.67 | 0 | 90 | 37.40 |
| 0.35 | 0.5 | 3.6 | 0.26 | 0.25 | 5 | 365 | 47.17 |
| 0.08 | 0.5 | 3.13 | 0.31 | 0.08 | 0 | 21 | 22.98 |
| 0 | 0.52 | 2.93 | 0.37 | 0 | 0 | 7 | 22.70 |
| 1.2 | 0.5 | 3.99 | 0.13 | 1.5 | 0 | 28 | 27.02 |
| 0.25 | 0.52 | 2.88 | 0.2 | 0.25 | 17.8 | 56 | 42.88 |
| 0 | 0.5 | 4 | 0.33 | 0 | 0 | 7 | 24.55 |
| 0 | 0.5 | 3.3 | 0.3 | 0 | 12.1 | 56 | 31.44 |
| 0.14 | 0.5 | 2.99 | 0.3 | 0.11 | 1.51 | 90 | 40.98 |
| 0.38 | 0.5 | 3.13 | 0.25 | 0.38 | 0 | 28 | 23.81 |
| 0.08 | 0.53 | 3.18 | 0.32 | 0.05 | 0 | 28 | 38.46 |
| 0.25 | 0.52 | 4.2 | 0.34 | 0.11 | 6 | 7 | 15.64 |
| 1.17 | 0.42 | 3.16 | 0.2 | 1.5 | 0 | 28 | 27.09 |
| 0.31 | 0.5 | 3.13 | 0.26 | 0.31 | 0 | 28 | 26.33 |
| 0.6 | 0.4 | 2.5 | 0.14 | 1.46 | 0 | 28 | 40.06 |
| 0.13 | 0.51 | 2.88 | 0.22 | 0.11 | 17.8 | 28 | 41.32 |
| 0.85 | 0.42 | 3.72 | 0.38 | 0 | 0 | 14 | 22.69 |
| 0.69 | 0.52 | 2.93 | 0.22 | 0.67 | 0 | 28 | 32.17 |
| 0.39 | 0.42 | 3.16 | 0.33 | 0.25 | 0 | 7 | 27.69 |
| 0.14 | 0.5 | 2.99 | 0.3 | 0.11 | 1.51 | 365 | 43.48 |
| 0 | 0.47 | 2.98 | 0.33 | 0 | 0 | 28 | 32.28 |
| 0.29 | 0.5 | 2.99 | 0.26 | 0.25 | 1.51 | 365 | 44.15 |
| 0.15 | 0.55 | 3 | 0.3 | 0.11 | 0 | 7 | 28.12 |
| 0.2 | 0.45 | 1.9 | 0.51 | 0.11 | 0 | 7 | 25.35 |

| | | | | | | | |
|---|---|---|---|---|---|---|---|
| 0 | 0.5 | 2.99 | 0.33 | 0 | 1.51 | 7 | 19.93 |
| 0.03 | 0.52 | 4.2 | 0.35 | 0.01 | 6 | 7 | 19.47 |
| 0.61 | 0.44 | 2.86 | 0.24 | 0.67 | 0 | 28 | 29.28 |
| 0.61 | 0.44 | 2.86 | 0.24 | 0.67 | 0 | 180 | 31.36 |
| 0 | 0.45 | 1.9 | 0.51 | 0 | 0 | 28 | 28.52 |
| 0.29 | 0.5 | 2.99 | 0.26 | 0.25 | 1.51 | 28 | 36.08 |
| 0.15 | 0.44 | 2.86 | 0.33 | 0.11 | 0 | 180 | 36.56 |
| 0 | 0.44 | 2.86 | 0.35 | 0 | 0 | 180 | 37.17 |
| 0 | 0.5 | 2.99 | 0.33 | 0 | 1.51 | 90 | 34.88 |
| 0.14 | 0.5 | 2.99 | 0.3 | 0.11 | 1.51 | 28 | 36.01 |
| 0.51 | 0.54 | 2.88 | 0.1 | 1 | 17.8 | 56 | 35.24 |
| 0 | 0.5 | 3.99 | 0.33 | 0 | 0 | 28 | 40.63 |
| 0.78 | 0.42 | 3.16 | 0.27 | 0.67 | 0 | 28 | 35.73 |
| 0.59 | 0.45 | 1.9 | 0.51 | 0.43 | 0 | 7 | 22.38 |
| 0.15 | 0.47 | 2.98 | 0.3 | 0.11 | 0 | 28 | 33.15 |
| 0.27 | 0.43 | 2.99 | 0.34 | 0.18 | 0 | 7 | 32.69 |
| 0.07 | 0.5 | 2.99 | 0.31 | 0.05 | 1.51 | 365 | 40.56 |
| 0.07 | 0.5 | 2.99 | 0.31 | 0.05 | 1.51 | 90 | 38.58 |
| 0.61 | 0.47 | 2.47 | 0.27 | 0.67 | 0 | 28 | 39.08 |
| 0.46 | 0.44 | 2.86 | 0.27 | 0.43 | 0 | 90 | 34.36 |
| 0 | 0.44 | 2.86 | 0.35 | 0 | 0 | 90 | 37.42 |
| 0.35 | 0.5 | 3.6 | 0.26 | 0.25 | 5 | 28 | 32.67 |
| 0.78 | 0.42 | 3.16 | 0.27 | 0.67 | 0 | 14 | 31.56 |
| 0.75 | 0.55 | 3 | 0.17 | 1 | 0 | 7 | 25.99 |
| 0.17 | 0.52 | 2.93 | 0.33 | 0.11 | 0 | 7 | 23.97 |
| 0.29 | 0.43 | 2.8 | 0.3 | 0.25 | 0 | 28 | 37.81 |
| 0 | 0.42 | 2.53 | 0.33 | 0 | 3.67 | 7 | 27.24 |
| 0.22 | 0.43 | 2.8 | 0.31 | 0.18 | 0 | 7 | 31.93 |
| 0.15 | 0.47 | 2.47 | 0.36 | 0.11 | 0 | 28 | 35.13 |
| 0.4 | 0.45 | 1.9 | 0.51 | 0.25 | 0 | 28 | 23.54 |
| 0.39 | 0.42 | 3.16 | 0.33 | 0.25 | 0 | 28 | 33.20 |
| 0.44 | 0.5 | 3.3 | 0.21 | 0.43 | 15.86 | 365 | 37.55 |
| 0 | 0.43 | 2.57 | 0.41 | 0 | 0 | 28 | 32.32 |
| 0 | 0.55 | 3 | 0.33 | 0 | 0 | 7 | 26.76 |
| 0.22 | 0.5 | 2.99 | 0.28 | 0.18 | 1.51 | 90 | 41.82 |
| 0 | 0.43 | 2.7 | 0.31 | 0 | 0 | 28 | 28.29 |
| 0.51 | 0.52 | 4.2 | 0.3 | 0.25 | 6 | 28 | 28.22 |
| 0.2 | 0.4 | 2.5 | 0.24 | 0.25 | 0 | 7 | 27.25 |
| 0.23 | 0.5 | 3.13 | 0.28 | 0.23 | 0 | 21 | 24.40 |
| 0.46 | 0.47 | 2.47 | 0.3 | 0.43 | 0 | 28 | 37.42 |
| 0.25 | 0.42 | 2.53 | 0.26 | 0.25 | 3.67 | 90 | 46.79 |
| 0.42 | 0.45 | 0.93 | 0.69 | 0.25 | 0 | 7 | 33.96 |
| 0 | 0.42 | 3.16 | 0.38 | 0 | 0 | 7 | 27.87 |
| 0.08 | 0.5 | 3.13 | 0.31 | 0.08 | 0 | 14 | 19.94 |
| 0.77 | 0.44 | 2.86 | 0.21 | 1 | 0 | 28 | 25.12 |
| 1.04 | 0.56 | 3.6 | 0.13 | 1.5 | 5 | 28 | 29.77 |
| 0.09 | 0.43 | 2.99 | 0.36 | 0.05 | 0 | 28 | 33.94 |
| 1.17 | 0.42 | 3.16 | 0.2 | 1.5 | 0 | 7 | 23.96 |
| 0.29 | 0.5 | 2.99 | 0.26 | 0.25 | 1.51 | 365 | 44.15 |
| 0.51 | 0.54 | 2.88 | 0.1 | 1 | 17.8 | 28 | 31.94 |
| 0 | 0.5 | 4 | 0.33 | 0 | 0 | 28 | 40.52 |
| 0.38 | 0.45 | 2.43 | 0.35 | 0.25 | 0 | 7 | 32.74 |
| 1.17 | 0.42 | 3.16 | 0.2 | 1.5 | 0 | 14 | 25.09 |
| 0.69 | 0.51 | 3.6 | 0.19 | 0.67 | 5 | 28 | 36.48 |
| 0.23 | 0.5 | 3.13 | 0.28 | 0.23 | 0 | 28 | 26.99 |
| 0 | 0.5 | 3.6 | 0.32 | 0 | 5 | 28 | 36.12 |
| 0.15 | 0.44 | 2.86 | 0.33 | 0.11 | 0 | 7 | 23.33 |

**Table A-2. Elastic modulus**

| WFS/C | W/C | CA/C | FA/TA | WFS/FA | 1000SP/C | Age | E_WFS |
|---|---|---|---|---|---|---|---|
| **Training set** | | | | | | | |
| 0.83 | 0.48 | 2.97 | 0.34 | 0.54 | 0.00 | 28 | 33.30 |
| 0.21 | 0.40 | 2.13 | 0.45 | 0.11 | 0.00 | 7 | 37.98 |
| 0.21 | 0.40 | 1.92 | 0.50 | 0.10 | 0.00 | 14 | 41.03 |
| 0.64 | 0.40 | 2.13 | 0.35 | 0.43 | 0.00 | 7 | 41.08 |
| 0.59 | 0.48 | 2.97 | 0.37 | 0.33 | 0.00 | 7 | 25.00 |
| 0.85 | 0.40 | 1.71 | 0.40 | 0.50 | 0.00 | 14 | 30.74 |
| 0.25 | 0.40 | 2.53 | 0.26 | 0.25 | 3.67 | 90 | 33.30 |
| 0.00 | 0.42 | 2.53 | 0.33 | 0.00 | 3.67 | 90 | 30.60 |
| 0.00 | 0.40 | 2.53 | 0.33 | 0.00 | 3.67 | 90 | 31.70 |
| 0.38 | 0.50 | 3.13 | 0.25 | 0.38 | 0.00 | 28 | 23.43 |
| 0.18 | 0.42 | 2.53 | 0.28 | 0.18 | 3.67 | 365 | 34.10 |
| 0.29 | 0.50 | 3.30 | 0.24 | 0.25 | 15.86 | 28 | 27.60 |
| 0.00 | 0.40 | 2.13 | 0.50 | 0.00 | 0.00 | 14 | 40.44 |
| 0.38 | 0.50 | 3.13 | 0.25 | 0.38 | 0.00 | 90 | 24.60 |
| 0.64 | 0.40 | 2.13 | 0.35 | 0.43 | 0.00 | 14 | 44.48 |
| 0.18 | 0.40 | 2.53 | 0.28 | 0.18 | 3.67 | 28 | 31.80 |
| 0.59 | 0.48 | 2.97 | 0.37 | 0.33 | 0.00 | 3 | 20.20 |
| 0.15 | 0.50 | 3.30 | 0.27 | 0.11 | 15.86 | 90 | 29.20 |
| 0.83 | 0.48 | 2.97 | 0.34 | 0.54 | 0.00 | 3 | 20.90 |
| 0.18 | 0.42 | 2.53 | 0.28 | 0.18 | 3.67 | 28 | 31.34 |
| 0.22 | 0.50 | 2.99 | 0.28 | 0.18 | 1.51 | 90 | 25.80 |
| 1.28 | 0.40 | 1.49 | 0.35 | 0.86 | 0.00 | 28 | 32.15 |
| 1.28 | 0.40 | 1.49 | 0.35 | 0.86 | 0.00 | 7 | 22.81 |
| 0.21 | 0.40 | 2.13 | 0.45 | 0.11 | 0.00 | 14 | 42.02 |
| 0.00 | 0.40 | 2.13 | 0.50 | 0.00 | 0.00 | 28 | 42.81 |
| 0.44 | 0.50 | 3.30 | 0.21 | 0.43 | 15.86 | 56 | 30.30 |
| 0.45 | 0.45 | 3.00 | 0.21 | 0.43 | 0.00 | 28 | 35.00 |
| 0.45 | 0.55 | 3.00 | 0.23 | 0.43 | 0.00 | 28 | 30.50 |
| 0.14 | 0.50 | 2.99 | 0.30 | 0.11 | 1.51 | 7 | 21.30 |
| 0.22 | 0.50 | 2.99 | 0.28 | 0.18 | 1.51 | 7 | 21.90 |
| 0.12 | 0.40 | 2.53 | 0.30 | 0.11 | 3.67 | 90 | 32.90 |
| 0.06 | 0.40 | 2.53 | 0.31 | 0.05 | 3.67 | 28 | 30.40 |
| 0.15 | 0.50 | 3.30 | 0.27 | 0.11 | 15.86 | 7 | 23.60 |
| 0.00 | 0.40 | 2.13 | 0.50 | 0.00 | 0.00 | 28 | 42.81 |
| 0.15 | 0.50 | 3.30 | 0.27 | 0.11 | 15.86 | 56 | 28.40 |
| 0.15 | 0.50 | 3.30 | 0.27 | 0.11 | 15.86 | 28 | 26.75 |
| 0.00 | 0.50 | 3.13 | 0.33 | 0.00 | 0.00 | 7 | 20.41 |
| 0.00 | 0.50 | 3.30 | 0.30 | 0.00 | 12.10 | 28 | 25.10 |
| 0.00 | 0.55 | 3.00 | 0.33 | 0.00 | 0.00 | 28 | 30.00 |
| 0.43 | 0.40 | 2.13 | 0.40 | 0.25 | 0.00 | 28 | 45.67 |
| 0.64 | 0.40 | 1.49 | 0.50 | 0.30 | 0.00 | 7 | 38.13 |
| 0.18 | 0.42 | 2.53 | 0.28 | 0.18 | 3.67 | 90 | 32.19 |
| 0.00 | 0.48 | 2.97 | 0.44 | 0.00 | 0.00 | 28 | 31.70 |
| 0.07 | 0.50 | 2.99 | 0.31 | 0.05 | 1.51 | 90 | 24.90 |
| 0.83 | 0.48 | 2.97 | 0.34 | 0.54 | 0.00 | 3 | 18.40 |
| 0.00 | 0.40 | 2.13 | 0.50 | 0.00 | 0.00 | 7 | 35.04 |
| 0.44 | 0.50 | 3.30 | 0.21 | 0.43 | 15.86 | 90 | 31.20 |
| 0.07 | 0.50 | 2.99 | 0.31 | 0.05 | 1.51 | 365 | 26.40 |

| | | | | | | | |
|---|---|---|---|---|---|---|---|
| 0.00 | 0.50 | 2.99 | 0.33 | 0.00 | 1.51 | 365 | 25.80 |
| 0.29 | 0.50 | 3.30 | 0.24 | 0.25 | 15.86 | 56 | 29.30 |
| 0.00 | 0.42 | 2.53 | 0.33 | 0.00 | 3.67 | 365 | 32.30 |
| 0.43 | 0.40 | 1.71 | 0.50 | 0.20 | 0.00 | 14 | 41.87 |
| 0.21 | 0.40 | 2.13 | 0.45 | 0.11 | 0.00 | 28 | 44.33 |
| 0.00 | 0.50 | 3.13 | 0.33 | 0.00 | 0.00 | 28 | 23.60 |
| 0.12 | 0.42 | 2.53 | 0.30 | 0.11 | 3.67 | 28 | 30.77 |
| 0.44 | 0.50 | 3.30 | 0.21 | 0.43 | 15.86 | 28 | 28.40 |
| 0.00 | 0.50 | 2.99 | 0.33 | 0.00 | 1.51 | 7 | 20.50 |
| 0.00 | 0.48 | 2.97 | 0.44 | 0.00 | 0.00 | 7 | 24.30 |
| 0.00 | 0.42 | 2.53 | 0.33 | 0.00 | 3.67 | 7 | 25.70 |
| 0.31 | 0.50 | 3.13 | 0.26 | 0.31 | 0.00 | 7 | 22.21 |
| 0.31 | 0.50 | 3.13 | 0.26 | 0.31 | 0.00 | 28 | 25.40 |
| 0.00 | 0.40 | 2.13 | 0.50 | 0.00 | 0.00 | 14 | 40.44 |
| 0.44 | 0.50 | 3.30 | 0.21 | 0.43 | 15.86 | 7 | 24.20 |
| 0.43 | 0.40 | 1.92 | 0.45 | 0.22 | 0.00 | 28 | 43.11 |
| 0.15 | 0.50 | 3.13 | 0.30 | 0.15 | 0.00 | 28 | 24.78 |
| 0.08 | 0.50 | 3.13 | 0.31 | 0.08 | 0.00 | 28 | 24.24 |
| 0.00 | 0.40 | 2.13 | 0.50 | 0.00 | 0.00 | 14 | 40.39 |
| 0.00 | 0.50 | 3.13 | 0.33 | 0.00 | 0.00 | 90 | 24.83 |
| 0.43 | 0.40 | 1.92 | 0.45 | 0.22 | 0.00 | 14 | 40.07 |
| 0.43 | 0.40 | 2.13 | 0.40 | 0.25 | 0.00 | 14 | 43.05 |
| 0.29 | 0.50 | 3.30 | 0.24 | 0.25 | 15.86 | 7 | 23.80 |
| 0.59 | 0.48 | 2.97 | 0.37 | 0.33 | 0.00 | 28 | 33.40 |
| 1.05 | 0.45 | 3.00 | 0.12 | 2.33 | 0.00 | 28 | 34.50 |
| 0.59 | 0.48 | 2.97 | 0.37 | 0.33 | 0.00 | 3 | 23.90 |
| 0.83 | 0.48 | 2.97 | 0.34 | 0.54 | 0.00 | 7 | 23.40 |
| 0.59 | 0.48 | 2.97 | 0.37 | 0.33 | 0.00 | 7 | 24.50 |
| 0.00 | 0.40 | 2.13 | 0.50 | 0.00 | 0.00 | 7 | 35.12 |
| 0.22 | 0.50 | 2.99 | 0.28 | 0.18 | 1.51 | 28 | 25.20 |
| 0.00 | 0.48 | 2.97 | 0.44 | 0.00 | 0.00 | 3 | 22.50 |
| 0.00 | 0.40 | 2.53 | 0.33 | 0.00 | 3.67 | 28 | 29.90 |
| 0.38 | 0.50 | 3.13 | 0.25 | 0.38 | 0.00 | 7 | 20.40 |
| 0.83 | 0.48 | 2.97 | 0.34 | 0.54 | 0.00 | 7 | 27.60 |
| 0.23 | 0.50 | 3.13 | 0.28 | 0.23 | 0.00 | 90 | 25.59 |
| 0.00 | 0.50 | 3.30 | 0.30 | 0.00 | 12.10 | 365 | 27.70 |
| 0.12 | 0.42 | 2.53 | 0.30 | 0.11 | 3.67 | 90 | 31.79 |
| 0.00 | 0.42 | 2.53 | 0.33 | 0.00 | 3.67 | 28 | 29.90 |
| 0.83 | 0.48 | 2.97 | 0.34 | 0.54 | 0.00 | 28 | 32.60 |
| 0.12 | 0.42 | 2.53 | 0.30 | 0.11 | 3.67 | 365 | 33.71 |
| 0.15 | 0.50 | 3.13 | 0.30 | 0.15 | 0.00 | 90 | 25.19 |
| 0.08 | 0.50 | 3.13 | 0.31 | 0.08 | 0.00 | 7 | 20.81 |
| 0.29 | 0.50 | 3.30 | 0.24 | 0.25 | 15.86 | 365 | 30.60 |
| 0.44 | 0.50 | 3.30 | 0.21 | 0.43 | 15.86 | 365 | 31.80 |
| 0.59 | 0.48 | 2.97 | 0.37 | 0.33 | 0.00 | 28 | 31.70 |
| 0.25 | 0.42 | 2.53 | 0.26 | 0.25 | 3.67 | 7 | 27.20 |
| 0.18 | 0.42 | 2.53 | 0.28 | 0.18 | 3.67 | 7 | 27.70 |
| 0.21 | 0.40 | 1.92 | 0.50 | 0.10 | 0.00 | 28 | 43.10 |
| 0.00 | 0.50 | 3.30 | 0.30 | 0.00 | 12.10 | 56 | 26.40 |
| 0.00 | 0.45 | 3.00 | 0.25 | 0.00 | 0.00 | 28 | 34.50 |

| | | | | | | | |
|---|---|---|---|---|---|---|---|
| 0.29 | 0.50 | 2.99 | 0.26 | 0.25 | 1.51 | 90 | 25.70 |
| 0.07 | 0.50 | 2.99 | 0.31 | 0.05 | 1.51 | 7 | 21.10 |
| 0.29 | 0.50 | 2.99 | 0.26 | 0.25 | 1.51 | 365 | 25.70 |
| 0.15 | 0.45 | 3.00 | 0.24 | 0.11 | 0.00 | 28 | 37.00 |
| 0.25 | 0.42 | 2.53 | 0.26 | 0.25 | 3.67 | 90 | 31.98 |
| 0.29 | 0.50 | 2.99 | 0.26 | 0.25 | 1.51 | 7 | 21.50 |
| 0.75 | 0.45 | 3.00 | 0.17 | 1.00 | 0.00 | 28 | 35.50 |
| 0.00 | 0.40 | 2.13 | 0.50 | 0.00 | 0.00 | 7 | 35.12 |
| 0.06 | 0.40 | 2.53 | 0.31 | 0.05 | 3.67 | 90 | 32.50 |
| 0.64 | 0.40 | 1.49 | 0.50 | 0.30 | 0.00 | 28 | 45.12 |
| 1.28 | 0.40 | 1.49 | 0.35 | 0.86 | 0.00 | 14 | 26.30 |
| 0.75 | 0.55 | 3.00 | 0.17 | 1.00 | 0.00 | 28 | 29.50 |
| Validation set | | | | | | | |
| 0.06 | 0.42 | 2.53 | 0.31 | 0.05 | 3.67 | 28 | 30.40 |
| 0.00 | 0.50 | 2.99 | 0.33 | 0.00 | 1.51 | 28 | 23.80 |
| 0.12 | 0.42 | 2.53 | 0.30 | 0.11 | 3.67 | 7 | 27.10 |
| 0.23 | 0.50 | 3.13 | 0.28 | 0.23 | 0.00 | 28 | 25.19 |
| 0.00 | 0.50 | 3.30 | 0.30 | 0.00 | 12.10 | 90 | 27.10 |
| 0.15 | 0.50 | 3.30 | 0.27 | 0.11 | 15.86 | 365 | 29.50 |
| 0.25 | 0.42 | 2.53 | 0.26 | 0.25 | 3.67 | 28 | 31.07 |
| 0.22 | 0.50 | 2.99 | 0.28 | 0.18 | 1.51 | 365 | 27.50 |
| 0.15 | 0.50 | 3.13 | 0.30 | 0.15 | 0.00 | 7 | 21.22 |
| 0.15 | 0.55 | 3.00 | 0.30 | 0.11 | 0.00 | 28 | 30.00 |
| 0.06 | 0.42 | 2.53 | 0.31 | 0.05 | 3.67 | 7 | 26.60 |
| 0.43 | 0.40 | 1.92 | 0.45 | 0.22 | 0.00 | 7 | 34.89 |
| 0.25 | 0.42 | 2.53 | 0.26 | 0.25 | 3.67 | 365 | 33.60 |
| 0.06 | 0.42 | 2.53 | 0.31 | 0.05 | 3.67 | 90 | 31.00 |
| 0.64 | 0.40 | 1.49 | 0.50 | 0.30 | 0.00 | 14 | 42.32 |
| 0.21 | 0.40 | 1.92 | 0.50 | 0.10 | 0.00 | 7 | 37.00 |
| 0.29 | 0.50 | 3.30 | 0.24 | 0.25 | 15.86 | 90 | 30.00 |
| 0.43 | 0.40 | 1.71 | 0.50 | 0.20 | 0.00 | 28 | 44.09 |
| 0.85 | 0.40 | 1.71 | 0.40 | 0.50 | 0.00 | 7 | 27.19 |
| 0.14 | 0.50 | 2.99 | 0.30 | 0.11 | 1.51 | 90 | 25.40 |
| 0.06 | 0.42 | 2.53 | 0.31 | 0.05 | 3.67 | 365 | 32.90 |
| 0.08 | 0.50 | 3.13 | 0.31 | 0.08 | 0.00 | 90 | 25.01 |
| 0.00 | 0.50 | 2.99 | 0.33 | 0.00 | 1.51 | 90 | 24.60 |
| 0.31 | 0.50 | 3.13 | 0.26 | 0.31 | 0.00 | 90 | 25.73 |
| 0.00 | 0.40 | 2.13 | 0.50 | 0.00 | 0.00 | 28 | 42.81 |
| 0.85 | 0.40 | 1.71 | 0.40 | 0.50 | 0.00 | 28 | 36.22 |
| 0.23 | 0.50 | 3.13 | 0.28 | 0.23 | 0.00 | 7 | 21.80 |
| 0.43 | 0.40 | 1.71 | 0.50 | 0.20 | 0.00 | 7 | 37.44 |
| 1.05 | 0.55 | 3.00 | 0.10 | 2.33 | 0.00 | 28 | 30.50 |
| 0.14 | 0.50 | 2.99 | 0.30 | 0.11 | 1.51 | 365 | 27.20 |
| 0.12 | 0.40 | 2.53 | 0.30 | 0.11 | 3.67 | 28 | 31.40 |
| 0.43 | 0.40 | 2.13 | 0.40 | 0.25 | 0.00 | 7 | 39.90 |
| 0.64 | 0.40 | 2.13 | 0.35 | 0.43 | 0.00 | 28 | 46.65 |
| 0.00 | 0.50 | 3.30 | 0.30 | 0.00 | 12.10 | 7 | 22.00 |
| 0.18 | 0.40 | 2.53 | 0.28 | 0.18 | 3.67 | 90 | 33.60 |
| 0.25 | 0.40 | 2.53 | 0.26 | 0.25 | 3.67 | 28 | 31.20 |

**Table A-3. Split tensile strength**

| WFS/C | W/C | CA/C | FA/TA | WFS/FA | 1000SP/C | Age | STS_WFS |
|---|---|---|---|---|---|---|---|
| **Training set** | | | | | | | |
| 0.17 | 0.50 | 3.60 | 0.29 | 0.11 | 5.00 | 28 | 1.84 |
| 0.35 | 0.50 | 3.60 | 0.26 | 0.25 | 5.00 | 28 | 1.98 |
| 0.52 | 0.50 | 3.60 | 0.23 | 0.43 | 5.00 | 28 | 2.58 |
| 0.86 | 0.53 | 3.60 | 0.16 | 1.00 | 5.00 | 28 | 2.38 |
| 1.04 | 0.56 | 3.60 | 0.13 | 1.50 | 5.00 | 28 | 1.72 |
| 0.00 | 0.50 | 3.60 | 0.32 | 0.00 | 5.00 | 90 | 2.66 |
| 0.17 | 0.50 | 3.60 | 0.29 | 0.11 | 5.00 | 90 | 2.35 |
| 0.52 | 0.50 | 3.60 | 0.23 | 0.43 | 5.00 | 90 | 3.33 |
| 0.69 | 0.51 | 3.60 | 0.19 | 0.67 | 5.00 | 90 | 3.26 |
| 0.86 | 0.53 | 3.60 | 0.16 | 1.00 | 5.00 | 90 | 3.19 |
| 1.04 | 0.56 | 3.60 | 0.13 | 1.50 | 5.00 | 90 | 2.16 |
| 0.17 | 0.50 | 3.60 | 0.29 | 0.11 | 5.00 | 365 | 2.66 |
| 0.35 | 0.50 | 3.60 | 0.26 | 0.25 | 5.00 | 365 | 2.86 |
| 0.52 | 0.50 | 3.60 | 0.23 | 0.43 | 5.00 | 365 | 3.50 |
| 0.69 | 0.51 | 3.60 | 0.19 | 0.67 | 5.00 | 365 | 3.42 |
| 1.04 | 0.56 | 3.60 | 0.13 | 1.50 | 5.00 | 365 | 2.52 |
| 0.13 | 0.51 | 2.88 | 0.22 | 0.11 | 17.80 | 7 | 4.10 |
| 0.38 | 0.53 | 2.88 | 0.17 | 0.43 | 17.80 | 7 | 3.40 |
| 0.00 | 0.46 | 2.88 | 0.24 | 0.00 | 17.80 | 28 | 4.60 |
| 0.13 | 0.51 | 2.88 | 0.22 | 0.11 | 17.80 | 28 | 4.20 |
| 0.51 | 0.54 | 2.88 | 0.10 | 1.00 | 17.80 | 28 | 3.70 |
| 0.13 | 0.51 | 2.88 | 0.22 | 0.11 | 17.80 | 56 | 4.40 |
| 0.25 | 0.52 | 2.88 | 0.20 | 0.25 | 17.80 | 56 | 4.10 |
| 0.38 | 0.53 | 2.88 | 0.17 | 0.43 | 17.80 | 56 | 3.90 |
| 0.51 | 0.54 | 2.88 | 0.10 | 1.00 | 17.80 | 56 | 3.83 |
| 0.00 | 0.46 | 2.88 | 0.24 | 0.00 | 17.80 | 90 | 4.85 |
| 0.13 | 0.51 | 2.88 | 0.22 | 0.11 | 17.80 | 90 | 4.50 |
| 0.25 | 0.52 | 2.88 | 0.20 | 0.25 | 17.80 | 90 | 4.15 |
| 0.00 | 0.50 | 3.30 | 0.30 | 0.00 | 12.10 | 7 | 1.89 |
| 0.15 | 0.50 | 3.30 | 0.27 | 0.11 | 15.86 | 7 | 1.96 |
| 0.29 | 0.50 | 3.30 | 0.24 | 0.25 | 15.86 | 7 | 2.05 |
| 0.44 | 0.50 | 3.30 | 0.21 | 0.43 | 15.86 | 7 | 2.08 |
| 0.15 | 0.50 | 3.30 | 0.27 | 0.11 | 15.86 | 28 | 2.85 |
| 0.29 | 0.50 | 3.30 | 0.24 | 0.25 | 15.86 | 28 | 2.90 |
| 0.44 | 0.50 | 3.30 | 0.21 | 0.43 | 15.86 | 28 | 3.00 |
| 0.00 | 0.50 | 3.30 | 0.30 | 0.00 | 12.10 | 56 | 2.93 |
| 0.44 | 0.50 | 3.30 | 0.21 | 0.43 | 15.86 | 56 | 3.24 |
| 0.00 | 0.50 | 3.30 | 0.30 | 0.00 | 12.10 | 90 | 2.99 |
| 0.15 | 0.50 | 3.30 | 0.27 | 0.11 | 15.86 | 90 | 3.13 |
| 0.29 | 0.50 | 3.30 | 0.24 | 0.25 | 15.86 | 90 | 3.21 |
| 0.00 | 0.50 | 3.30 | 0.30 | 0.00 | 12.10 | 365 | 3.10 |
| 0.29 | 0.50 | 3.30 | 0.24 | 0.25 | 15.86 | 365 | 3.32 |
| 0.00 | 0.40 | 2.53 | 0.33 | 0.00 | 3.67 | 7 | 2.77 |
| 0.06 | 0.40 | 2.53 | 0.31 | 0.05 | 3.67 | 7 | 3.09 |
| 0.00 | 0.40 | 2.53 | 0.33 | 0.00 | 3.67 | 28 | 4.23 |
| 0.25 | 0.40 | 2.53 | 0.26 | 0.25 | 3.67 | 28 | 4.51 |
| 0.00 | 0.40 | 2.53 | 0.33 | 0.00 | 3.67 | 90 | 4.32 |

| | | | | | | | |
|---|---|---|---|---|---|---|---|
| 0.06 | 0.40 | 2.53 | 0.31 | 0.05 | 3.67 | 90 | 4.45 |
| 0.00 | 0.50 | 3.13 | 0.33 | 0.00 | 0.00 | 7 | 1.80 |
| 0.23 | 0.50 | 3.13 | 0.28 | 0.23 | 0.00 | 7 | 2.10 |
| 0.31 | 0.50 | 3.13 | 0.26 | 0.31 | 0.00 | 7 | 2.20 |
| 0.38 | 0.50 | 3.13 | 0.25 | 0.38 | 0.00 | 7 | 1.80 |
| 0.31 | 0.50 | 3.13 | 0.26 | 0.31 | 0.00 | 28 | 2.80 |
| 0.38 | 0.50 | 3.13 | 0.25 | 0.38 | 0.00 | 28 | 2.10 |
| 0.00 | 0.44 | 2.86 | 0.35 | 0.00 | 0.00 | 7 | 2.77 |
| 0.31 | 0.44 | 2.86 | 0.30 | 0.25 | 0.00 | 7 | 2.60 |
| 0.61 | 0.44 | 2.86 | 0.24 | 0.67 | 0.00 | 7 | 2.31 |
| 0.77 | 0.44 | 2.86 | 0.21 | 1.00 | 0.00 | 7 | 2.21 |
| 0.00 | 0.44 | 2.86 | 0.35 | 0.00 | 0.00 | 28 | 2.81 |
| 0.15 | 0.44 | 2.86 | 0.33 | 0.11 | 0.00 | 28 | 2.76 |
| 0.31 | 0.44 | 2.86 | 0.30 | 0.25 | 0.00 | 28 | 2.67 |
| 0.46 | 0.44 | 2.86 | 0.27 | 0.43 | 0.00 | 28 | 2.60 |
| 0.77 | 0.44 | 2.86 | 0.21 | 1.00 | 0.00 | 28 | 2.32 |
| 0.00 | 0.44 | 2.86 | 0.35 | 0.00 | 0.00 | 90 | 2.81 |
| 0.31 | 0.44 | 2.86 | 0.30 | 0.25 | 0.00 | 90 | 2.68 |
| 0.77 | 0.44 | 2.86 | 0.21 | 1.00 | 0.00 | 90 | 2.33 |
| 0.00 | 0.44 | 2.86 | 0.35 | 0.00 | 0.00 | 180 | 2.73 |
| 0.15 | 0.44 | 2.86 | 0.33 | 0.11 | 0.00 | 180 | 2.66 |
| 0.31 | 0.44 | 2.86 | 0.30 | 0.25 | 0.00 | 180 | 2.66 |
| 0.46 | 0.44 | 2.86 | 0.27 | 0.43 | 0.00 | 180 | 2.59 |
| 0.61 | 0.44 | 2.86 | 0.24 | 0.67 | 0.00 | 180 | 2.46 |
| 0.77 | 0.44 | 2.86 | 0.21 | 1.00 | 0.00 | 180 | 2.44 |
| 0.00 | 0.47 | 2.47 | 0.38 | 0.00 | 0.00 | 28 | 2.75 |
| 0.31 | 0.47 | 2.47 | 0.33 | 0.25 | 0.00 | 28 | 2.98 |
| 0.61 | 0.47 | 2.47 | 0.27 | 0.67 | 0.00 | 28 | 3.40 |
| 0.77 | 0.47 | 2.47 | 0.24 | 1.00 | 0.00 | 28 | 3.12 |
| 0.68 | 0.47 | 2.75 | 0.26 | 0.67 | 0.00 | 28 | 3.04 |
| 0.77 | 0.47 | 3.09 | 0.26 | 0.67 | 0.00 | 28 | 2.91 |
| 0.65 | 0.47 | 2.60 | 0.27 | 0.67 | 0.00 | 28 | 3.61 |
| 0.66 | 0.47 | 2.67 | 0.27 | 0.67 | 0.00 | 28 | 3.67 |
| 0.00 | 0.52 | 4.20 | 0.38 | 0.00 | 6.00 | 28 | 3.30 |
| 0.25 | 0.52 | 4.20 | 0.34 | 0.11 | 6.00 | 28 | 1.87 |
| 0.51 | 0.52 | 4.20 | 0.30 | 0.25 | 6.00 | 28 | 2.85 |
| 0.03 | 0.52 | 4.20 | 0.35 | 0.01 | 6.00 | 28 | 2.08 |
| 0.06 | 0.52 | 4.20 | 0.32 | 0.03 | 6.00 | 28 | 2.64 |
| 0.00 | 0.40 | 2.13 | 0.50 | 0.00 | 0.00 | 7 | 3.13 |
| 0.21 | 0.40 | 1.92 | 0.50 | 0.10 | 0.00 | 7 | 3.15 |
| 0.43 | 0.40 | 1.71 | 0.50 | 0.20 | 0.00 | 7 | 3.23 |
| 0.21 | 0.40 | 2.13 | 0.45 | 0.11 | 0.00 | 7 | 3.26 |
| 0.43 | 0.40 | 2.13 | 0.40 | 0.25 | 0.00 | 7 | 3.44 |
| 0.64 | 0.40 | 2.13 | 0.35 | 0.43 | 0.00 | 7 | 3.63 |
| 0.00 | 0.40 | 2.13 | 0.50 | 0.00 | 0.00 | 7 | 3.13 |
| 0.85 | 0.40 | 1.71 | 0.40 | 0.50 | 0.00 | 7 | 2.18 |
| 1.28 | 0.40 | 1.49 | 0.35 | 0.86 | 0.00 | 7 | 1.69 |
| 0.00 | 0.40 | 2.13 | 0.50 | 0.00 | 0.00 | 14 | 3.59 |
| 0.21 | 0.40 | 1.92 | 0.50 | 0.10 | 0.00 | 14 | 3.69 |
| 0.64 | 0.40 | 1.49 | 0.50 | 0.30 | 0.00 | 14 | 3.92 |

| | | | | | | | |
|---|---|---|---|---|---|---|---|
| 0.21 | 0.40 | 2.13 | 0.45 | 0.11 | 0.00 | 14 | 3.78 |
| 0.64 | 0.40 | 2.13 | 0.35 | 0.43 | 0.00 | 14 | 4.23 |
| 0.00 | 0.40 | 2.13 | 0.50 | 0.00 | 0.00 | 14 | 3.59 |
| 0.85 | 0.40 | 1.71 | 0.40 | 0.50 | 0.00 | 14 | 2.66 |
| 1.28 | 0.40 | 1.49 | 0.35 | 0.86 | 0.00 | 14 | 2.25 |
| 0.00 | 0.40 | 2.13 | 0.50 | 0.00 | 0.00 | 28 | 4.03 |
| 0.21 | 0.40 | 1.92 | 0.50 | 0.10 | 0.00 | 28 | 4.15 |
| 0.00 | 0.40 | 2.13 | 0.50 | 0.00 | 0.00 | 28 | 4.03 |
| 0.21 | 0.40 | 2.13 | 0.45 | 0.11 | 0.00 | 28 | 4.26 |
| 0.43 | 0.40 | 2.13 | 0.40 | 0.25 | 0.00 | 28 | 4.43 |
| 0.43 | 0.40 | 1.92 | 0.45 | 0.22 | 0.00 | 28 | 3.95 |
| 0.85 | 0.40 | 1.71 | 0.40 | 0.50 | 0.00 | 28 | 3.26 |
| 1.28 | 0.40 | 1.49 | 0.35 | 0.86 | 0.00 | 28 | 2.93 |
| 0.00 | 0.48 | 2.97 | 0.44 | 0.00 | 0.00 | 3 | 2.70 |
| 0.59 | 0.48 | 2.97 | 0.37 | 0.33 | 0.00 | 3 | 1.80 |
| 0.83 | 0.48 | 2.97 | 0.34 | 0.54 | 0.00 | 3 | 2.10 |
| 0.59 | 0.48 | 2.97 | 0.37 | 0.33 | 0.00 | 3 | 2.30 |
| 0.83 | 0.48 | 2.97 | 0.34 | 0.54 | 0.00 | 3 | 2.10 |
| 0.59 | 0.48 | 2.97 | 0.37 | 0.33 | 0.00 | 7 | 3.20 |
| 0.59 | 0.48 | 2.97 | 0.37 | 0.33 | 0.00 | 7 | 3.50 |
| 0.83 | 0.48 | 2.97 | 0.34 | 0.54 | 0.00 | 7 | 2.50 |
| 0.59 | 0.48 | 2.97 | 0.37 | 0.33 | 0.00 | 28 | 3.60 |
| 0.59 | 0.48 | 2.97 | 0.37 | 0.33 | 0.00 | 28 | 4.00 |
| 0.00 | 0.40 | 2.50 | 0.29 | 0.00 | 0.00 | 28 | 4.30 |
| 0.60 | 0.40 | 2.50 | 0.14 | 1.46 | 0.00 | 28 | 3.15 |
| 0.00 | 0.55 | 2.16 | 0.44 | 0.00 | 0.00 | 7 | 3.13 |
| 0.17 | 0.55 | 2.16 | 0.42 | 0.11 | 0.00 | 7 | 2.93 |
| 0.35 | 0.55 | 2.16 | 0.40 | 0.24 | 0.00 | 7 | 3.00 |
| 0.71 | 0.55 | 2.16 | 0.33 | 0.67 | 0.00 | 7 | 3.21 |
| 0.90 | 0.55 | 2.16 | 0.29 | 1.00 | 0.00 | 7 | 3.33 |
| 0.00 | 0.55 | 2.16 | 0.44 | 0.00 | 0.00 | 28 | 3.51 |
| 0.17 | 0.55 | 2.16 | 0.42 | 0.11 | 0.00 | 28 | 3.73 |
| 0.35 | 0.55 | 2.16 | 0.40 | 0.24 | 0.00 | 28 | 3.59 |
| 0.71 | 0.55 | 2.16 | 0.33 | 0.67 | 0.00 | 28 | 3.99 |
| 0.18 | 0.50 | 3.38 | 0.33 | 0.11 | 0.00 | 7 | 1.92 |
| 0.36 | 0.50 | 3.38 | 0.30 | 0.25 | 0.00 | 7 | 2.01 |
| 0.72 | 0.50 | 3.38 | 0.24 | 0.67 | 0.00 | 7 | 2.02 |
| 0.18 | 0.50 | 3.38 | 0.33 | 0.11 | 0.00 | 28 | 2.45 |
| 0.36 | 0.50 | 3.38 | 0.30 | 0.25 | 0.00 | 28 | 2.54 |
| 0.72 | 0.50 | 3.38 | 0.24 | 0.67 | 0.00 | 28 | 2.52 |
| 0.00 | 0.50 | 3.38 | 0.35 | 0.00 | 0.00 | 56 | 2.92 |
| 0.18 | 0.50 | 3.38 | 0.33 | 0.11 | 0.00 | 56 | 3.04 |
| 0.36 | 0.50 | 3.38 | 0.30 | 0.25 | 0.00 | 56 | 3.18 |
| 0.54 | 0.50 | 3.38 | 0.27 | 0.43 | 0.00 | 56 | 3.31 |
| 0.72 | 0.50 | 3.38 | 0.24 | 0.67 | 0.00 | 56 | 3.09 |
| 0.00 | 0.50 | 3.38 | 0.35 | 0.00 | 0.00 | 90 | 3.59 |
| 0.54 | 0.50 | 3.38 | 0.27 | 0.43 | 0.00 | 90 | 4.07 |
| 0.72 | 0.50 | 3.38 | 0.24 | 0.67 | 0.00 | 90 | 3.87 |
| 0.00 | 0.43 | 2.57 | 0.41 | 0.00 | 0.00 | 7 | 2.20 |
| 0.18 | 0.43 | 2.99 | 0.35 | 0.11 | 0.00 | 7 | 2.58 |

| | | | | | | | |
|---|---|---|---|---|---|---|---|
| 0.27 | 0.43 | 2.99 | 0.34 | 0.18 | 0.00 | 7 | 2.53 |
| 0.36 | 0.43 | 2.99 | 0.32 | 0.25 | 0.00 | 7 | 2.16 |
| 0.15 | 0.43 | 2.80 | 0.32 | 0.11 | 0.00 | 7 | 2.72 |
| 0.29 | 0.43 | 2.80 | 0.30 | 0.25 | 0.00 | 7 | 2.12 |
| 0.00 | 0.43 | 2.57 | 0.41 | 0.00 | 0.00 | 28 | 3.30 |
| 0.18 | 0.43 | 2.99 | 0.35 | 0.11 | 0.00 | 28 | 3.87 |
| 0.27 | 0.43 | 2.99 | 0.34 | 0.18 | 0.00 | 28 | 3.77 |
| 0.36 | 0.43 | 2.99 | 0.32 | 0.25 | 0.00 | 28 | 2.93 |
| 0.00 | 0.43 | 2.80 | 0.34 | 0.00 | 0.00 | 28 | 3.21 |
| 0.29 | 0.43 | 2.80 | 0.30 | 0.25 | 0.00 | 28 | 3.25 |
| 0.39 | 0.42 | 3.16 | 0.33 | 0.25 | 0.00 | 7 | 2.20 |
| 0.78 | 0.42 | 3.16 | 0.27 | 0.67 | 0.00 | 7 | 3.26 |
| 1.17 | 0.42 | 3.16 | 0.20 | 1.50 | 0.00 | 7 | 2.62 |
| 0.95 | 0.42 | 3.33 | 0.38 | 0.00 | 0.00 | 7 | 2.83 |
| 0.90 | 0.42 | 3.51 | 0.38 | 0.00 | 0.00 | 7 | 2.24 |
| 0.85 | 0.42 | 3.72 | 0.38 | 0.00 | 0.00 | 7 | 2.16 |
| 0.00 | 0.42 | 3.16 | 0.38 | 0.00 | 0.00 | 14 | 2.98 |
| 0.39 | 0.42 | 3.16 | 0.33 | 0.25 | 0.00 | 14 | 3.15 |
| 1.17 | 0.42 | 3.16 | 0.20 | 1.50 | 0.00 | 14 | 3.36 |
| 0.95 | 0.42 | 3.33 | 0.38 | 0.00 | 0.00 | 14 | 3.53 |
| 0.90 | 0.42 | 3.51 | 0.38 | 0.00 | 0.00 | 14 | 2.62 |
| 0.00 | 0.42 | 3.16 | 0.38 | 0.00 | 0.00 | 28 | 3.67 |
| 0.39 | 0.42 | 3.16 | 0.33 | 0.25 | 0.00 | 28 | 3.78 |
| 0.78 | 0.42 | 3.16 | 0.27 | 0.67 | 0.00 | 28 | 4.16 |
| 0.90 | 0.42 | 3.51 | 0.38 | 0.00 | 0.00 | 28 | 3.01 |
| 0.85 | 0.42 | 3.72 | 0.38 | 0.00 | 0.00 | 28 | 2.83 |
| 0.00 | 0.45 | 0.93 | 0.69 | 0.00 | 0.00 | 28 | 3.27 |
| 0.42 | 0.45 | 0.93 | 0.69 | 0.25 | 0.00 | 28 | 3.32 |
| 0.63 | 0.45 | 0.93 | 0.69 | 0.43 | 0.00 | 28 | 3.14 |
| 0.00 | 0.45 | 1.90 | 0.51 | 0.00 | 0.00 | 28 | 3.31 |
| 0.20 | 0.45 | 1.90 | 0.51 | 0.11 | 0.00 | 28 | 3.24 |
| 0.40 | 0.45 | 1.90 | 0.51 | 0.25 | 0.00 | 28 | 3.20 |
| 0.59 | 0.45 | 1.90 | 0.51 | 0.43 | 0.00 | 28 | 3.15 |
| 0.00 | 0.53 | 3.18 | 0.33 | 0.00 | 0.00 | 28 | 3.08 |
| 0.08 | 0.53 | 3.18 | 0.32 | 0.05 | 0.00 | 28 | 3.24 |
| Validation set | | | | | | | |
| 0.24 | 0.53 | 3.18 | 0.28 | 0.18 | 0.00 | 28 | 3.51 |
| 0.32 | 0.53 | 3.18 | 0.27 | 0.25 | 0.00 | 28 | 3.63 |
| 0.40 | 0.53 | 3.18 | 0.25 | 0.33 | 0.00 | 28 | 3.73 |
| 0.48 | 0.53 | 3.18 | 0.23 | 0.43 | 0.00 | 28 | 3.79 |
| 0.56 | 0.53 | 3.18 | 0.22 | 0.54 | 0.00 | 28 | 3.91 |
| 0.64 | 0.53 | 3.18 | 0.20 | 0.67 | 0.00 | 28 | 2.86 |
| 0.17 | 0.52 | 2.93 | 0.33 | 0.11 | 0.00 | 7 | 2.44 |
| 0.35 | 0.52 | 2.93 | 0.30 | 0.25 | 0.00 | 7 | 2.82 |
| 0.52 | 0.52 | 2.93 | 0.26 | 0.43 | 0.00 | 7 | 2.41 |
| 0.69 | 0.52 | 2.93 | 0.22 | 0.67 | 0.00 | 7 | 2.40 |
| 0.00 | 0.52 | 2.93 | 0.37 | 0.00 | 0.00 | 28 | 3.50 |
| 0.17 | 0.52 | 2.93 | 0.33 | 0.11 | 0.00 | 28 | 3.85 |
| 0.35 | 0.52 | 2.93 | 0.30 | 0.25 | 0.00 | 28 | 4.24 |
| 0.52 | 0.52 | 2.93 | 0.26 | 0.43 | 0.00 | 28 | 3.65 |

| | | | | | | | |
|---|---|---|---|---|---|---|---|
| 0.69 | 0.52 | 2.93 | 0.22 | 0.67 | 0.00 | 28 | 3.60 |
| 0.15 | 0.55 | 3.00 | 0.30 | 0.11 | 0.00 | 28 | 2.35 |
| 0.45 | 0.55 | 3.00 | 0.23 | 0.43 | 0.00 | 28 | 2.50 |
| 0.75 | 0.55 | 3.00 | 0.17 | 1.00 | 0.00 | 28 | 2.40 |
| 1.05 | 0.55 | 3.00 | 0.10 | 2.33 | 0.00 | 28 | 2.60 |
| 0.00 | 0.45 | 3.00 | 0.25 | 0.00 | 0.00 | 28 | 2.85 |
| 0.45 | 0.45 | 3.00 | 0.21 | 0.43 | 0.00 | 28 | 2.90 |
| 0.75 | 0.45 | 3.00 | 0.17 | 1.00 | 0.00 | 28 | 2.90 |
| 1.05 | 0.45 | 3.00 | 0.12 | 2.33 | 0.00 | 28 | 2.90 |
| 0.00 | 0.50 | 2.99 | 0.33 | 0.00 | 1.51 | 7 | 2.15 |
| 0.14 | 0.50 | 2.99 | 0.30 | 0.11 | 1.51 | 7 | 2.38 |
| 0.00 | 0.42 | 2.53 | 0.33 | 0.00 | 3.67 | 7 | 2.77 |
| 0.06 | 0.42 | 2.53 | 0.31 | 0.05 | 3.67 | 7 | 3.10 |
| 0.12 | 0.42 | 2.53 | 0.30 | 0.11 | 3.67 | 7 | 3.20 |
| 0.18 | 0.42 | 2.53 | 0.28 | 0.18 | 3.67 | 7 | 3.28 |
| 0.25 | 0.42 | 2.53 | 0.26 | 0.25 | 3.67 | 7 | 3.10 |
| 0.00 | 0.50 | 2.99 | 0.33 | 0.00 | 1.51 | 28 | 4.23 |
| 0.07 | 0.50 | 2.99 | 0.31 | 0.05 | 1.51 | 28 | 4.58 |
| 0.14 | 0.50 | 2.99 | 0.30 | 0.11 | 1.51 | 28 | 4.76 |
| 0.22 | 0.50 | 2.99 | 0.28 | 0.18 | 1.51 | 28 | 4.77 |
| 0.00 | 0.42 | 2.53 | 0.33 | 0.00 | 3.67 | 28 | 4.23 |
| 0.06 | 0.42 | 2.53 | 0.31 | 0.05 | 3.67 | 28 | 4.38 |
| 0.12 | 0.42 | 2.53 | 0.30 | 0.11 | 3.67 | 28 | 4.58 |
| 0.18 | 0.42 | 2.53 | 0.28 | 0.18 | 3.67 | 28 | 4.67 |
| 0.25 | 0.42 | 2.53 | 0.26 | 0.25 | 3.67 | 28 | 4.50 |
| 0.07 | 0.50 | 2.99 | 0.31 | 0.05 | 1.51 | 90 | 4.59 |
| 0.29 | 0.50 | 2.99 | 0.26 | 0.25 | 1.51 | 90 | 4.72 |
| 0.00 | 0.42 | 2.53 | 0.33 | 0.00 | 3.67 | 90 | 4.31 |
| 0.06 | 0.42 | 2.53 | 0.31 | 0.05 | 3.67 | 90 | 4.45 |
| 0.18 | 0.42 | 2.53 | 0.28 | 0.18 | 3.67 | 90 | 4.80 |
| 0.00 | 0.50 | 2.99 | 0.33 | 0.00 | 1.51 | 365 | 3.96 |
| 0.07 | 0.50 | 2.99 | 0.31 | 0.05 | 1.51 | 365 | 4.10 |
| 0.22 | 0.50 | 2.99 | 0.28 | 0.18 | 1.51 | 365 | 4.36 |
| 0.29 | 0.50 | 2.99 | 0.26 | 0.25 | 1.51 | 365 | 4.29 |
| 0.00 | 0.42 | 2.53 | 0.33 | 0.00 | 3.67 | 365 | 4.38 |
| 0.06 | 0.42 | 2.53 | 0.31 | 0.05 | 3.67 | 365 | 4.60 |
| 0.12 | 0.42 | 2.53 | 0.30 | 0.11 | 3.67 | 365 | 4.78 |
| 0.25 | 0.42 | 2.53 | 0.26 | 0.25 | 3.67 | 365 | 4.90 |
| 0.00 | 0.45 | 2.43 | 0.44 | 0.00 | 0.00 | 7 | 3.21 |
| 0.19 | 0.45 | 2.43 | 0.40 | 0.11 | 0.00 | 7 | 3.35 |
| 0.38 | 0.45 | 2.43 | 0.35 | 0.25 | 0.00 | 7 | 3.48 |
| 0.58 | 0.45 | 2.43 | 0.31 | 0.43 | 0.00 | 7 | 3.11 |
| 0.77 | 0.45 | 2.43 | 0.26 | 1.00 | 0.00 | 7 | 2.83 |
| 0.00 | 0.45 | 2.43 | 0.44 | 0.00 | 0.00 | 28 | 4.53 |
| 0.19 | 0.45 | 2.43 | 0.40 | 0.11 | 0.00 | 28 | 4.67 |
| 0.58 | 0.45 | 2.43 | 0.31 | 0.43 | 0.00 | 28 | 4.39 |